From the Institute of Molecular Medicine II

at the Heinrich Heine University Düsseldorf

Novel therapeutic strategies and modulators of anti-tumor immunity in melanoma

Dissertation

to obtain the academic title of Doctor of Philosophy (PhD) in Medical Sciences from the Faculty of Medicine at Heinrich Heine University Düsseldorf

submitted by

Wei Liu

(2021)

As an inaugural dissertation printed by permission of the Faculty of Medicine at Heinrich Heine University Düsseldorf

signed:

Dean:

Examiners:

Prof. Dr. med. Philipp Lang

Institute of Molecular Medicine II,

Medical faculty, Heinrich-Heine-University, Düsseldorf

Prof. Dr. med. Bernhard Homey,

Department of Dermatology,

Medical faculty, Heinrich-Heine-University, Düsseldorf

List of publications

1. **Wei Liu**, Paweł Stachura, Haifeng C. Xu, Nikkitha Umesh Ganesh, Fiona Cox, Ruifeng Wang, Karl S. Lang, Jay Gopalakrishnan, Dieter Häussinger, Bernhard Homey, Philipp A. Lang, Aleksandra A. Pandyra. (2020). **Repurposing the serotonin agonist Tegaserod as an anticancer agent in melanoma: molecular mechanisms and clinical implications**. Journal of Experimental & Clinical Cancer Research, 39(1), 1-16.
2. **Wei Liu,** Paweł Stachura, Haifeng C. Xu, Sanil Bhatia, Arndt Borkhardt, Philipp A. Lang, Aleksandra A. Pandyra. (2020). **Senescent Tumor CD8+ T Cells: Mechanisms of Induction and Challenges to Immunotherapy**. Cancers, 12(10), 2828. (**review**)

I Zusammenfassung

Maligne Melanome sind für einen Großteil der krebsbedingten Todesfälle verantwortlich. Neue Therapien für Melanome sind dringend erforderlich, insbesondere für Patienten im Spätstadium, die nicht auf Immuntherapien und Kinasehemmer ansprechen. Im ersten Abschnitt der Dissertation haben wir ein pharmakologisches Screening durchgeführt, um neuartige Wirkstoffe gegen Melanome zu identifizieren. Das Screening bestand aus der NIH Clinical Collection (NCC) von 770 *small molecules*, die entweder von der FDA zugelassen waren oder zuvor in klinischen Studien am Menschen erprobt wurden. Jedes der Moleküle wurde in der murinen B16.F10-Zelllinie gescreent und die halbmaximale Hemmkonzentration (IC 50) bestimmt. Von den Substanzen, deren IC 50 -Werte im niedrigen mikromolaren Bereich lagen, wurde Tegaserod (TM), ein Serotoninrezeptor 4 (HTR4) -Agonist, erfolgreich in sekundären Screening-Experimenten mit menschlichen Melanomzelllinien BRAF WT und $BRAF^{V600E}$ validiert. Die Wirksamkeit von TM gegen Krebs wurde in *in-vitro*- und *in-vivo*-Studien näher untersucht. TM hat in der murinen Melanomzelllinie B16.F10, sowie in mehreren menschlichen Melanomzelllinien dosis- und zeitabhängig Apoptose induziert. *In vivo* zeigte TM eine gute Verträglichkeit. Die antitumorale Wirkung wurde in einem syngenen Melanom-Modell validiert, in dem das Wachstum und die Metastasierung des Primärtumors untersucht wurden. Darüber hinaus gleicht die Wirksamkeit von TM der Wirksamkeit von Vemurafenib, welches $BRAF^{V600E}$ in menschlichen Melanomzellinien mit derselben Mutation hemmt. TM hemmt *in vitro* und *in vivo* die PI3K / Akt /mTOR Signaltransduktion, indem es das ribosmale Protein S6 (Rps6) inhibiert. Die Hemmung des PI3K / Akt / mTOR-Signalwegs ist wahrscheinlich für die proapoptotische und antimetastatische Wirkung von TM in Melanomzelllinien verantwortlich. Die pharmakologische Hemmung des Signalwegs mittels spezifischer Inhibitoren erzielte den gleichen apoptotischen Phänotyp und bestätigte die Sensitivität von Melanomzellen gegenüber der Inhibition des PI3K / Akt / mTOR-Signalwegs. Zusammengefasst haben wir ein gegen Melanome wirksames Medikament identifiziert, das potenziell sowohl bei $BRAF^{V600E}$- als auch bei BRAF

WT-Melanomen mit Standardmedikamenten wie Vemurafenib und Cobimetinib kombiniert werden kann.

Andererseits beruhen viele neue Therapien wie Zytokin-, Impfstoff- und Antikörper-basierte Therapien darauf, das Immunsystem zur Bekämpfung von Tumoren auszunutzen. Das Tumormikromilieu (Tumormicroenvironment oder auch TME) solider Tumoren ist ein komplexes Milieu, das aus infiltrierenden Immunzellen, Stromazellen, Gefäßen und Tumorzellen besteht. Dessen Zusammensetzung wird durch verschiedene Faktoren wie Zytokine, Chemokine, Wachstumsfaktoren und Metaboliten innerhalb des Milieus geprägt. Aufgrund der inhärenten Komplexität des TME sind weitere Untersuchungen erforderlich, um den Beitrag der verschiedenen Komponenten einschließlich der darin enthaltenen Zytokine besser zu verstehen. Der zweite Teil dieser Dissertation befasst sich mit der Untersuchung der Auswirkungen des Cytokin-B-Zell-Aktivierungsaktors (BAFF) auf die antitumorale Immunität bei Melanomen.

Obwohl die Rolle von BAFF für das Überleben von B-Zellen und als Prognosefaktor bei Autoimmunerkrankungen und bösartigen hämatologischen Tumoren bekannt ist, ist unklar, wie sich BAFF auf das Wachtum solider Tumorarten auswirkt. Wir haben BAFF-überexprimierende B16.F10.gp33 (BAFF) Melanomzellen generiert. C57BL/6 Mäuse, die mit BAFF Zellen behandelt wurden, hatten im Vergleich zu mit WT Zellen behandelten Mäusen eine signifikant kleineres Tumorvolumen. Die Charakterisierung von BAFF- und Kontrolltumoren zeigte bei BAFF-Tumoren einen erhöhten Grad an Apoptose und eine Abnahme der Expression von immunsuppressiven Faktoren, einschließlich des programmierten Zelltod-1-Liganden 1 (PD-L1). BAFF-Tumoren wiesen nicht nur eine geringere Anzahl infiltrierender myeloischer Zellen auf, auch die PD-L1-Expression infiltrierender Monozyten in BAFF-Tumoren war verringert. Die funktionelle Abhängigkeit des unterschiedlichen Tumorwachstums zwischen BAFF- und Kontrolltumoren von Monozyten und der PDL1-Expression konnte durch die Depletion von Monozyten, sowie die Behandlung mit einem anti-PD-L1 Antikörper bestätigt werden. Die RNA-Seq-Analyse von Monozyten, welche aus BAFF- und Kontrolltumoren isoliert wurden, bestätigte des Weiteren, dass aus BAFF-Tumoren isolierte Monozyten durch einen verminderten Exhaustion-Phänotyp

gekennzeichnet waren und die Expression von Genen , die adaptive Immunantworten und NF-κB-Signale aktivieren, erhöht war. Mittels der Verwendung einer Kombination von Knockout-Mäusen und Depletionsantikörpern wurde festgestellt, dass der Phänotyp durch NK-Zellen beeinflusst wird. Zusammenfassend haben wir gezeigt, dass BAFF das Tumorwachstum durch eine verringerte Tumorinfiltration von Monozyten und aktivierten NK-Zellen beeinflusst.

II Summary

Melanoma accounts for a large proportion of cancer-related deaths. New therapies are urgently needed in melanoma, particularly in late-stage patients not responsive to immunotherapies and kinase inhibitors. In the first section of the dissertation, we conducted a pharmacologic screen composed of the NIH Clinical Collection (NCC) of 770 small molecules, FDA-approved or which have been previously used in human clinical trials to identify novel anti-melanoma agents. Each molecule was screened in the murine B16.F10 cell line and its half maximal inhibitory concentrations (IC50) was determined. Amongst the compounds whose IC50 values were in the low micromolar range, Tegaserod (TM), a serotonin receptor 4 (HTR4) agonist, validated successfully in secondary screening approaches with BRAF WT and $BRAF^{V600E}$ human melanoma cell lines. The anti-cancer efficacy of TM was further evaluated in *in vitro* and *in vivo* studies. TM induced apoptosis in a dose and time dependent manner in the B16.F10 murine melanoma cell line as well as several human melanoma cell lines. *In vivo*, TM was well-tolerated and anti-tumoral effects were validated in a syngeneic melanoma model testing primary tumor growth and metastasis. Furthermore, TM strongly synergized with the standard of care $BRAF^{V600E}$ targeting Vemurafenib in human melanoma cell lines with this mutation. Mechanistically, TM inhibited PI3K/Akt/mTOR signaling converging on ribosomal protein S6 (S6) *in vitro* and *in vivo*. Inhibition of the PI3K/Akt/mTOR pathway was likely responsible for TM's pro-apoptotic effects and anti-metastatic effects in melanoma cell lines. Pharmacological inhibition of the pathway using specific inhibitors recapitulated the apoptotic phenotype confirming the sensitivity of melanoma cells to PI3K/Akt/mTOR pathway perturbation. Taken together, we have identified a drug with anti-melanoma activity that has the potential to be combined with the standard of care agent Vemurafenib and Cobimetinib in both $BRAFV^{600E}$ and BRAF WT melanoma.

On the other hand, many new therapies, such as cytokine, vaccine, and antibody-based therapies, rely on exploiting the immune system to fight tumors. In solid tumors, the tumor microenvironment (TME) is a complex milieu composed of infiltrating

immune cells, stromal cells, vasculature, and tumor cells whose composition is shaped by the different factors including cytokines, chemokines, growth factors and metabolites within it. Due to the TME's inherent complexity, further research is needed to understand the contribution of the different components including cytokines within it. The second portion of the dissertation focuses on dissecting the effects of the cytokine B cell activating factor (BAFF) on anti-tumoral immunity in melanoma.

While the role of BAFF in the survival of B cells and as a prognostic factor in autoimmune diseases and hematological malignancies is well known, it is unclear how BAFF impacts solid tumor growth. We generated a BAFF-overexpressing B16.F10.gp33 (BAFF) system in melanoma cells. The expression of BAFF inhibits tumor growth. Characterization of BAFF and control tumors indicated increased tumor apoptosis and a decrease in the expression of immunosuppressive factors including Programmed Cell Death 1 Ligand 1 (PD-L1) in BAFF tumors. Not only did BAFF tumors have lower numbers of myeloid infiltrates, but the PD-L1 expression on infiltrating monocytes in BAFF tumors was also decreased. Depletion of monocytes as well as treatment with an anti-PD-L1 antibody confirmed the functional dependence of the difference in tumor growth between BAFF and control tumors on monocytes and PD-L1 expression. RNA-Seq analysis of monocytes isolated from BAFF and control tumors further confirmed that monocytes isolated from BAFF tumors where characterized by a decreased exhaustive phenotype and enriched for in genes activating adaptive immune responses and NF-κB signaling. Using knockout mice and depletion antibodies, the phenotype was found to be influenced by NK cells. In summary, we have shown that BAFF impacts tumor growth through decreased tumor infiltrating monocytes and activated NK cells.

III Abbreviations

ACT: Adoptive T cell therapy

AEs: Adverse events

AJCC: American Joint Committee on Cancer

ALT: Alanine aminotransaminase

AST: Aspartate transaminase

ATCC: American Type Culture Collection

BAFF-Tg mice: BAFF transgenic mice

BAFF: B cell activating factor

BAFF-R: B cell activating factor receptor

BCMA: B-Cell maturation antigen

BCNU: bis-chloroethylnitrosourea, Carmustine

BCR: B cell receptor

BMI: Body mass index

cAMP: cyclic adenosine monophosphate

CCL2: Chemokine (C-C motif) ligand 2

CCL5: Chemokine (C-C motif) ligand 5

CCLE: Cancer Cell Line Encyclopedia

CCNU: 1-(2-chloroethyl)-3-cyclohexyl-1-nitrosourea, Lomustine

CCR2: C-C chemokine receptor type 2

CDK: Cyclin-dependent kinase

CDK4: Cyclin-dependent kinase 4

CDKN2A: Cyclin-dependent kinase inhibitor 2A

CI: Confidence interval

CNS: Central nervous system

CREB: cAMP response element-binding protein

CTLA4: Cytotoxic T-lymphocyte-associated protein 4

CTLs: Cytotoxic T lymphocytes

CV: Cardiovascular

DCR: Disease control rate

DNA: Deoxyribonucleic acid

DTH: Delayed-type hypersensitivity

ED75: Effective dose for 75% of the population

ED90: Effective dose for 90% of the population

ELISA: Enzyme-linked immunosorbent assay

ER: Endoplasmic reticulum

ERK: Extracellular signal-regulated kinase

FDA: Food and Drug Administration

FGFR1: Fibroblast growth factor receptor 1

Fig.: Figure

GAPDH: Glyceraldehyde 3-phosphate dehydrogenase

GSEA: Gene set enrichment analysis

GZMB: Granzyme B

HED: Human equivalent dose

HT: 5-hydroxytryptamine

HTRs: 5-hydroxytryptamine receptors

IBS: Irritable bowel syndrome

IC50: Half-maximal inhibitory concentration

ICAM-1: Intercellular adhesion molecule 1

IFNs: Interferons

IL-2: Interleukin-2

IL-4: Interleukin-2

IL-6: Interleukin-6

IL-10: Interleukin-10

IL-7R: Interleukin 7 receptor

IPA: Ingenuity pathway analysis

IRFs: IFN regulatory factors

KEGG: Kyoto Encyclopedia of Genes and Genomes

KLRG1: Killer cell lectin-like receptor subfamily G member 1

LDH: Lactate dehydrogenase

LMM: Lentigo malignant melanoma

LPS: Lipopolysaccharide

MAPK: Mitogen-activated protein kinases

mDC: Myeloid dendritic cells

MDSC: Myeloid-derived suppressor cells

MEK: Mitogen-activated protein kinase

MHC-I: Major histocompatibility complex I

MHC-II: Major histocompatibility complex II

MM: Multiple myeloma

MMP9: Matrix metallopeptidase 9

MMS: Mohs micrographic surgery

mTOR: Mammalian target of rapamycin

MZ: Marginal zone

NCC: NIH Clinical Collection

NF-κB: Nuclear factor kappa-B

NK cells: Natural killer cells

NR: Non-responders

NSCLC: Non-small cell lung carcinoma

OS: Overall survival

PD1: Programmed cell death protein 1

pDC: Plasmacytoid dendritic cells

PDK1: Phosphoinositide-dependent kinase 1

PDL1: Programmed death-ligand 1

PDL2: Programmed death-ligand 2

PFS: Progression-free survival

PI3K: Phosphoinositide 3-kinase

PR: Partial responses

rBAFF: Recombinant BAFF

rhBAFF: Recombinant human BAFF

RT: Radiation therapy

SBRT: Stereotactic body radiation therapy

SEM: Standard error of the mean

SLE: Systemic lupus erythematosus

SLNB: Sentinel Lymph Node Biopsy

SRS: Stereotactic radiosurgery

T1 B cells: Transitional type 1 B cells

T2 B cells: Transitional type 2 B cells

TACI: Transmembrane activator and CAML interactor

TAMs: Tumor-associated macrophages

TCGA: The Cancer Genome Atlas

TGFβ: Transforming growth factor beta

Th17 cells: T helper type17 cells

TILs: Tumor infiltrating lymphocytes

TLR: Toll-like receptors

TM: Tegaserod

TME: Tumor microenvironment

TNF: Tumor necrosis factor

Treg cells: Regulatory T-cells

TRAF: TNF receptor associated factors

TUNEL: Terminal deoxynucleotidyl transferase dUTP nick end labeling

T-VEC: Talimogene laherparepvec

UVR: Ultraviolet radiation

VEGF: Vascular endothelial growth factor

IV Table of contents

1 Introduction

Cancer is composed of a large group of heterogenous diseases and is the second leading cause of death world-wide. The annual number of cancer cases is on the rise. According to a report from the World Health Organization (WHO), the number of new cases in 2020 was over 19 million, up to one million from 2018. The total population of cancer cases tallied up to 2020 is around 779 million [1, 2]. The cancer burden continues to grow globally and is exerting tremendous social and economic burdens on society. In solid tumors, the tumor microenvironment (TME) is complex and therapy intrinsic and acquired resistance and metastasis are major obstacles in cancer patient care. Melanoma is one of the most lethal cancers and caused around fifty-seven thousand cancer-related deaths in 2020 [3]. Although the novel immunotherapeutic drugs have altered the treatment landscape in melanoma and dramatically increased the survival of some patients, response rates are still low and challenges remain. Many gaps in successfully treating melanoma exist and there is an urgent need for not only novel therapeutic options but also a deeper understanding of the immune mechanisms within the TME including how cytokines influence other immune populations and immunotherapeutic options. The first portion of the thesis focuses on uncovering novel anti-melanoma therapies using screening approaches and the second half on the role of the cytokine B cell activating factor (BAFF) in regulating anti-tumor immune responses.

1.1 Melanoma- etiology and treatment

1.1.1 Melanoma

Cancer is a disease driven by genetic changes in normal cells. One of the most crucial difference between cancer cells and normal cells is that cancer cells do not mature into distinct cell types with specific functions. Cancers which have different metabolic functions than normal cells are able to sustain proliferative signaling, evade growth suppressors and apoptosis-inducing signals. Compared to normal cells, cancer cells are also able to induce angiogenesis, invasion and metastasis and evade the immune system [4]. There are more than 100 types of cancers that usually named after originating organs or tissues. The most significant cancer population in 2020 was

composed of breast cancer patients (11.7%), followed by lung cancer (11.4%) and then colorectal cancer (10%). Melanoma is among the top 20 new tumor cases in 2020 [2].

Melanoma is a malignant tumor that arises from the uncontrolled proliferation of melanocyte pigment-containing cells [5-8] and mainly occurs in the skin (also called cutaneous melanoma, CM) and rarely in the eye (uvea, conjunctiva, and ciliary body), meninges, mouth, intestines, and on the various mucosal surface. Cutaneous melanoma is the most common malignant melanoma and the most aggressive and lethal form of skin cancer [9, 10]. The most common type of skin cancer is keratinocyte carcinoma (KC), but the actual number is difficult to estimate because cases are not required to be reported to cancer registries in the US. Approximately 5% of skin cancers are classified as CM, but it is amongst the deadliest as CM accounts for approximately three-quarters of all skin cancer related deaths [11].

1.1.2 Etiology and risk factors

Melanoma arises from multiple factors, including environmental exposure, physical factors, and genetic susceptibility [12]. The most important environmental risk factor is ultraviolet radiation (UVR) via sun exposure. UVR induces unrepairable DNA damage in skin cells and triggers mutations that lead to uncontrolled proliferation, eventually forming malignant tumors [13, 14]. A study estimated that 62.3% of melanoma in Canada could be attributed to UVR exposure, and a 50% reduction in sun exposure or other UVR behavior could decrease up to 11,980 melanoma cases by 2042 [15]. Another meta-analysis summarized 57 studies carried out in multiple countries on sun exposure and melanoma and found that intermittent sun exposure increased melanoma risk by 60% (summary relative risk (SRR):1.61; 95% CI: 1.31-1.99) [16]. Additionally, physical factors can influence the association of sun exposure with melanoma risks such as skin, hair, and eye color as well as freckles [13]. Similar to other cancers, melanoma risk is also influenced by the body mass index (BMI). A meta-analysis demonstrated that a high BMI or obesity inversely correlated with telomere length [17]. Melanoma patients have different responses to immunotherapy depending on their fat distribution. Patients with higher subcutaneous fat and strong muscle mass

experienced better responses than those with low muscle mass and high-fat mass [18]. In addition, previous retrospective studies showed vitamin D to play a significant role in melanoma outcomes. Specifically, low serum vitamin D levels were indicative of a negative prognosis in melanoma [19, 20].

Melanoma susceptibility genes have been classified by their frequency and the degree of risk. Some rare mutation variants have been shown to have a high risk of melanoma development. Cyclin-dependent kinase inhibitor 2A (CDKN2A) which inhibits cyclin-dependent kinase (CDK), regulates cell cycle checkpoints. In multiple case-family studies, germline mutations in *CDKN2A* confer age and geography-associated risk, and the penetrance (a mean age-specific cumulative risk) at age 80 years is 76% in the USA and 91% in Australia[21, 22]. In general population-based studies as opposed to case-family studies, the lifetime risk was 28% [23]. Mutations in cyclin-dependent kinase 4 (CDK4) are rare and present in less than 1% of familial cases of melanoma, but the penetrance at the age of 50 years is 74% [24]. In addition to these two high-risk susceptibility genes, high-throughput sequencing studies found more high-risk genes, including *TERT*, *POT1*, *ACD*, and *TERF2IP*, which encode proteins that control telomere length, and *BAP1, RAD51B*, and *POLE*, which encode proteins related to DNA repair [25-30]. Some frequent variants including genes associated with pigmentation (*OCA2, ASIP, TYR* [*OCA1*]*, TYRP1* [*OCA3*]*, MATP, SCLC45A2* [*OCA4*]*, KIT*, and *PARP1*) showed a low individual effect on the risk of developing melanoma. However, when combined, these low-risk variants may account for up to 78% of non-familial melanomas [22, 31-33].

Melanocytes naevi commonly known as moles, are generally benign but can also lead to melanoma [34]. The gene mutations predominantly in the RAS/RAF/MEK/ERK pathway cause proliferation of melanocytes naevi. The most common mutations are $BRAF^{V600E}$ and NRAS. A study reported that 78% of common acquired naevi, 60% of dysplastic naevi, 7% of blue and 6% of Spitz naevi are driven by BRAF mutations. 95% of giant pigmented congenital naevi, 70% small/naevi, and 2% blue and Spitz naevi are driven by NRAS mutations [35]. Data collected from an online data source showed the frequency of mutations in melanoma to be mainly in BRAF (37%-50%) followed by

NRAS (13–25%), *NF1* (12%), *MEK1* (6–7%), *KIT* (2–8%), *CTNNB1* (2-4%), *GNA11* (1%), and *GNAQ* (1%) [34]. In some cases, copy number changes also influence melanoma development and are more common in acral lentiginous melanomas[36]. Specifically, amplification of *AURKA* [37], *GAB2/PAK1* [38, 39], *CCND1* [39, 40], *CDK4* [39, 41] or deletion of *NF1* [39, 42], *CDKN2A* [42] have been found in acral lentiginous melanomas.

Some mutations affect several signaling pathways and induce aberrant signaling and malignant transformation. For example, mutations in the RAS/RAF/MEK/ERK pathway account are frequently mutated in melanoma. The $BRAF^{V600E}$ mutation destabilizes the inactive conformation of BRAF kinase. This leads to continuous downstream signaling of the MAPK pathway, including ERK activation and results in increased cell proliferation and survival [43]. RAS is an upstream regulator of RAF. The RAS proteins are GTPase's including different homologous proteins KRAS, HRAS, and NRAS. RAS can stimulate PI3K and RAF to regulate cell proliferation, survival and differentiation [44, 45]. RAS mutations occur in approximately 30% of all human cancers, and NRAS mutations are the most common RAS mutations in melanoma. NRAS mutation or loss of PTEN can activate the PI3K/AKT/mTOR pathway leading to increased cell proliferation and survival [44-46]. Considering that RAS can affect both RAF and PI3K, NRAS-mutant positive melanoma relies on aberrantly activated RAS/RAF/MEK/ERK and PI3K/Akt pathways to induce malignant transformation [47]. Taken together, melanoma development is influenced by a complex interplay of environmental, physical, and genetic factors.

1.1.3 Melanoma therapy

1.1.3.1 Surgical management

For localized, invasive melanoma, surgery remains the best option. Appropriate surgical management is essential for the diagnosing, staging, and optimal treatment of invasive primary cutaneous melanoma [48]. For the primary localized cutaneous melanoma, wide local excision is the current standard therapy. Mohs micrographic surgery (MMS) is used in the clinic to gradually remove individual layers of cancer

which are then examined under the microscope until all cancer tissue is removed. The advantages of MMS are that this type of surgery removes as little normal tissue as possible and enables tissue preservation [49]. In ill-defined lentigo maligna lesions with 5-year follow-up studies, MMS was found to be superior to traditional surgical excisions [50]. However, MMS is not generally supported for invasive melanoma.

Sentinel lymph node biopsy (SLNB) and lymphatic mapping are the standard approaches for diagnosing whether patients with melanoma have a substantial risk of regional node metastasis. Previous research reported the overall sensitivity rate of SLNB to be 95.3%, 84.5% for the neck basins, 95.3% for the axilla and 99.3% for the groin [51]. A study demonstrated that positive SLNB is the best predictor of recurrence and survival in clinically node-negative cutaneous melanoma [52]. The overall complication rate of sentinel node biopsy is 5%, including sensory nerve injury (0.2%), lymphedema (0.7%), infection (1%) and hematoma/seroma (2%) [53]. Moreover, a meta-analysis study showed the rate of false-negative SLNB in thin melanomas is 12.5% [54]. Another study reported a high false-positive rate of 18-29% in head and neck melanoma [55]. Overall, sentinel node biopsy has a substantial risk of a false-negative/positive sentinel node diagnosis.

Although surgery is not appropriate for metastatic melanoma, for transit or satellite metastases confined to the skin and subcutaneous tissue, the most appropriate management is still complete excision with a small margin [56]. Although in most widespread metastatic disease, complete resection is associated with prolonged survival in up to 40% of cases [57].

1.1.3.2 Radiation therapy for melanoma

Melanoma is considered a relative radioresistant tumor due to its intrinsic capacity to repair sublethal DNA damage [58]. However, several studies suggest that given melanoma's heterogeneity it should not be considered radioresistant [59-62]. Therefore, radiation therapy remains a valid treatment option for melanoma patients.

For patients with lentigo malignant melanoma (LMM), mucosal melanoma, and ocular melanoma, definitive radiation therapy (RT) has been a good primary treatment modality with acceptable cosmetic and functional outcomes [63-68]. The side effects

of radiation treatment are commonly mild and include erythema, telangiectasia, and pigment change [69]. Definitive radiation therapy is considered safe and is generally well-tolerated. For patients with cutaneous melanoma primary lesions, RT is typically offered after surgical excision to reduce the local recurrence rate. For patients with regional nodal metastases, adjuvant RT following lymphadenectomy effectively decreases local and regional recurrence risk. In a retrospective analysis, patients at high risk of regional failure who received adjuvant RT, had a lower 5-year local recurrence rate (10%) compared with patients who did not receive RT (41%) [70]. For patients with advanced-stage and metastatic disease, RT is highly effective for symptom palliation. New RT techniques, such as stereotactic radiosurgery (SRS) and stereotactic body radiation therapy (SBRT) are effective in the treatment of patients with limited metastases [71]. However, the prognosis of patients with more severe disease, including brain metastasis, remains poor after systemic, surgical or radiation therapy.

1.1.3.3 Cytotoxic chemotherapy

In advanced melanoma, chemotherapy is no longer used as a frontline therapy. However, in the progressing melanoma without BRAF, NRAS, or KIT mutations, chemotherapy is the first option after immunotherapy and is used as a common salvage regimen in the clinic.

Commonly used chemotherapeutics include dacarbazine, temozolomide, nitrosoureas, carboplatin and taxanes [72]. Dacarbazine is an alkylating agent used as a standard chemotherapy treatment option for metastatic melanoma patients since its FDA approval in 1975 [72]. Dacarbazine induces DNA adducts and is cytotoxic to cells [73, 74] and has side effects common to many chemotherapeutic agents such as nausea, vomiting, and myelosuppression. Another alkylating agent, temozolomide, was approved by the FDA for the treatment of glioblastoma [75, 76]. Several studies have evaluated the use of temozolomide versus dacarbazine in metastatic melanoma. Side effects of temozolomide include headache, nausea, vomiting, and myelosuppression [77]. As temozolomide can cross the blood-brain barrier [75], it is often considered the better option in treating metastatic brain melanoma [78]. However, in clinical practice there is generally no significant difference between dacarbazine and temozolomide, and

these two agents are similar and interchangeable. The nitrosoureas, such as carmustine (BCNU) and lomustine (CCNU), are also alkylating agents that have been used in the treatment of advanced-stage melanoma. BCNU or CCNU have been shown to provide benefit in treating patients with brain metastases but their use is associated with significant side effects [79]. Carboplatin is cytotoxic to cancer cells by inducing DNA crosslink formation and inhibiting cell replication and transcription. A study investigating the use of carboplatin in a phase II trial of advanced-stage melanoma demonstrated there was 19% response rate (95% CI, 8-38%) [80]. The taxane microtubule inhibitors, paclitaxel and docetaxel, induce dysfunctional mitotic spindle complexes and cell death. Paclitaxel treatment showed partial responses (PR) 12% (95% CI, 3-13%) in chemotherapy-naïve melanoma patients and considerable side effects including neutropenia, alopecia, lower extremity bone pain, and peripheral neuropathy [81]. Docetaxel demonstrated similar activity and side effects in advanced-stage melanoma [82].

Due to the low response rates of single chemotherapy agents, combinations (CVD (cisplatin, vinblastine or vindesine with dacarbazine) or the Dartmouth regimen (carmustine, dacarbazine, cisplation, and tamoxifen)) have been used in the treatment of advanced melanoma. But a number of studies demonstrated similar response rates in CVD and Dartmouth regimens compared with single-agent dacarbazine treatment [83-85]. Moreover, there were no long-term or survival benefits with Dartmouth regimen treatment, but the toxicities were significantly increased [85-88]. These chemotherapeutic combination therapies do not increase response rates significantly but instead increased side effects and toxicities. Overall, dacarbazine is still used as a standard chemotherapy regimen, and the combination therapies would need more evaluation in future trials.

1.1.3.4 Targeted therapy

In cutaneous melanoma, around 70% of patients harbor mutations in genes involved in crucial mitogenic signaling pathways associated with tumor cell proliferation [89]. Therefore, inhibitors specifically targeting members of these pathways are used in the clinical treatment of melanoma. The selective oral BRAF-

mutant inhibitor, vemurafenib, was approved by the FDA in 2011 to treat unresectable or metastatic melanomas with activating $BRAF^{V600E}$ mutations [86, 90]. In $BRAF^{V600E}$ mutated melanoma patients, vemurafenib slowed 90% tumor regression and improved clinical response rates, PFS and OS, compared with chemotherapy [86]. Another selective BRAF-mutant inhibitor, dabrafenib, was approved by the FDA in 2013 [90, 91]. Several clinical trials with single dabrafenib treatment or dabrafenib combined with other targeted inhibitors or dabrafenib combined with radiotherapy are ongoing [92]. Some other inhibitors such MEK (trametinib), CKIT (imatinib), VEGF (bevacizumab), PI3K-AKT-mTOR pathway inhibitors (PI-103, a PI3K inhibitor; rapamycin, mTOR inhibitor), and Cyclin-dependent kinase (CDK) inhibitors (ribociclib) are being explored in melanoma treatment [92].

Although these different types of treatment represent an advancement for melanoma patients, they still face several obstacles. Overcoming the intrinsic and acquired resistance mechanisms, minimizing side effects, increasing response rates, prolonging survival and reducing recurrence pose continuous challenges in the successful treatment of melanoma.

1.1.3.5 Immunotherapy

Within the tumor microenvironment (TME), the interaction between the tumor and the hosts' immune system is complicated. Tumor-infiltrating lymphocytes (TILs) recognize tumor-specific antigens and differentiate to cytotoxic effector $CD8^+$ T cells to clear the tumor cells and improve survival [93, 94]. On the other hand, regulatory T-cells (Treg cells), tumor-associated macrophages (TAMs), and the expression of programmed death-ligand 1 (PD-L1) on tumor and immune cells suppress T cell anti-tumor activity and promote a pro-tumorigenic environment. Cytokines such as interleukin IL-2 and interferons (IFNs) also play an essential role in the TME. IL-2 is a cytokine primarily produced by activated $CD4^+$ T cells and activated $CD8^+$ T cells. FDA approved IL-2 as a treatment in metastatic melanoma in 1998 [95]. Previous studies showed that the partial response of IL-2 was 12.5%, complete response rate 4% and overall response 19.7% [96]. However, IL-2 treatment is associated with many side effects including hypotension, tachycardia, peripheral edema, and cardiac arrhythmias

[97]. IL-2 is still being used in clinical trials in combination with chemotherapy, radiotherapy, targeted therapies, and other immunotherapies [92]. IFNs are cytokines that have antitumor, antiangiogenic, antiproliferative, and anti-viral properties [98-101]. For the resected stage IIB/III melanoma treatment, the FDA approved IFN-α-2b as adjuvant therapy in 1995 [101, 102]. In melanoma, IFN-α stimulates histocompatibility complex class I (MHCI) expression on melanoma and immune cells and inhibits tumor cell proliferation [103]. Adjuvant IFN-α treatment demonstrated significant benefit in reducing the risk of recurrence and improving the survival of melanoma patients [104], but only a small proportion of patients respond to interferon therapy [105]. IFN-α is used as adjuvant therapy with other immunotherapies and targeted therapies [92].

T cell exhaustion in TME is one of the critical features of tumor immune evasion. Programmed cell death protein 1 (PD1) expression on T cells is a marker for T cell exhaustion. Tumor cells and antigen-presenting cells express the PD1 ligand (PD-L1 and PDL-2) which binds to PD1 and suppresses T cells activation and induces T cell exhaustion. Therefore, an anti-PD1 monoclonal antibody, nivolumab, was approved by the FDA to treat metastatic melanoma patients in 2014 [106]. The PD1-PDL1 blockade induces T cell antitumor activity that reduces tumor progression [107]. Another anti-PD1 antibody, pembrolizumab, was approved by the FDA to treat advanced melanoma patients in 2015 as a new treatment for ipilimumab refractory melanoma [108-110]. Several studies have reported nivolumab to be more effective (PFS (progression-free survival), 6.9 months) than chemotherapy (PFS, 2.2 months) or ipilimumab (PFS, 2.9 months) [107]. Pembrolizumab induced less high-grade toxicity than ipilimumab and led to prolonged PFS and OS (overall survival) [108]. Ipilimumab is an anti-CTLA-4 (cytotoxic T-lymphocyte-associated protein 4) monoclonal antibody approved by the FDA for the treatment of advanced melanoma in 2011. CTLA-4 is expressed on T cells and it is an inhibitory receptor when it binds to CD80 or CD86 on the surface of antigen-presenting cells (APCs). Binding of CTLA-4 to CD80 or CD86 suppresses T cell activation and induces immune tolerance [111, 112]. Ipilimumab blocks these inhibitory effects, enhances pro-inflammatory T-cell cytokine production and increases T cell

infiltration in tumors [113, 114]. However, the response rates are still not that high with these immunotherapies.

New immune therapies for refractory melanoma, such as gp100 peptide vaccine therapy, TLR agonist therapy, oncolytic virus therapy, and adoptive T cell therapy (ACT) are currently being explored in clinical trials. Gp100 is a glycoprotein expressed on melanoma cells but not in healthy tissues, which can be recognized by cytotoxic T lymphocytes (CTLs) and then enhance CTLs reactivity [115, 116]. Although gp100 is not effective in a monotherapeutic setting, it is being tested as an adjuvant therapy in clinical trials [115]. Activation of innate immune receptors, the Toll-like receptors (TLRs), induces the IFN-α and IL-12 production to improve local immune responses [117] and enhance antitumor immunity [118]. Previous research showed that a TLR 7/8 agonist, resiquimod, can active myeloid dendritic cells (mDC) (TLR8) and plasmacytoid dendritic cells (pDC) (TLR7) in patients with advanced melanomas [119]. In another experimental study, resiquimod was used as an adjuvant therapy combined with gp100 vaccination in metastases melanoma, induced upregulation of type I IFN and IFNγ, and improved antitumor response [119]. Oncolytic virus (OV) therapy is an engineered nonpathogenic viral strain directly injected specifically into a metastatic melanoma nodule. OVs only replicate in melanoma cells leading to tumor lysis and tumor-specific antigens release. These tumor-specific antigens are recognized by APCs which subsequently activate CTL antitumor responses. The first oncolytic virus for melanoma treatment was approved in 2015 by the FDA as talimogene laherparepvec (T-VEC). T-VEC is a genetically modified herpes simplex virus type 1 used in refractory stage IV or unresectable stage III melanomas. T-VEC is safe and the adverse events are not severe [120]. More clinical trials with T-VEC and other oncolytic viruses are still ongoing. The approach of transferring *ex vivo* expanded and genetically manipulated melanoma-specific T-cells into patients to enhance the antitumor activity is called adoptive cell transfer (ACT) therapy. However, this approach is difficult and time-consuming [121].

Taken together, although there are a number of different therapies available, treating melanoma patients is challenging due to resistance, low response rates and

toxicity especially in combinatorial approaches. For example, due to the poor prognosis of patients with metastatic melanoma, radiation therapy is usually combined with other therapies, such as BRAF inhibitors and immunotherapies. However, BRAF inhibitors have the undesirable side effect of increasing radiation-induced skin toxicities [122-125]. Several studies reported that the combination of SRS and BRAF inhibitors increases survival [126-128]. Hypo-fractionated radiation can induce PD-L1, PD-L2, and CTLA-4 expression [129-131], which can enhance the effect of immunotherapy. However, despite the advantages of combination of RT therapy, the adverse side effects are also increased. The treatment of melanoma is multidisciplinary, and optimal combination strategies and novel therapies need to be further explored.

1.2 Brief introduction of BAFF

The tumor microenvironment (TME) consists of cancer cells, stromal tissue (including vascular tissue, myofibroblasts, fibroblasts, immune cells, and cytokines), and extracellular matrix [132]. The immune cells and cytokines produced within the TME milieu can have important anti-tumoral or pro-tumoral function within TME. The cytotoxic $CD8^+$ T cells can suppress tumors by direct cytotoxic effector functions or by producing IFNγ and IL-2 [133]. $CD8^+$ T cells are influenced by $CD4^+$ T helper 1 (Th1) cells. Th2 cells can support B cell responses by producing IL-4, IL-5, and IL-13. TH17 cells produce IL-17A, IL-17F, IL-21 and IL-22 and promote the anti-microbial tissue inflammation in tumors [133]. Natural killer (NK) cells and natural killer T (NKT) cells are associated with good prognosis, but NK cells' tumor-killing function can be inhibited by TGFß within the TME [133]. B cells can play a dual role in the TME. In some breast and ovarian cancers, B cell infiltration was associated with good prognosis [134, 135]. However B cells demonstrated tumor-promoting functions in the genetic mouse model of skin cancer [136, 137]. Other immune cells, such as tumor-associated macrophages (TAMs), tumor-associated neutrophils (TANs), and dendritic cells (DCs) also have dual role in the TME [138]. While monocytes usually tend to have immunosuppressive functions within the TME [139]. Cytokines also play a very important role in the TME by regulating cancer cells and immune cells and are often

the bridging link between the different populations. In this section, the function of a B cell activating factor (BAFF) will be discussed.

1.2.1 B cell activating factor (BAFF)

B cell activating factor (BAFF, *Tnfsf13b*), a member of the tumor necrosis factor (TNF) family, is a cytokine critical for B cell development and survival [140]. BAFF is produced by myeloid cells [141], malignant B cells [142], activated T cells and bone marrow stromal cells [143]. Transcriptionally, BAFF is positively controlled by IFN regulatory factors (IRFs), such as IRF1 and IRF2. IRF4 and IRF8 negatively regulate BAFF expression [144]. BAFF exerts its biological function through binding with a high affinity to the BAFF receptor (BAFF-R) and the transmembrane activator and CAML interactor (TACI) receptors and with lower affinity to the B cell maturation antigen (BCMA) receptor [145, 146]. Although there is some overlap in signaling between the three receptors, BAFF binding to the different receptors, controls subset specific aspects of B cell development, maintenance, and survival. In addition to B cells, BAFF has also been shown to affect T cells and other innate immune cells.

1.2.2 BAFF effects on B cells

1.2.2.1 Function of BAFF in B cell development

In 1990, Pascal Schneider et al. showed that BAFF stimulated B cell growth and played an essential role as a co-stimulator of B cell proliferation and function [147]. Batten et al. treated splenocytes with BAFF *in vitro* and found BAFF to specifically induce survival of transitional type 2 (T2) B cells and to promote differentiation of T2 B cells into mature B cells. Further experiments in BAFF transgenic (BAFF-Tg) mice, demonstrated that the number of T2 and marginal zone(MZ) B cells were elevated in the spleen [148]. Other research performed in BAFF-deficient mice confirmed that BAFF does indeed play an important role during the T1-T2 transition, and the BAFF deficient mice have decreased numbers of T2, follicular, and MZ B cells [149, 150]. However, the high level of BAFF did not affect the number of B1 cells in lymphoid organs and the peritoneal cavity in BAFF-Tg mice [151, 152]. In BAFF, TACI, BAFF-R and BCMA deficient mice, the number of B1 cells was also found to be normal [149,

150, 153-155]. Overall, these studies showed that systemic BAFF improved survival and differentiation of T2 B cells but not B1 cells.

1.2.2.2 BAFF effects on B cell survival and metabolic fitness

Previous research about BAFF activity on B cell survival was performed by Schneider P et al. in 1999 [147]. Human peripheral blood B cells were cultured with or without soluble BAFF *in vitro*. Results showed that BAFF treated B cells were more viable and BAFF increased immunoglobulin (Ig) secretion along with anti-IgM stimulation. Further evidence demonstrating that BAFF promoted B cell survival *in vivo* in the BAFF-Tg mice model, and all BAFF-Tg mice had B-cell hyperplasia, autoantibody production, and systemic lupus erythematosus (SLE)-like autoimmune phenotype with nephritis symptoms [146, 151, 152]. In BAFF-deficient mice, T2, MZ, and mature B cells were almost completely absent and the amount of circulating Ig was significantly reduced. Furthermore, the T-dependent and independent immune responses were impaired [149, 150]. All these studies indicated that BAFF is significantly important for B cell survival.

Both B-cell receptor (BCR) and BAFF-R signals are important for B cell survival. Lack of BCR on mature B cells leads to B cell death [156, 157]. Similarly, inactivating BAFF or BAFF-R mutations reduce B cell life span and lead to immunodeficiency [145, 146, 149, 150, 158, 159]. BAFF binding to the BAFF-R initiates signaling through the non-canonical NF-κB pathway. Specifically, BAFF binding to the BAFF-R is followed by recruitment of the intracellular adaptor TNF receptor associated factors (TRAF) to the BAFF-R followed by release of the NF-κB-inducing kinase (NIK). NIK phosphorylates IκB kinase alpha which in turn causes the phosphorylation of NF-κB2 precursor protein p100. Once phosphorylated, NF-κB2 p100 is processed to the active p52 form. The active p52 form then initiates transcription of antiapoptotic genes including members of the Bcl-2 family [160, 161]. Signaling through the BAFF-R also activates Akt [162]. Moreover, BAFF-TACI/BAFF-BCMA signaling improve B cell survival and proliferation through canonical NF-κB pathway [162].

Treating mature B cells with BAFF *in vitro* drastically changes the state of B cell metabolism. BAFF increased B cell size, cellular protein content, and mitochondrial

membrane potential. Preincubation of B cells with BAFF accelerated proliferation in response to BCR stimulation compared with BCR only triggered cells. BAFF also upregulated cell cycle progression proteins such as cyclin D and cyclin E, cyclin-dependent kinase 4 (Cdk4), mini-chromosome maintenance protein 2 and 3 (Mcm2 and 3), the proliferation marker Ki-67, and induced phosphorylation of the critical cell cycle controlling retinoblastoma (Rb) protein [163]. Moreover, T. Matsushita, et al. showed BAFF could increase IL-6^+ effector B (Beff) cells but attenuates IL-10^+ regulatory B (Breg) cells in mice while BAFF inhibition attenuates IL-6^+ Beff cells [164]. Taken together, BAFF upregulates several proteins and cytokines on B cells.

1.2.3 BAFF-mediated effects on T cells

1.2.3.1 BAFF production by T cells

Although evidence showing that murine T cells express BAFF is lacking, Huard et al. detected low levels of BAFF transcription in human T cells [165]. Other studies detected intracellular BAFF in blood by flow cytometry and salivary gland samples from active SLE and Sjogren's syndrome patients and found that $CD4^+$ and $CD8^+$ T cells expressed intracellular BAFF which was not detectable in normal control subjects [166, 167]. Yoshimoto et al. induced a robust expression of BAFF on T cells of SLE patients following TCR stimulation with anti-CD3 antibody but not on T cells from healthy controls. This experiment indicated that BAFF expression could be induced in T cells under pathological conditions [168].

1.2.3.2 Effects of BAFF on T cells

Previous research showed that BAFF co-stimulation with anti-CD3 upregulates Bcl-2 expression and drives T cell proliferation in active T cells, indicating that BAFF might function as a survival factor in a similar manner as in B cells [169, 170]. Treatment of mice with recombinant BAFF (rBAFF) increased $CD4^+$ T lymphocytes including memory T cells and effector T cells, but not $CD8^+$ T cells [171]. Interestingly, in an *in vitro* assay, recombinant human BAFF (rhBAFF) decreased human $CD8^+$ T cell apoptosis and promoted survival of $CD8^+$ T cells but did not affect $CD4^+$ T cells [172]. The study by Shanshan et al. cultured splenic T cells with rhBAFF *in vitro* and found

that the T lymphocyte viability was significantly increased as was the production of IL-2, IL-4, IFNγ and TGFß [173]. Collectively, these studies demonstrated BAFF to have a significant positive function on T cell activation and this was T cell subset dependent. For example, in BAFF-Tg mice, elevated BAFF levels exacerbated the severity of Th1-mediated delayed-type hypersensitivity(DTH) responses [169, 174]. However, in a Th2-mediated allergic airway disease model, overexpression of BAFF suppressed Th2-mediated responses and reduced antigen (Ag)-specific T cell proliferation [174]. A possible explanation for this differential effect between Th1 and Th2 responses might be that BAFF-enhanced Th1 responses are B cell dependent, whereas the suppressed Th2 responses are B cell independent [174]. Several studies showed BAFF to promote Th17 cell production, expanded $CD4^{+}CD62L^{low}CD44^{high}$ activated memory T cells, and increased the number of functional $CD4^{+}Foxp3^{+}$ regulatory T cells [151, 174-177]. In BAFF-Tg mice, the constitutive overexpression of BAFF promoted Th17 cell generation *in vitro* and *in vivo* and exacerbated Th17 cell-driven disease [176]. Silencing BAFF gene expression by shRNA suppressed generation of plasma cells and Th17 cells [177].

Mouse T cells express the BAFF receptors, BAFF-R and TACI, but not BCMA [169, 178, 179]. T cells from $BAFF\text{-}R^{-/-}$ mice failed to respond to BAFF, indicating that BAFF provides co-stimulatory signals to T cells via BAFF-R other than TACI [169, 179]. Scapini et al. found that $BAFF\text{-}R^{-/-}$ T cells failed to be activated when transferred to $lyn^{-/-}$ mice, whose myeloid cells overproduce BAFF, indicating that BAFF stimulated T cell activation can occur in a BAFF-R dependent manner [178]. Another study found that rhBAFF promoted the expression of BCMA, TACI, and BAFF-R in mouse T cells *in vitro* and that treatment with TACI-Fc reduced BAFF-induced T cell viability and cytokine production. RhBAFF increased the viability and activation of T cells through the BAFF-BAFFR-PI3K-Akt pathway. Overall, these studies collectively show that BAFF can upregulate BAFF receptor expression on T cells and regulates T cells mainly through the BAFF-R pathway and not the TACI pathway [173]. Taken together, in some contexts, BAFF has been shown to have an immunoregulatory function on T cell responses through the BAFF-BAFFR-PI3K-Akt signaling pathway.

1.2.4 BAFF and other innate immune cells

BAFF is partially produced by myeloid lineage cells such as monocytes, macrophages and DCs [141, 180] but it can also have effects on these cells. BAFF induced DCs activation and maturation through the BAFF-BAFF receptors (mainly TACI) signaling pathways [181, 182]. Further, it was shown the BAFF upregulated costimulatory molecules on DCs, production of inflammatory cytokines and chemokines including IL-1, IL-6, monocyte chemoattractant protein (CCL2), and CCL5 [183]. Moreover, BAFF treated DCs promoted allogeneic $CD4^+$ T cell proliferation. When knockdown BAFF on DCs, cells remain in an immature state and fail to produce the IL6 required to differentiate T helper type17 (Th17) cells [177]. These studies indicate that BAFF can help DCs to recruit immune cells to inflammatory sites and enhance the proinflammatory activity of T cells.

Human monocytic cell lines THP1 and U937 express high level of BAFF and its receptors after PMA stimulation [184] . When THP1 cells were treated with rhBAFF or receptor antibodies, IL-8 expression was increased in a dose-dependent manner. However, when the expression of all three BAFF receptors was blocked by siRNAs, IL-8 expression was suppressed. That study indicated that BAFF can activate THP1 cells through the forward BAFF-BAFF receptor signaling pathway. On the other hand, upon blocking receptor expression, THP1 cells treated with an anti-BAFF antibody still induced the expression of IL-8, inflammatory mediators MMP9, and ICAM-1. These data indicate that both a forward signal through BAFF receptor and a reverse signal through BAFF can induce THP1 cell activation, and then regulate B cells [185] . Production of BAFF in different immune cells and signaling through the different receptors BAFF binds to is illustrated in Graphical Fig. 1.

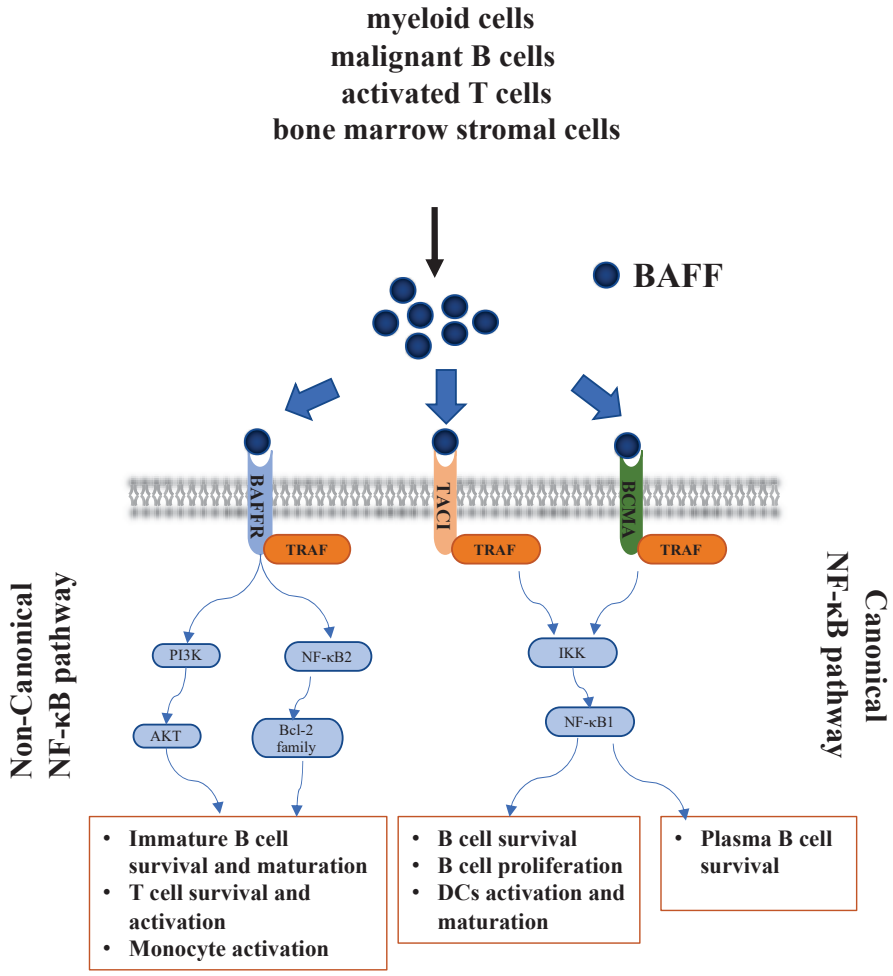

Graphical Fig. 1. Schematic summary of BAFF-mediated receptor signaling pathways. BAFF plays crucial role in the survival, proliferation ad activation of B cells, T cells and other immune cells through BAFF-BAFFR/BAFF-TACI/BAFF-BCMA signaling pathways.

1.2.5 BAFF's role in with autoimmune diseases

BAFF depletion in mice results significant defects in peripheral B cell numbers, antibody responses and maturation of B cells [151, 186, 187]. Conversely, BAFF overexpressing mice have increased peripheral B cell numbers, elevated serum Ig levels and develop autoimmune disease [150, 188]. Increased BAFF levels have been observed in patients suffering from autoimmune diseases particularly lupus erythematosus [189], Sjögren's syndrome [186] and rheumatoid arthritis [190]. Recently, elevated levels of soluble BAFF in multiple sclerosis and systemic lupus erythematosus (SLE) were associated with an insertion-deletion TNFSF13B variant [191]. Higher BAFF levels in patients suffering from autoimmunity have been shown to functionally contribute to the development and maintenance of autoimmune diseases. This has led to the development of anti-BAFF monoclonal antibodies such as Belimumab, already approved for the treatment of SLE [192].

1.2.6 BAFF and cancer

In addition to the recognized role of BAFF in autoimmune diseases, there are reports indicating BAFF to be associated with cancer, particularly in haematological malignancies such as multiple myeloma (MM) and non-Hodgkin's lymphomas where patients have been shown to have elevated serum BAFF levels that negatively correlated with clinical outcome [193, 194]. The above findings are not surprising given that BAFF is a survival factor for normal plasma and B cells and would therefore also sustain the proliferation of malignant B cells. In solid tumors, however, the pathophysiological link between BAFF and cancer is tenuous. While elevated serum BAFF levels were observed in patients with neuroendocrine tumors [195], BAFF expression did not differ between normal and cancerous tissue in breast cancer patients [196]. BAFF serum levels were shown to be higher in patients with pancreatic ductal adenocarcinoma and accompanying in vitro studies demonstrated that BAFF promoted tumor invasion and metastasis [197]. When more specifically considering individual contributions of BAFF–affected immune cells to anti-tumor immunity, BAFF derived from dendritic cells improved antitumor efficacy [198] and loss of BAFF production in

the epithelium led to immune-surveillance tumor escape in the depletion of prostate-associated lymphocytes [199]. Importantly, Yarchoan et al. have shown that *in vitro* BAFF treatment upregulated multiple B cell co-stimulatory molecules, and when administered systemically at high doses in tumor-bearing mice, had multiple immunoregulatory functions [200]. Specifically, in the spleen, B cells and $FOXP3^+$ T regulatory cells (Tregs) accumulated. Within the tumor microenvironment (TME), Th1-associated T-Bet^+CD8^+ T cells and $FOXP3^+$ Tregs were increased [200]. Taken together, BAFF is an important emerging cytokine involved in anti-tumor immunity. While the role of BAFF in hematological malignancies may be better established, less can be conclusively ascertained about its prognostic or functional role in solid tumors although it is clear that BAFF is an important emerging cytokine involved in anti-tumor immunity.

1.3 Aim of this thesis research

Novel anti-melanoma therapeutic options are urgently needed. The application of drugs used for alternate diseases as novel anti-cancer therapeutics, known as drug repositioning, has been successfully implemented before in the clinical setting. These compounds can be a rich potential source of novel, readily available anti-cancer therapeutics. Therefore, in the first section of this thesis, we conducted a pharmacologic screen composed of the NIH Clinical Collection (NCC) of 770 small molecules, FDA-approved, or previously used in human clinical trials to identify novel anti-melanoma agents. Each molecule was screened in the murine B16F10 cell line and its half maximal inhibitory concentrations (IC50) would be determined. The anti-tumoral mechanism of candidate molecules were characterized *in vitro* and *in vivo*.

In addition to the screening of new molecules for melanoma treatment, more detailed studies of cytokines on the tumor microenvironment are also imminent. BAFF is well known in autoimmune diseases, but its function in TME is unclear. In the second section of this thesis, we generated BAFF-overexpressing (BAFF) murine cell lines to specifically examine the effects of local BAFF within the TME. We investigated BAFF's ability to impact primary tumor growth using murine knockout models and

depletion antibodies and found that intra-tumoral BAFF critically affects the number of tumor infiltrating monocytes and their immunosuppressive phenotype. The thesis overview is illustrated in Graphical Fig. 2.

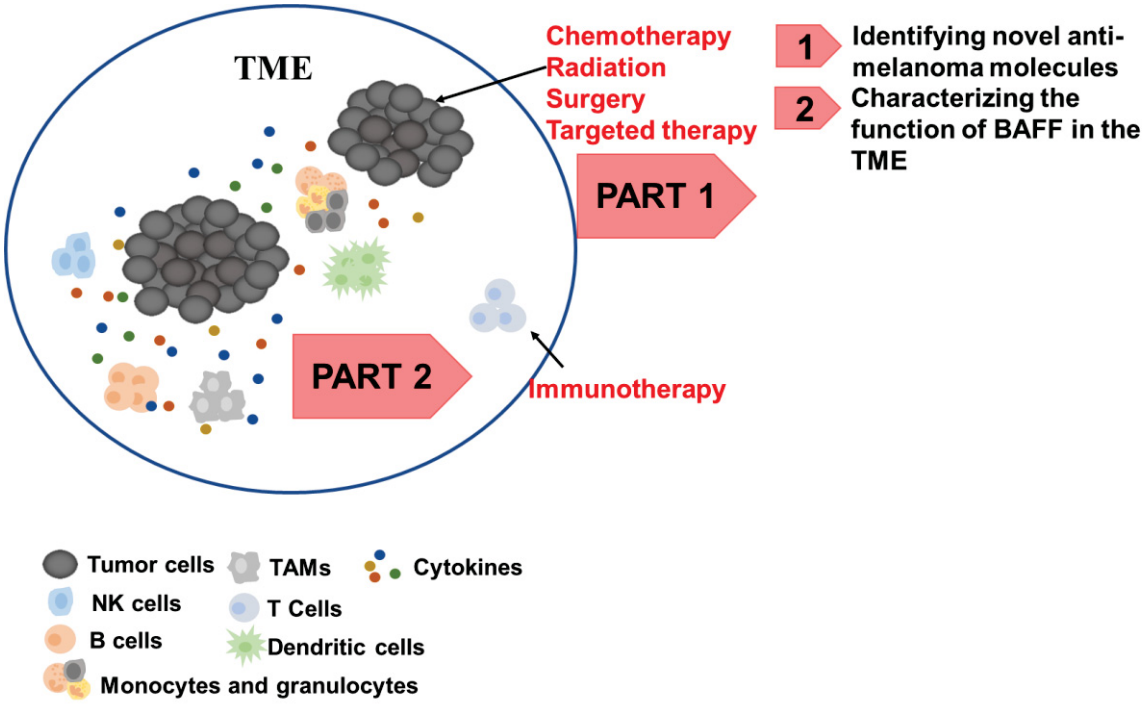

Graphical Fig. 2. Structural overview of the thesis. PART 1 explores the first aim of identifying novel anti-melanoma molecules; PART2 describes the second aim of characterizing the function of BAFF in the tumor microenvironment. TME: tumor microenvironment; TAMs: tumor-associated macrophages.

2 Materials and methods

2.1 Anti-tumor effect of small molecules in melanoma [201]

2.1.1 Cell culture and compounds

B16.F10, A375, SH4, RPMI-7951 and SK-MEL-24 melanoma cell lines were purchased from ATCC. MeWo and MEL-JUSO cell lines were kindly provided by Dr. A. Roesh (Universitätsklinikum Essen, Essen, Germany). The MEL-JUSO and MeWo cell lines were both originally purchased from ATCC. B16.F10 murine cells, A375 and SH4 human malignant melanoma cell lines were maintained Dulbecco Modified Eagle's Medium (DMEM). Human RPMI-7951 malignant melanoma cells were maintained in Eagle's MEM. SK-MEL-24 were maintained in Eagle in Earle's BSS with non-essential amino acids. MeWo and MEL-JUSO cell lines were maintained in Roswell Park Memorial Institute (RPMI) medium. All media were supplemented with 10% FCS (15% for SK-MEL-24) and penicillin streptomycin. Cells were incubated at 37°C in 5% CO_2, and all cell lines were routinely confirmed to be mycoplasma-free (MycoAlert Mycoplasma Detection Kit, Lonza). The NIH Clinical Collection (NCC) composed of 770 small molecules mainly dissolved in DMSO at a concentration of 10 μM was obtained from the NIH, Tegaserod (Sigma) was dissolved in DMSO, serotonin (Sigma) was dissolved in water. MK-2206, ZSTK474, KU-0063794, Vemurafenib, Cobimetinib (Selleckchem) were dissolved in DMSO.

2.1.2 MTT assays

For the MTT colorimetric assay, cells were seeded in 96 well plates and viability was assessed following addition of the MTT (Sigma) reagent. Half-maximal inhibitory concentrations (IC50) values were computed from dose–response curves using Prism (v5.0, GraphPad Software).

2.1.3 Flow cytometry

For Annexin V/7AAD apoptosis assays, trypsinized cells were washed and stained in Annexin V binding buffer (BD Biosciences). Melanoma cells were treated at doses of 2 × – 4 × IC50 values for TM and 2 × IC50 for PI3K/Akt/mTOR inhibitors. Tumors

were excised, weighed, crushed, strained through a 40 μm filter and re-suspended in FACS buffer (PBS, 1% FCS, 5 mM EDTA) and surface stained with anti-Ly-6G, Ly6C, CD8, CD3, NK1.1, CD11b, CD45.2, CD4, CD25, KLRG1, PD1 and CD95 (eBioscience). Staining of $CD4^+$ cells for FOXP3, RORγt and GATA3 and of $CD8^+$ cells for Granzyme B, perforin and IFNγ were performed using the Foxp3 mouse Treg cell staining buffer kit (eBioscience). Cells were analyzed using FACS (FACS Fortessa, BD Biosciences).

2.1.4 Immunofluorescence

For TUNEL staining, cells were seeded on cover slips, treated and 48 hours later fixed by 4% formaldehyde in PBS for 30 min, permeabilized with 0.1% Triton X-100, 0.1% sodium citrate in PBS for 2 min and stained using the TUNEL staining kit as per manufacturer's protocol (Roche). For p-S6 staining, cells seeded on cover slips were stained with primary anti-p-S6 antibody (Ser 235/6, Cell Signaling) overnight, followed by incubation with secondary anti-Rabbit IgG Cy3 conjugate antibody. Cover slips were incubated with DAPI in PBS for 30 min. Images were taken with an Axiocam 503 color microscope (ZEISS).

2.1.5 Immunoblotting

Cells were lysed using boiling hot SDS lysis buffer (1.1% SDS, 11% glycerol, 0.1 mol/L Tris, pH 6.8) with 10% β-mercaptoethanol. Tumor tissue was crushed using a tissue lyser (TissueLyser II, QIAGEN) and cells were gently lysed using Triton X-100. Blots were probed with anti-α-tubulin (Merck), anti-HTR4 (ThermoFischer), anti-cleaved Caspase 8, anti-Akt, anti-p-Akt (Ser 473), anti-S6, anti-p-S6 (Ser235/6, Ser240/4), anti-p70 S6, anti-p-p70 S6 (Thr421/Ser424), anti-p-ERK1/2, anti-ERK1/2, anti-p-CREB (Ser133) and anti-CREB (all from Cell Signaling) and detected using the Odyssey infrared imaging system (Odyssey Fc, LI-COR Biosciences). Immunoblots were quantified using ImageJ.

2.1.6 Combination index (CI) determination

Synergy between TM and Vemurafenib, and Cobimetinib was evaluated by calculating the CI [202]. Dose–response curves were generated for TM, Vemurafenib

and Cobimetinib alone and each drug in combination with TM at a constant ratio following compound exposure for 72 hours. Viability was assessed by the MTT assay. CompuSyn software was used to evaluate synergy using the median-effect model.

2.1.7 Histology

Histological analysis was performed on snap-frozen tissue. Briefly, snap-frozen tissue sections fixed in acetone, blocked with 10% FCS and stained with anti-active Caspase 3 (BD Biosciences), cleaved Caspase 8 (Cell Signaling). For p-S6 (Cell Signaling) staining, snap-frozen tissue sections were fixed in 10% neutral buffered formalin and blocked with 5% FCS/ 0.3% Triton X-100 in PBS. Images were taken with an Axiocam 503 color microscope (ZEISS) and quantified using Image J. For conventional immunohistochemistry tumor slides, IHC profiler Image J plugin was used and used as previously described in detail[203].

2.1.8 Serum biochemistry

Aspartate aminotransferase (AST), alanine aminotransferase (ALT) and L-Lactatdehydrogenase (LDH) were measured using the automated biochemical analyser Spotchem EZ SP-4430 (Arkray, Amstelveen, Netherlands) and the Spotchem EZ Reagent Strips Liver-1.

2.1.9 Quantitative RT-PCR

RNA was isolated using Trizol (Invitrogen) and RT-PCR analyses were performed using the iTaq™ Universal SYBR® GreenOne-Step RT-qPCR Kit (Biorad) according to the manufacturer's instructions. For analysis, expression levels were normalized to *GADPH.*

2.1.10 Intracellular CAMP assay

Intracellular CAMP levels were determined as per manfacturer's instructions (Enzo Life Biosciences).

2.1.11 Mice and *in vivo* treatments

C57BL/6J mice were maintained under specific pathogen-free conditions. 7-9 weeks old C57BL/6J mice were subcutaneously injected with 5×10^5 B16.F10 cells. 7

days post injection, when tumor volume reached approximately 50 mm^3, mice were randomized and treated daily for 5 consecutive days with Tegaserod or vehicle control (2.5% DMSO in PBS). Tegaserod and vehicle were administered intraperitoneally (i.p.). Tumors were measured using calipers and tumor volume was calculated using the following formula: (tumor length × $width^2$)/2. Experiments were performed under the authorization of LANUV (No.: 84-02.04.2016.A424; No.: 81-02.04.2018.A253; No.: 81-02.04.2019.A416; No.: 81-02.04.2020.A305) in accordance with German law for animal protection. Organ removal from mice is allowed under the O42/11 project which issued by ZETT (*Zentrale Einrichtung für Tierforschung und wissenschaftliche Tierschutzaufgaben*) in Heinrich Heine University Düsseldorf.

2.1.12 Data mining using the CCLE

RNA-Seq expression data (Affymetrix U133+2 arrays) from the Cancer Cell Line Encyclopedia (CCLE) [204] (Broad Institute and Genomics Institute of the Novartis Research Foundation) for the selected human melanoma cell lines was analyzed using Xena Functional Genomics Explorer [205] and visualized using the MORPHEUS matrix visualization software (https://software.broadinstitute.org/morpheus).

2.1.13 Statistical analyses

Data are expressed as mean ± S.E.M. Statistically significant differences between two groups were determined using the student's t-test and between three or more groups, the two-way ANOVA was used with a post-hoc test. Values of $P < 0.05$ were considered statistically significant. Statistical tests were carried out using Graph Pad Prism (version 6.0g)

2.2 Function of BAFF in melanoma

2.2.1 Cell culture

HEK293TV and B16.F10.gp33 (B16.gp33) (provided by Dr. H.P. Pircher, Freiburg) murine cell lines were maintained Dulbecco Modified Eagle's Medium (DMEM) supplemented with 10% FCS (GIBCO), 2 mM L-glutamin, and 100 U/ml penicillin-streptomycin and in the case of B16.gp33 with 200 µg/ml of Geneticin (Sigma). RMA/S, RMA cells were maintained in RPMI1640 supplemented with 10% FCS, 2 mM L-glutamine, 100 U/ml penicillin-streptomycin and 0.05 mM β-mercaptoethanol (Sigma).

2.2.2 Mice

Jht$^{-/-}$, *Cd8*$^{-/-}$, *Ifng*$^{-/-}$ and *Baffr*$^{-/-}$ mice were bred in a C57BL/6 background and maintained under specific pathogen-free conditions. Mice were maintained under specific pathogen-free conditions and experiments were performed under the authorization of LANUV, the same protocol as *Part 2.1.11*. 7–9-week-old C57BL/6J mice were subcutaneously injected with 5×10^5 B16.BAFF or B16.Control cells. Tumors were measured using calipers and tumor volume was calculated using the following formula: (tumor length × width^2)/2.

2.2.3 Cell depletions and blocking antibodies

NK cells were depleted with intravenous (*i.v.*) injections of anti-NK1.1 antibody (clone PK136) as previously described [206]. Monocytes were depleted using the anti-CCR2 antibody (clone MC-21) [207] and used with a Rat IgG2b isotype control (BioXCell, clone BE0090). 200 µg of murine anti-PD-L1 (Bioxcell, clone 10F.9G2) antibody or Rat IgG2b isotype control was injected every three days starting at day 0 post tumor injection for 5 times.

2.2.4 Histology

Histological analysis was performed on snap frozen tissue. Snap-frozen tissue sections fixed in acetone, blocked with 10% FCS and stained with anti-active Caspase 3 (BD Biosciences), anti-cleaved Caspase 8 (Cell Signaling), anti-PD-L1, anti-F4/80,

anti-Ly6C, anti-Ly6G (all from eBioscience) and anti-BAFF (R&D) antibodies. The same protocol as *Part 2.1.7*.

2.2.5 Flow cytometry

Tumors lysis and stained with anti-Ly-6G, Ly6C, CD8, CD3, NK1.1, CD11b, CD45.2, CD4, F4/80, KLRG1, ILR7, PD1, PD-L1, BAFFr and CD19 (eBioscience) are the same as *Part 2.1.3*. For tetramer staining, single suspended tumor cells were incubated with tetramer-gp33 (CD8) for 15 min, at 37°C. After incubation, surface antibodies anti-CD8 (eBioscience) were added for 30min at 4°C. For intracellular cytokine staining and re-stimulation, single suspended cells were stimulated with LCMV specific peptide gp33 for 1 hour after which Bredeldin A (eBiocience) was added for another 5 hours incubation at 37°C followed by anti-CD8 surface marker staining, fixation, permeabilization the Foxp3 mouse Treg cell staining buffer kit (eBiosciences) followed by staining with anti-IFNγ and anti-Granzyme B antibodies (eBiosciences). Annexin V/7AAD apoptosis assays are the same as *Part 2.1.3*. Experiments were performed using a FACS Fortessa and analyzed with FlowJo software.

2.2.6 NK cytotoxicity assays

NK cell cytotoxicity assays were carried out as previously described [208]. In addition to NK cells, 10^4 tumor-sorted monocytes were also co-cultured with RMA/S cells. For the BAFF treated NK cell killing assay, 250 ng/ml of recombinant mouse BAFF protein were used (BioLegend).

2.2.7 Immunoblotting

Cells were lysed as same as *Part 2.1.5*. Blots were probed with anti-actin (Merck), anti-Myc (Cell Signaling) and detected using the Odyssey infrared imaging system (Odyssey Fc, LI-COR Biosciences).

2.2.8 ELISA

IFN-γ and the TGFβ1 ELISA kits were purchased from eBioscience. The murine and human BAFF ELISA kit was purchased from R&D. All experiments were performed according to the manufacturers' instructions.

2.2.9 Quantitative RT-PCR

RNA isolation and RT-PCR analyses were performed using the same protocol as *Part 2.1.9*. For analysis, expression levels were normalized to *GADPH*.

2.2.10 Lentiviral transduction and cell line generation

Lentiviral particles were generated by calcium phosphate transfection of sub-confluent (50–60%) HEK293TV cells with 10 μg of BAFF or GFP expression plasmid constructs (BAFF pLenti-C-Myc-DDK and the pLenti-C-Myc-DDK-P2A-Puro tagged open reading frame (ORF) clones (Origene)), and 5 μg each of pMDG1.vsvg, pRSV-Rev and pMDLg/pRRE packaging plasmid constructs. Lentiviral particles were collected 24 and 48 hours later, filtered through a 0.45 μm filter and stored at −80°C. Control cell lines were infected with lentiviral particles. Monoclonal cell population were generated through clonal dilution. Poly-clonal populations were puromycin selected (1.5 μg/ml of puromycin) and maintained in puromycin throughout passaging.

2.2.11 RNA sequencing and gene set analysis

RNA was isolated using Trizol (Thermo Scientific, Germany) and 500 ng total RNA was processed using the TruSeq RNA Sample Preparation v2 Kit (low-throughput protocol; Illumina, San Diego, USA) to prepare the barcoded libraries. Libraries were validated and quantified using DNA 1000 and high-sensitivity chips on a Bioanalyzer (Agilent, Boeblingen, Germany); 7.5 pM denatured libraries were used as input into cBot (Illumina), followed by deep sequencing using HiSeq 2500 (Illumina) for 101 cycles, with an additional seven cycles for index reading. Fastq files were imported into Partek Flow (Partek Incorporated, Missouri, USA). Quality analysis and quality control were performed on all reads to assess read quality and to determine the amount of trimming required (both ends: 13 bases 5′and 1 base 3′). Trimmed reads were aligned against the mm10 genome using the STAR v2.4.1d aligner. Unaligned reads were further processed using Bowtie 2 v2.2.5 aligner. Aligned reads were combined before

quantifying the expression against the ENSEMBL (release 95) database by the Partek Expectation-Maximization algorithm using the counts per million normalization. Genes with missing values and with a mean expression less than one were filtered out. Finally, statistical gene set analysis was performed using a t-test to determine differential expression at the gene level ($p<0.05$, fold change ±2). Partek flow default settings were used in all analyses. Principal Component Analysis was performed using all genes using Covariance scaling and first three components.

2.2.12 Pathway analysis

GeneSet Enrichment Analysis (GSEA) was performed using the t-value from the t-test comparing BAFF vs Control tumors. Mouse gene sets were comprised of curated pathways from several databases including GO, Reactome, KEGG (August 01, 2018 version; http://download.baderlab.org/EM_Genesets/current_release/). Data was processed and visualized by using Cytoscape (www.cytoscape.org; $p\leq0.002$, $q\leq0.07$, similarity cutoff 0.5). Data was auto-annotated and visualized as clusters which were manually annotated. Heatmap visualization and unsupervised hierarchical clustering was performed using all significant, differentially regulated genes from a cluster of interested after normalizing mean expression to 0 with a standard deviation of 1 and using Pearson's dissimilarity algorithm and average linkage in Partek Genomics Suite (Partek Incorporated). Ingenuity pathway analysis (IPA, Qiagen) was conducted using genes with significant differential expression ($p\leq0.05$ and fold change ±2). The significance cut-off for IPA was set to $p\leq0.05$ and z score of ±1.5 for upstream regulators. Additionally, for upstream regulators we filtered out biological drugs, all chemical and miRNA entries.

2.2.13 Statistical analyses

The same as *Part 2.1.13*.

3 Results

3.1 Anti-tumor effect of small molecules in melanoma [201]

3.1.1 A screen of pharmacologically active drugs identifies Tegaserod (TM) as having anti-melanoma activity.

To identify drugs with novel anti-melanoma activities using an unbiased approach, we tested the NIH Clinical Collection (NCC) composed of 770 small molecules against the murine B16.F10 melanoma cell line. A murine cell line was chosen with the intent of testing sensitivity in an *in vivo* immune-competent syngeneic model where immune cell-host interactions could also be evaluated. B16.F10 cells were exposed to a concentration range (10 μM-78 nM) for 72 hours and the IC50 values for each compound were determined by assessing cell viability at each dose using the MTT assay (Fig. 1). From the compounds with determinable IC50 values, many had IC50 values in the low micromolar range (< 2 μM) that could be subdivided into broad pharmacological and/or functional classes (Fig. 2A). Positive hits included members of the statin, antifungal and anthelmintics categories, most of which are already being pre-clinically evaluated as therapeutics in melanoma or other cancers [209-211]. Others, belonging to the microtubule disruptors, antimetabolite and topoisomerase inhibitors are already in use as anti-cancer agents [212]. Secondary screening validation focused on compounds in the serotonin signaling categories. Tegaserod (TM), a serotonin agonist had IC50 values in the low micromolar ranges in B16.F10 cells as well as several human malignant melanoma cell lines (Fig. 2B). The chosen melanoma cell lines have both wildtype (WT) and mutated BRAF. Specifically, the A375, SH4 and RPMI-7951 (RPMI) and SK-MEL-24 harbor the $BRAF^{V600E}$ mutation while the B16.F10 murine cells and the human MeWo and MEL-JUSO cell lines are BRAF WT. As the MTT assay is only an indirect indicator of cell viability, we next assessed whether TM is capable of inducing apoptosis. There was a significant time and dose-dependent increase in apoptosis in all cell lines tested as determined by measuring Annexin V and 7AAD staining following treatment with TM (Fig. 2C).

To further verify and characterize cell death observed following treatment of melanoma cells with TM, we assessed apoptosis using TUNEL staining in two representative $BRAF^{V600E}$ and BRAF WT melanoma cell lines, RPMI and B16.F10 cell lines, respectively. Treatment with TM induced an increase in TUNEL staining relative to untreated controls (Fig. 2D). Taken together, we have identified a compound with previously unknown anti-melanoma activity that induces apoptosis in melanoma cell lines.

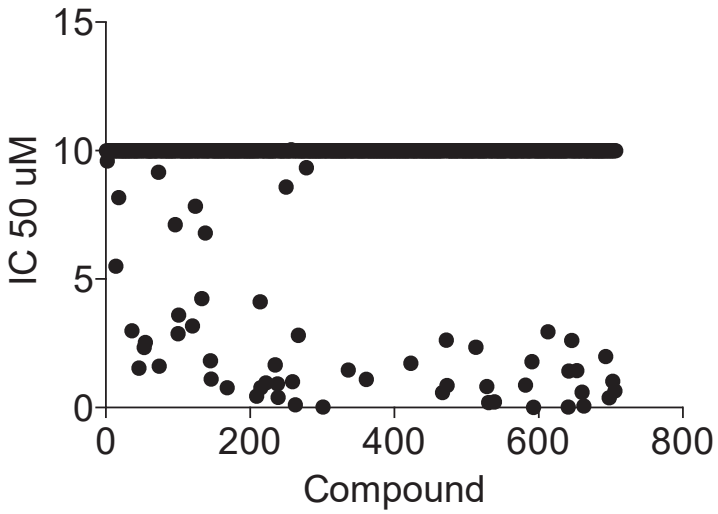

Fig. 1. **A pharmacological screen of active compounds was carried out in the B16.F10 murine melanoma cell line.** B16.F10 cells were exposed to a concentration range (10 μM- 78 nM) of the pharmacologically active compounds for 72 hours and the IC values were determined using the MTT assay. Compounds for which IC50 values were not determinable because the concentration used were too low to induce anti-proliferative effects or were above 10 μM were placed on the 10 μM line.

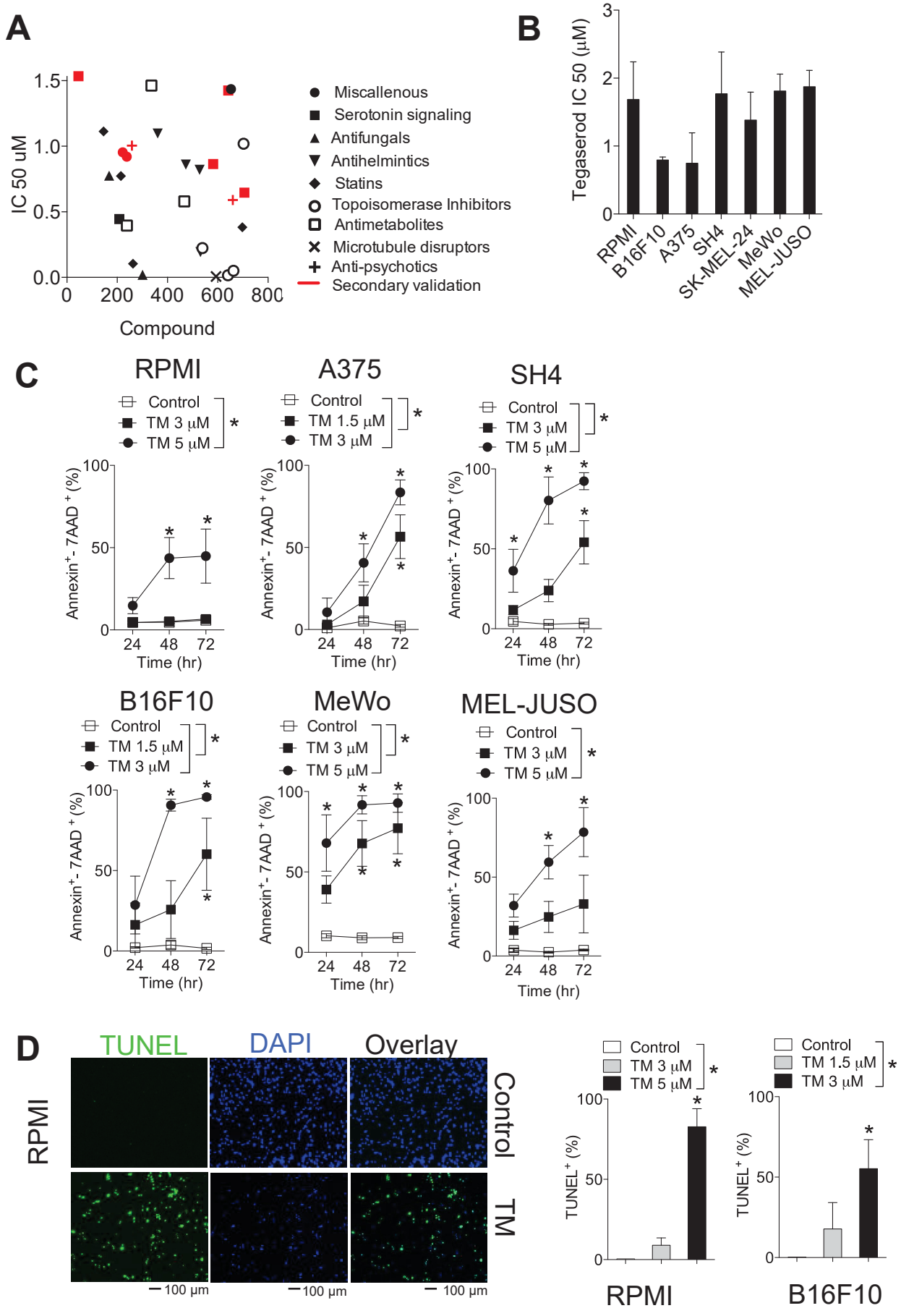
A
IC 50 uM
Compound
Miscallenous
Serotonin signaling
Antifungals
Antihelmintics
Statins
Topoisomerase Inhibitors
Antimetabolites
Microtubule disruptors
Anti-psychotics
Secondary validation
B
Tegaserod IC 50 (μM)
RPMI
B16F10
A375
SH4
SK-MEL-24
MeWo
MEL-JUSO
C
RPMI
A375
SH4
B16F10
MeWo
MEL-JUSO
Control
TM 3 μM
TM 5 μM
TM 1.5 μM
Annexin+- 7AAD+ (%)
Time (hr)
D
TUNEL
DAPI
Overlay
RPMI
Control
TM
100 μm
TUNEL+ (%)
B16F10

Fig. 2. A pharmacological screen identifies Tegaserod (TM) as having anti-melanoma activity. (A) B16.F10 murine melanoma cells were treated with 770 pharmacologically active compounds at a concentration range of 10 μM-78 nM. Several classes of compounds had anti-cancer activity with IC50 values in the low micromolar range as assessed by MTT assay following 72 hours of exposure. (B) Tageserod (TM), a serotonin agonist, was further validated and found to have anti-cancer effects in the B16.F10 cell line and a panel of human malignant melanoma cell lines, A375, RPMI-7951 (RPMI), SH4, SK-MEL-24, MeWo and MEL-JUSO (n = 3-6). (C) Treatment with low micromolar doses of TM induced apoptosis in a time and dose-dependent manner as assessed by Annexin V/7AAD staining (n = 3-6). Percent apoptosis was ascertained by summing up the Annexin $V^+/7AAD^-$ and Annexin $V^+/7AAD^+$ populations. *$P < 0.05$ as determined by a two-way ANOVA with a Dunnett's post-hoc test. (D, left panel) Immunofluorescent TUNEL staining of RPMI cells 48 hours post TM (5 μM) treatment is shown (A representative image of n = 3-5 is shown). *$P < 0.05$ as determined by a one-way ANOVA with a Dunnett's post-hoc test. Scale bar indicates 100 μm. (D, right panel) Quantification of the TUNEL apoptosis staining is shown (n = 3-5). Error bars in all experiments indicate SEM.

3.1.2 Tegaserod (TM) exerts its anti-cancer effects independently of serotonin signaling.

We wondered whether melanoma cancer cell lines express serotonin receptors 5-HTRs. We mined expression data from the Cancer Cell Line Encyclopedia (CCLE) [204] and found that some receptors particularly HTR7 have a high expression relative to the others in the human melanoma cell lines used in our system (Fig. 3A). TM was synthesized with the primary intent of functioning as a 5-HTR4 agonist [213]. HTR4 mRNA was weakly detected (not detectable in the MeWo cell line) but HTR4 protein expression was undetectable in all melanoma cell lines tested (Fig. 3B).

The main transduction mechanisms of the G-coupled 5-HTR1 and 5-HTR4-7's occur through modulation of cAMP levels [214]. We therefore wondered whether TM alters cAMP levels in melanoma cell lines. Treatment of melanoma cell lines with TM did not alter cAMP levels (Fig. 4A). The expression of genes that have been previously shown to be upregulated upon serotonin (5-HT) treatment through PKA signaling, *PDE2A, MET, TREM1, THBS1, SERPINB2,* and *S1PR1* [215] was not changed following TM treatment (Fig. 4B). As expected, with the lack of change in cAMP levels, there was no significant increase in the phosphorylation of cAMP response element binding protein (CREB) in RPMI, B16.F10, A375, SK-MEL-24, MeWo cells, although p-CREB was increased in SH4 and MEL-JUSO cells (Fig. 5A). To further address the question of whether serotonin agonist signaling is responsible for the apoptotic phenotype, we treated melanoma cancer cells with a wide range (100 μM-0.4 μM) of 5-HT. Treatment with 5-HT had little effect on the melanoma cells (Fig. 5B) and co-treatment of 5-HT with TM had no effect on apoptosis induced by TM (Fig. 5C). Taken together, the anti-melanoma effects caused by TM are likely not being mediated through 5-HTR4 signaling.

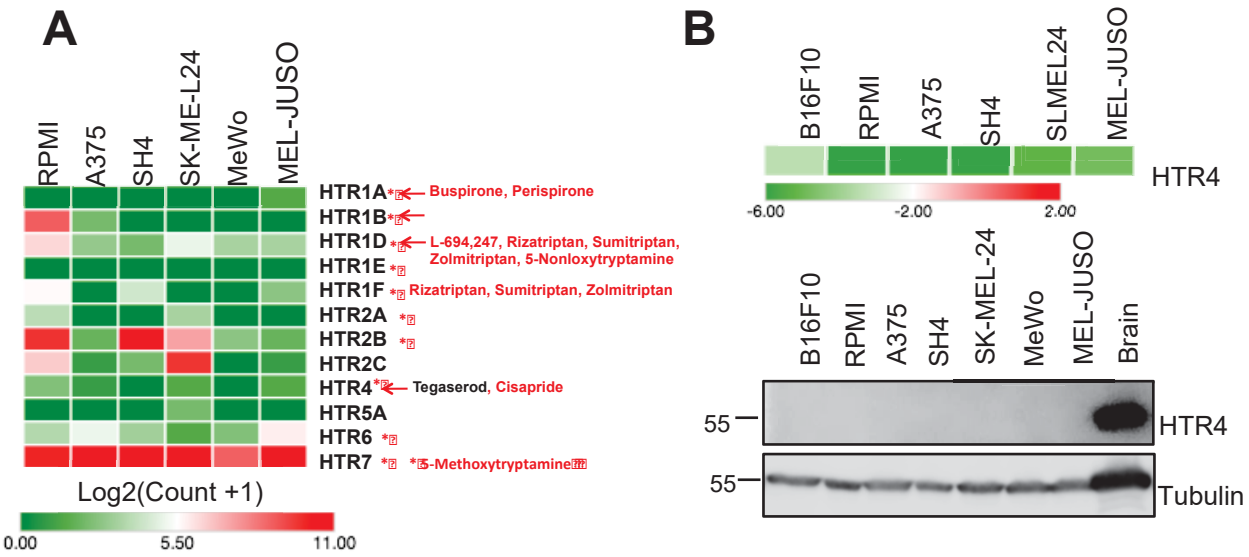

Fig. 3. Low expression of serotonin receptors in melanoma cell lines. (A) Expression of the different serotonin receptors (5-HTRs) in our panel of human melanoma cell lines. Data was mined from the Cancer Cell Line Encyclopedia. (B, upper panel) mRNA expression of 5-HTR4 which is targeted by TM is shown. Expression values are represented as Log10 (CT*HTR4*- CT*GAPDH*) and visualized through Morpheus software (Broad Institute) (n = 3-5). (B, lower panel) Protein expression of HTR4 in melanoma cell lines is shown using mouse brain as a positive control (A representative immunoblot of n = 3 is shown).

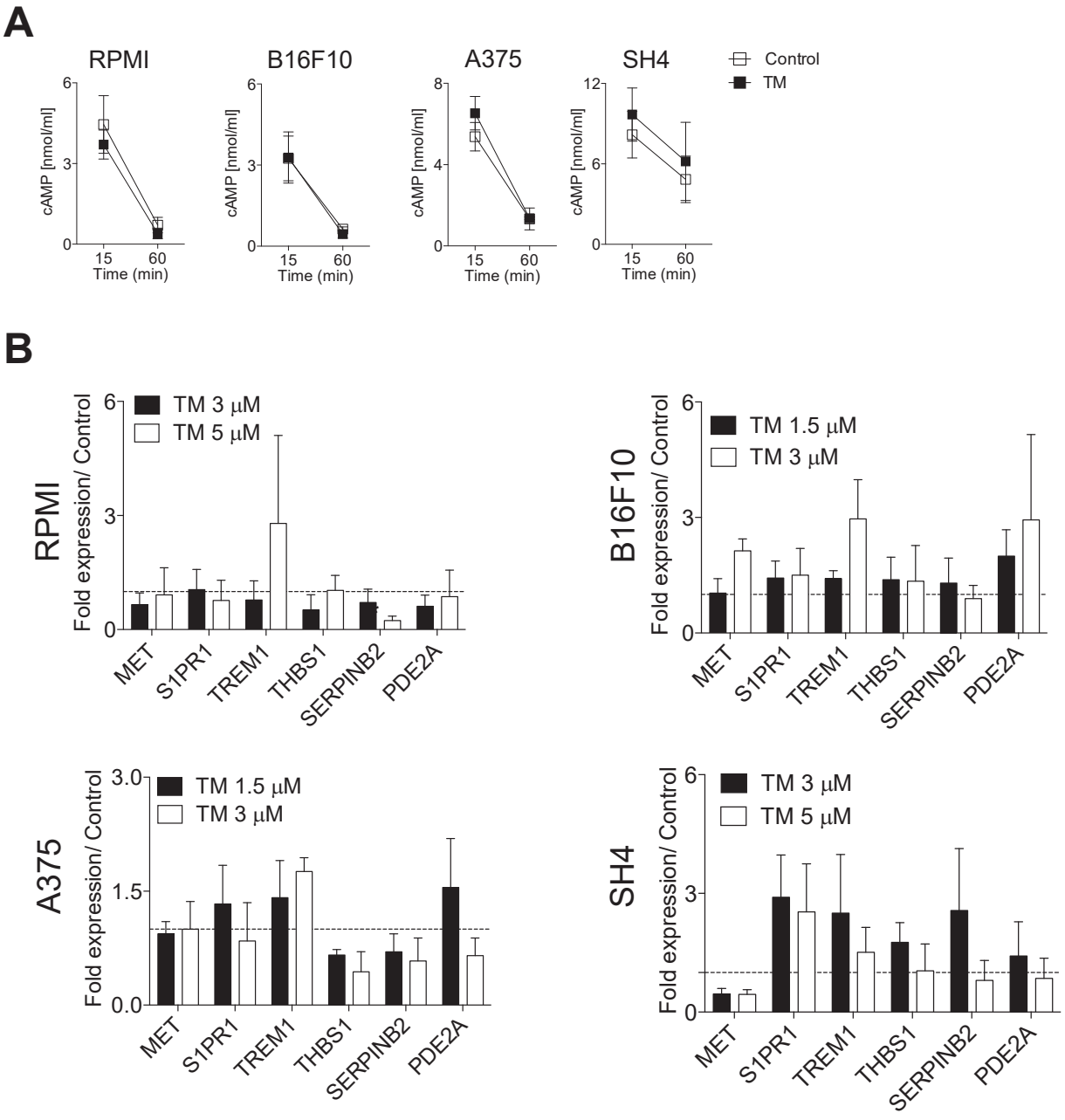
A
RPMI
B16F10
A375
SH4
Control
TM
cAMP [nmol/ml]
Time (min)
B
RPMI
B16F10
A375
SH4
Fold expression/ Control
TM 3 μM
TM 5 μM
TM 1.5 μM
TM 3 μM
MET
S1PR1
TREM1
THBS1
SERPINB2
PDE2A

Fig. 4. **TM did not alter the expression of genes known to be upregulated in response to serotonin treatment.** (A) Treatment at the indicated time points with TM (3 μM for B16F10 and A375 and 5 μM for RPMI and SH4) did not induce changes in cAMP levels in melanoma cell lines (n = 3). *P < 0.05 as determined by a Student´s t-test (unpaired, 2 tailed). (B) Treatment with TM for 18 hours did not induce changes in *MET, S1PR1, TREM1, TREM1, THBS1, SERP1B2* and *PDE2A.* Expression was normalized to *GAPDH* (n = 3-4). *P < 0.05 as determined by a one-way ANOVA with a Dunnett's post-hoc test. Error bars in all experiments indicate SEM.

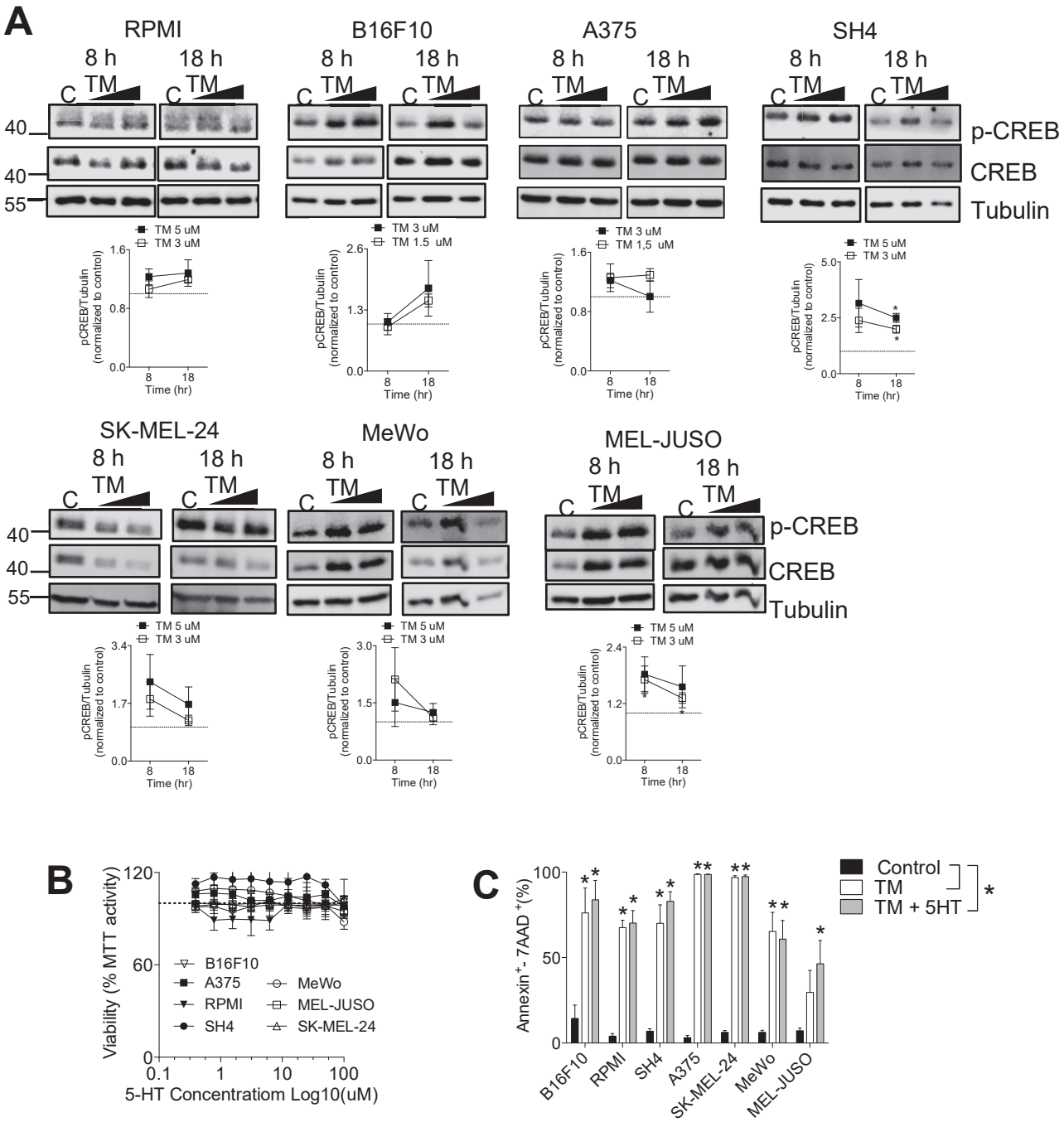
A
RPMI
B16F10
A375
SH4
SK-MEL-24
MeWo
MEL-JUSO
8 h
18 h
C
TM
40
40
55
p-CREB
CREB
Tubulin
TM 5 uM
TM 3 uM
TM 1,5 uM
pCREB/Tubulin (normalized to control)
Time (hr)

B
Viability (% MTT activity)
B16F10
A375
RPMI
SH4
MeWo
MEL-JUSO
SK-MEL-24
5-HT Concentratiom Log10(uM)

C
Annexin+- 7AAD +(%)
Control
TM
TM + 5HT
B16F10
RPMI
SH4
A375
SK-MEL-24
MeWo
MEL-JUSO

Fig. 5. TM induces apoptosis independently of serotonin signaling. (A) (A, upper panel) Changes in phosphorylation of the transcription factor CREB 8 and 18 hours post TM treatment are shown (A representative immunoblot of n = 3-4 is shown). Quantification of immunoblots is shown in A (lower panel). (B) Treatment with serotonin (5-HT) for 72 hours did not have anti-proliferative effects in melanoma cells (n = 3-4). (C) Co-treatment of TM (3 μM for B16.F10 and A375 and 5 μM for RPMI, SH4, MeWo and MelJuso melanoma cells) with serotonin (5-HT, 100 μM) did not impact the anti-melanoma effects of TM and did not alter TM induced apoptosis as assessed 72 hours post treatment using the Annexin V/7AAD assay (n = 3-6). Error bars in the all experiments indicate SEM; *P < 0.05 as determined by a Student´s t-test (unpaired, 2 tailed), or a one-way ANOVA with a Dunnett's post-hoc test.

3.1.3 Tegaserod (TM) blunts of ribosomal protein S6 (S6) phosphorylation through the PI3K/Akt/mTOR pathway.

We wondered what signaling pathways perturbed by treatment with TM are responsible for the apoptotic phenotype in melanoma cells. Common driver oncogenic pathways critical to melanoma pathogenesis are the MAPK and PI3K/Akt and mTOR pathways [216]. ERK phosphorylation was not significantly affected following treatment of melanoma cells with TM at early time-points, 8 and 18 hours, prior to apoptosis induction (Fig. 6). Phosphorylation of ribosomal protein S6 (S6) on the $Ser^{235/236}$ phosphorylation sites was inhibited in all human melanoma cell lines tested (Fig. 7A+B). Phosphorylation of S6 on the $Ser^{240/244}$ phosphorylation sites was also inhibited in the RPMI and SH4 cells lines (Fig. 8). As there was no difference in S6 phosphorylation between control and TM treated B16.F10 cells at 8 and 18 hours we also assessed earlier time-points. At 2 and 4 hours post TM treatment, p-S6 was also blunted as assessed by immunofluorescence staining (Fig. 7C).

S6 is phosphorylated by the p70 S6 kinase directly downstream of the mammalian target of rapamycin (mTOR) complex 1 (TORC1) [217]. TORC1 converges on multiple upstream signaling pathways including the MAPK [218] and PI3K/Akt/mTOR pathways [219-221]. The MAPK pathway activity, as assessed by ERK phosphorylation was unperturbed in response to TM treatment (Fig. 6). Through the PI3K/Akt pathways, activated Akt can activate TORC1 through tuberous sclerosis complex 2 (TSC2) or PRAS40 phosphorylation [221, 222]. Akt phosphorylation on Ser473 was suppressed at 8 or 18 hours post treatment with TM in RPMI, SH4 and B16.F10 cells (Fig. 7A). Not surprisingly, phosphorylation of the kinase directly upstream of S6, p70 S6 at Thr 421/Ser 424, was also decreased in RPMI, B16.F10 and SH4 cells post TM treatment (Fig. 7A). Maximal Akt activation occurs through phosphorylation of two key residues, Ser 473 by mTORC2 [223] or DNA-dependent protein kinase (DNA-PK) [224] and by phosphoinositide-dependent kinase 1 (PDK1) at Thr 308 [225]. However, as PDK1 phosphorylation at Ser 241 was not blunted following treatment with TM (Fig. 8) and phospho-Akt at residue Thr 308 was not detectable in our system under normal cell growth conditions (data not shown). Akt

activity by TM might be rather suppressed through mTORC2 or DNA-PK. However, there is the possibility that suppression of phosphorylation at alternative Akt sites occurs through other regulators such CK2 [226] or GSK-3α [227] and this would have to be further explored.

To confirm that melanoma cells used in our system are sensitive to PI3K/Akt/mTOR inhibition, we treated melanoma cells with specific inhibitors of AKT (MK-2206, a highly selective Akt1/2/3 inhibitor), PI3K (ZSTK474, a class I PI3K isoforms inhibitor) and mTOR (KU-0063794, a specific dual-mTOR inhibitor of mTORC1 and mTORC2). All our tested melanoma cell lines both $BRAF^{V600E}$ and BRAF WT were sensitive to Akt, PI3K and pan-mTOR inhibition with IC50 values in a similar range as that of TM (Fig. 9A and Table 1). TSTK474 and/or MK-2206 and/or KU-0063794 also induced apoptosis in both $BRAF^{V600E}$ and BRAF WT melanoma cell lines (Fig. 9B).

Taken together, TM suppresses p-S6 through blunting PI3K/Akt/mTOR signaling in melanoma cells, an effect that is likely responsible for the pro-apoptotic effects observed as treatment with various inhibitors of the pathway was able to recapitulate the phenotype.

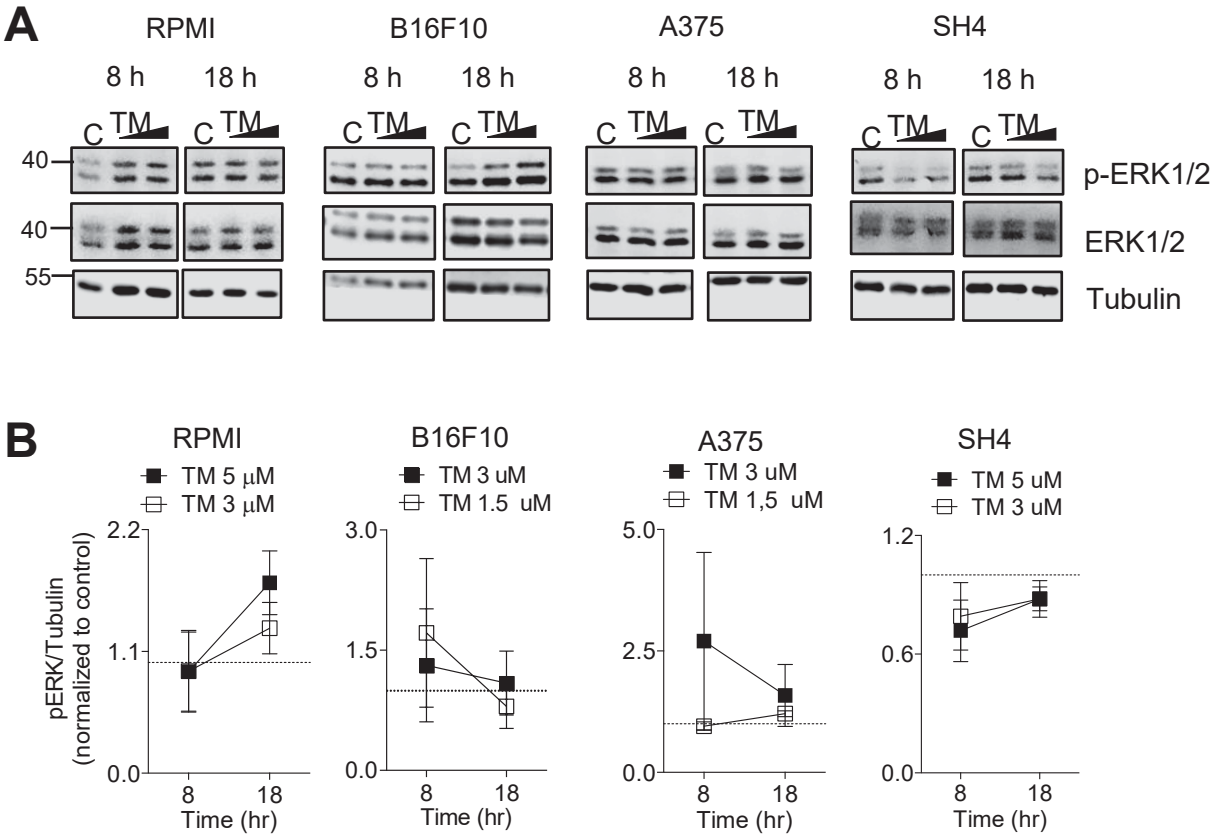

Fig. 6. TM did not affect the MAPK pathway. (A) Melanoma cells were treated as indicated time points with increasing concentrations of TM and probed for phosphorylated ERK1/2, total ERK1/2 and tubulin (representative immunoblots of n = 3 are shown). Blots are quantified in (B). Error bars in the all experiments indicate SEM. *P < 0.05 as determined by a one-way ANOVA with a Dunnett's post-hoc test.

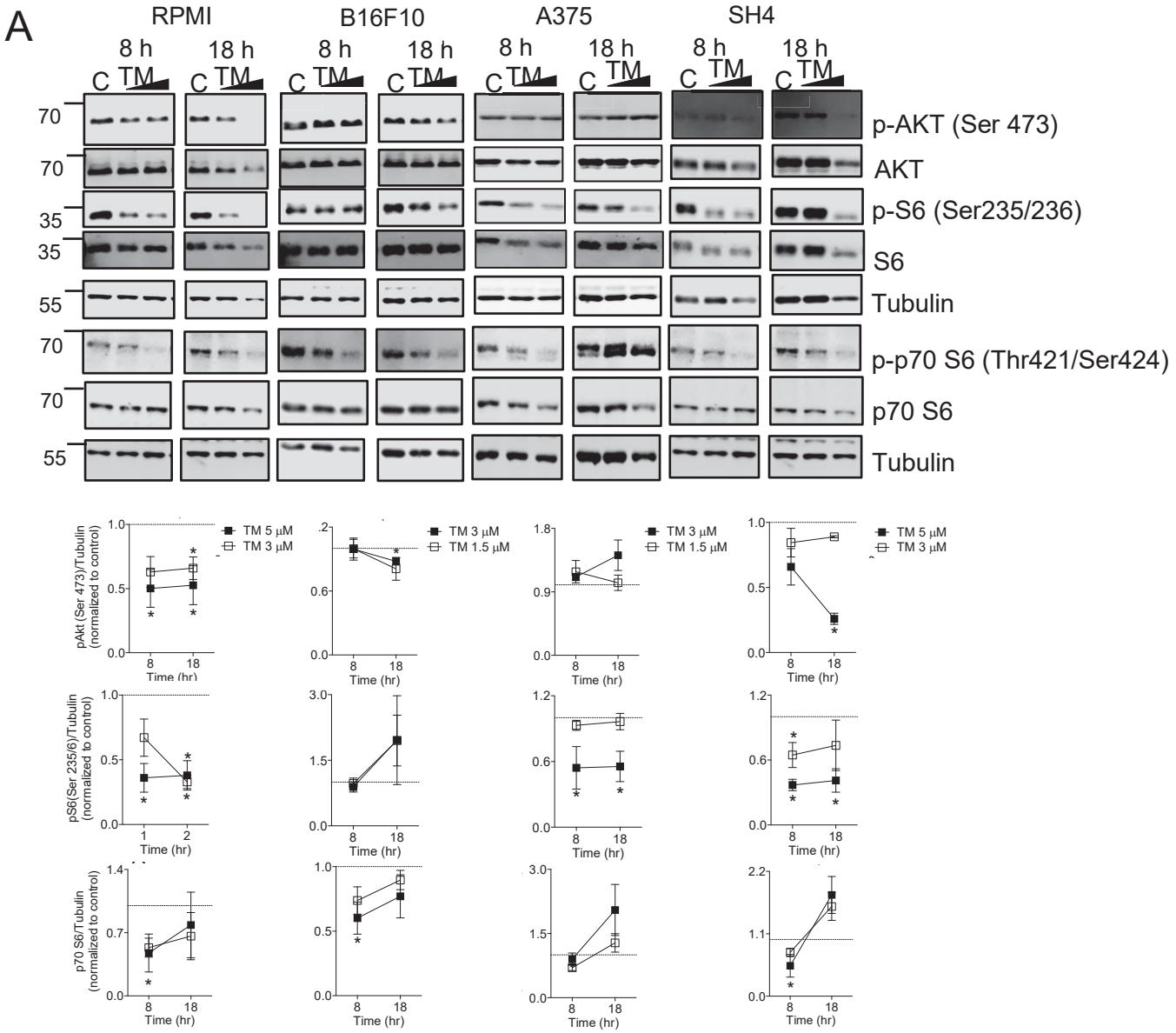
A
RPMI
B16F10
A375
SH4
8 h
18 h
C
TM
70
70
35
35
55
70
70
55
p-AKT (Ser 473)
AKT
p-S6 (Ser235/236)
S6
Tubulin
p-p70 S6 (Thr421/Ser424)
p70 S6
Tubulin
pAkt (Ser 473)/Tubulin (normalized to control)
pS6(Ser 235/6)/Tubulin (normalized to control)
p70 S6/Tubulin (normalized to control)
TM 5 µM
TM 3 µM
TM 1.5 µM
Time (hr)

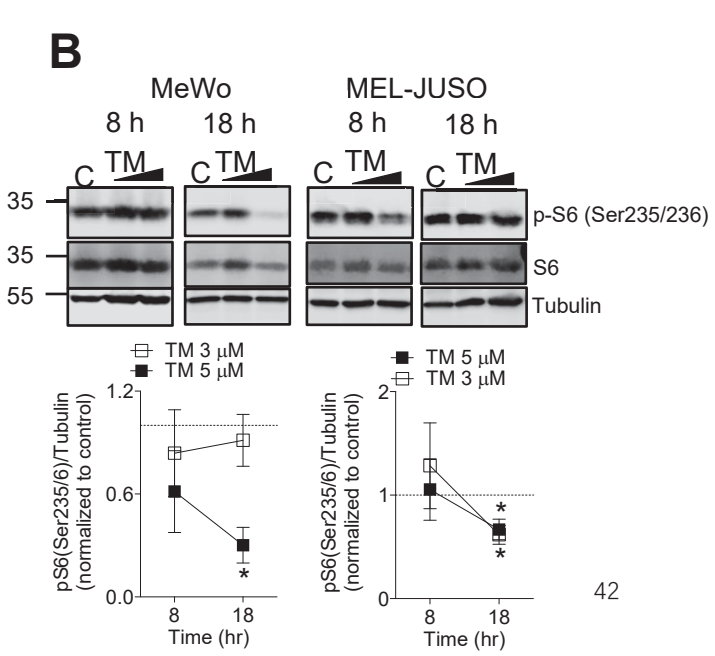
B
MeWo
MEL-JUSO
8 h
18 h
C
TM
35
35
55
p-S6 (Ser235/236)
S6
Tubulin
TM 3 µM
TM 5 µM
pS6(Ser235/6)/Tubulin (normalized to control)
Time (hr)

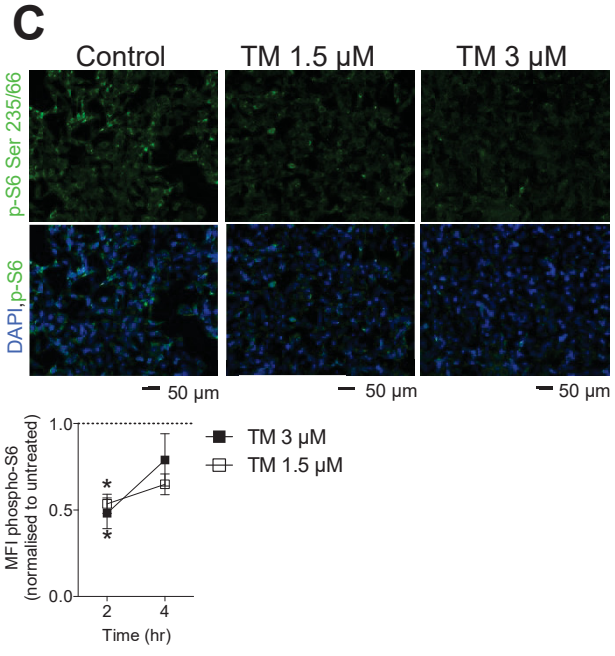
C
Control
TM 1.5 µM
TM 3 µM
p-S6 Ser 235/66
DAPI,p-S6
50 µm
MFI phospho-S6 (normalised to untreated)
TM 3 µM
TM 1.5 µM
Time (hr)

Fig. 7. TM inhibits phosphorylation of ribosomal protein S6 (S6) on the Ser235/236 phosphorylation sites in melanoma cell lines. (A-B) Treatment with increasing doses of TM at the indicated time-points prior to apoptosis induction decreased phosphorylation of Akt (p-Akt) at Ser 473, phospho-S6 (p-S6) at Ser235/6 and phospho-p70 S6 (p-p70 S6) in RPMI, B16F10, A375, RPMI, MeWo and MEL-JUSO melanoma cells (representative immunoblots of n = 3-6 are shown) and quantified below. (C) Immunofluorescent p-S6 staining of B16.F10 cells treated with TM for 2 hours is shown (A representative image of n = 3 is shown) and quantified in B, lower panel). Scale bar indicates 50 µm. Error bars in the all experiments indicate SEM. *P < 0.05 as determined by a Student´s t-test (unpaired, 2 tailed) or a one-way ANOVA with a Dunnett's post-hoc test.

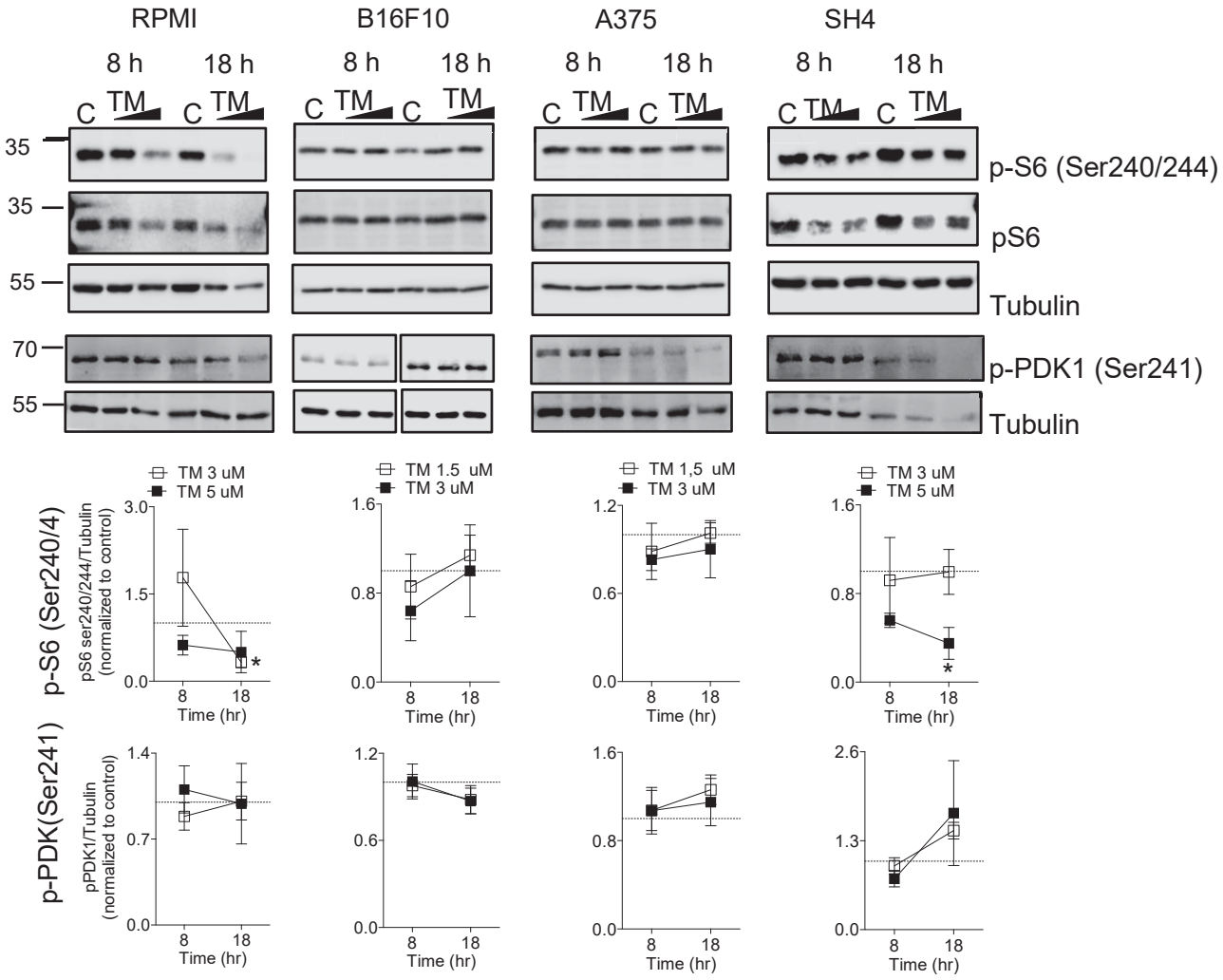

Fig. 8. TM blunts ribosomal protein S6 (S6) phosphorylation on the Ser240/244 phosphorylation sites in melanoma cell lines. Changes in p-S6 (Ser240/244) (n = 3) and p-PDK1 (Ser241) (n =3-4) following treatment with TM are shown quantified below. Error bars in all experiments indicate SEM. *P < 0.05 as determined by a one-way ANOVA with a Dunnett's post-hoc test.

Table 1: Melanoma cell line sensitivity to PI3K/Akt and mTOR pathway inhibition

Compound	Target	IC50±SEM					
		B16.F10	A375	RPMI	SH4	MeWo	MEL-JUSO
MK-2206	Pan-AKT	0.29±0.05	4.76±0.58	1.92±0.36	3.11±0.91	1.26±0.01	3.03±0.35
ZSTK474	PI3K	0.95±0.33	2.69±1.14	0.51±0.05	2.80±0.81	1.06±0.07	3.47±0.28
KU-0063794	Pan-mTOR	0.68±0.26	1.90±1.45	1.63±0.28	1.71±0.86	0.97±0.05	1.84±0.12

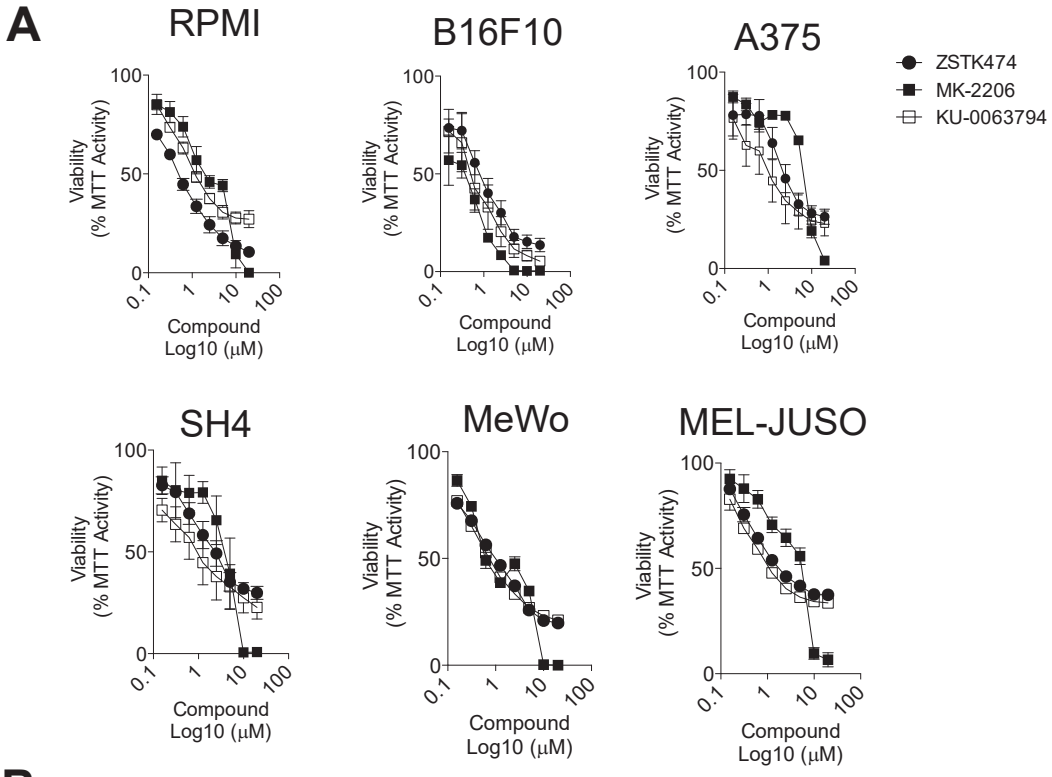

Fig. 9. Melanoma cells lines are sensitive to the anti-cancer effects of PI3K/Akt/mTOR inhibitors. (A) Melanoma cells are similarly sensitive to PI3K/Akt and mTOR pathway inhibition as they are to TM treatment. Dose response curves following treatment with the PI3K inhibitor ZSTK474, pan-Akt inhibitor MK-2206 and mTORC1/mTORC2 inhibitor KU-0063794 are shown (n = 3-4). (B) Treatment with the PI3K inhibitor ZSTK474 (2 μM for MeWo, 6 μM for MEL-JUSO and A375 and 1 μM for RPMI), pan-Akt inhibitor MK-2206 (2 μM for MeWo, 6 μM for MEL-JUSO, 10 μM for A375 and 4 μM for RPMI) and mTORC1/mTORC2 inhibitor KU-0063794 (2 μM for MeWo and 4 μM for all other cell lines) induced apoptosis in melanoma cells as assessed by Annexin V/7AAD staining (n = 3-6). Percent apoptosis was ascertained by summing up the Annexin $V^+/7AAD^-$ and Annexin $V^+/7AAD^+$. Error bars in the all experiments indicate SEM. *$P < 0.05$ as determined by a one-way ANOVA with a Dunnett's post-hoc test.

3.1.4 Tegaserod (TM) delays tumor growth, reduces metastases, and suppresses p-S6 *in vivo*.

To evaluate the efficacy of TM against melanoma tumor growth we used a syngeneic immune-competent model. Mice were subcutaneously inoculated with B16.F10 cells, and 7 days later, randomized and treated with daily injections of TM or vehicle for 5 days. Treatment significantly decreased tumor growth (Fig.10A) and resulted in only slight decreases in weight following treatment (Fig. 10B). There were no changes in liver damage markers AST, LDH and ALT (Fig. 10C). The *in vitro* TM-mediated PI3K/Akt/mTOR signaling inhibition was re-capitulated *in vivo.* When immunohistochemical staining of tumor tissue harvested at day13 post inoculation was performed for phosphorylation of S6 (Ser235/236), one third of control tumor slides were classified as having a high positive score. This is sharp contrast to tumors from TM treated mice where only one slide scored as having a high positive score (Fig. 11A). Images were scored for positive staining using the IHC profiler which employs an automated, unbiased approach to evaluate antibody staining in tissue sections [203]. Furthermore, tumor lysates from TM treated mice had significantly lower Akt and S6 phosphorylation levels (Fig. 11B).

To assess tumor apoptosis, immunohistochemical staining of tumor tissue harvested 13 days post inoculation was performed for cleaved Caspase-3 and cleaved Caspase-8 (Fig. 12A-D). 50 % of tumor slides from TM-treated mice stained for cleaved Caspase-3 had a positive score and the other 50% were scored as low positive (Fig. 12A). In contrast, tumor slides from vehicle-treated mice were 5% negative for cleaved Caspase-3, and only 27% scored positive and 68 % scored low positive (Fig. 12B). There was a significantly higher contribution from the high positive stained areas for cleaved Caspase-3 in the tumors of TM-treated mice (Fig. 12B), indicating that TM treatment caused tumor cell apoptosis *in vivo*. When tumor lysates were probed for cleaved Caspase-8, tumors from TM treated mice demonstrated a trend towards increased cleaved Caspase-8, but differences were not significant (Fig. 12E).

To evaluate the ability of TM to decrease metastasis *in vivo,* we intravenously injected B16.F10 melanoma cells into C57BL/6J mice and monitored lung metastases

in control and TM treated mice. Mice treated with TM had significantly less lung metastases (Fig. 13). Taken together, we have shown that *in vivo* TM is well tolerated, can retard tumor growth, induces tumor apoptosis and blunts p-S6.

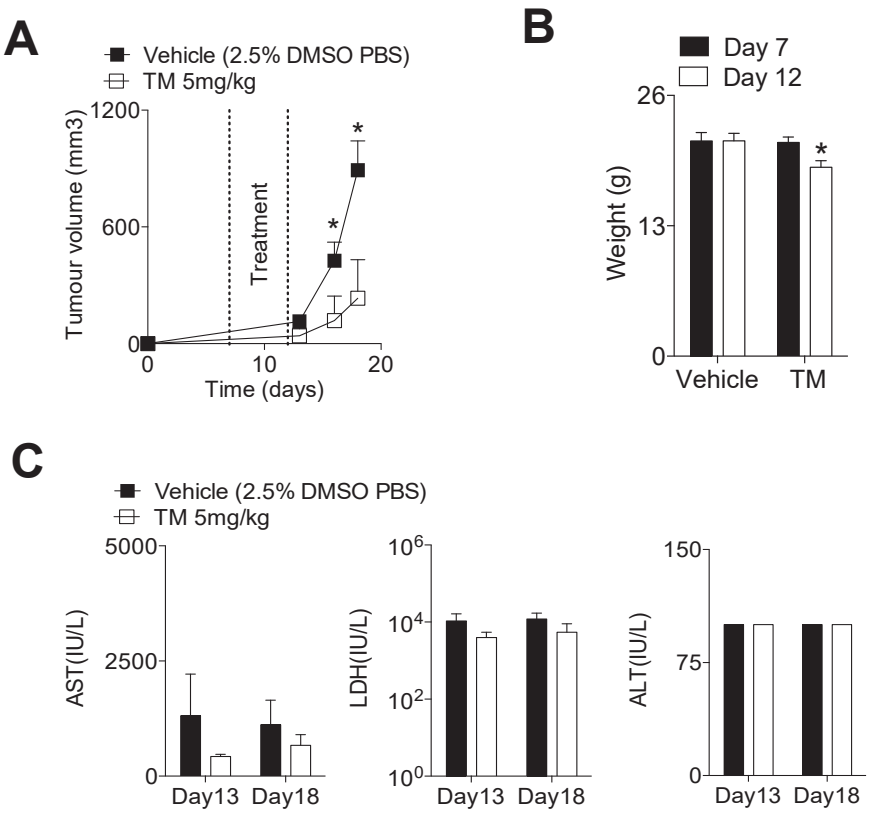

Fig. 10. TM blunts tumor growth without toxicity in mice. C57BL/6J mice were subcutaneously injected with 5×10^5 B16.F10 cells. 7 days post-tumor injection, mice were randomized and into two groups and treated daily with Tegaserod or vehicle for five consecutive days. (A) Tumor volume was measured for 18 days after which mice were sacrificed (n = 6-8). (B) The group receiving the TM treatment experienced only a small decrease in body weight (≈ 12%). Data is pooled from two independent *in vivo* experiments (n = 6-8). (C) Treatment with TM did not significantly alter liver damage parameters AST, LDH and ALT relative to vehicle treated group (n = 3). Error bars in the all experiments indicate SEM. *P < 0.05 as determined by a Student´s t-test (unpaired, 2 tailed).

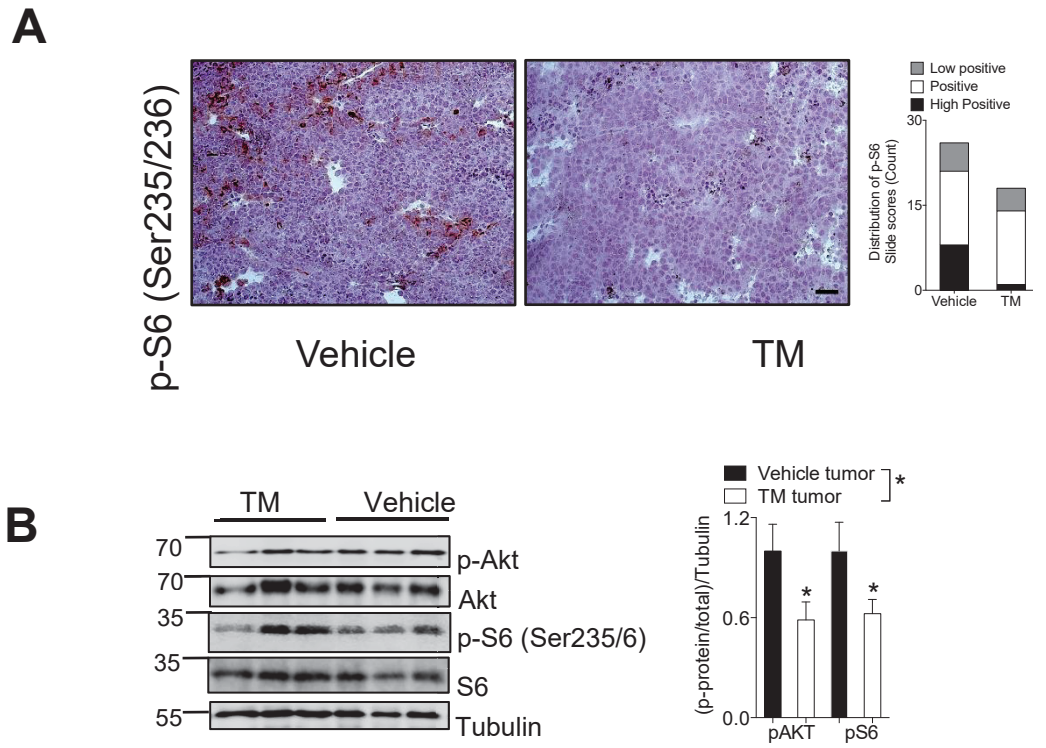

Fig. 11. Tegaserod (TM) inhibits Akt and p-S6 phosphorylation in vivo. C57BL/6J mice were subcutaneously injected with 5×10^5 B16.F10 cells. 7 days post-tumor injection, mice were randomized and into two groups and treated daily with Tegaserod or vehicle for five consecutive days. (A) Mice were sacrificed on Day 13 post tumor-inoculation and immunohistochemical staining of tumor tissue for p-S6 is shown (a representative image of n = 6 is shown). A third of pictures from tumors of mice treated with vehicle were classified as 'high positive' for p-S6 compared to only 1 slide from TM treated mice (3-5 pictures from different fields of view were obtained of tumors from each independent mouse, for a total of 26 and 18 tumor pictures for vehicle and TM treated mice respectively). (B, left panel) Immunoblots of tumor lysates from TM or control treated mice confirmed decreased Akt (Ser473) and S6 (Ser235/6) phosphorylation (n = 6-9 mice, with 3 mice are shown on one immunoblot) quantified in (B, right panel). Scale bars indicate 50 μm. Error bars in the all experiments indicate SEM. *P < 0.05 as determined by a Student´s t-test (unpaired, 2 tailed).

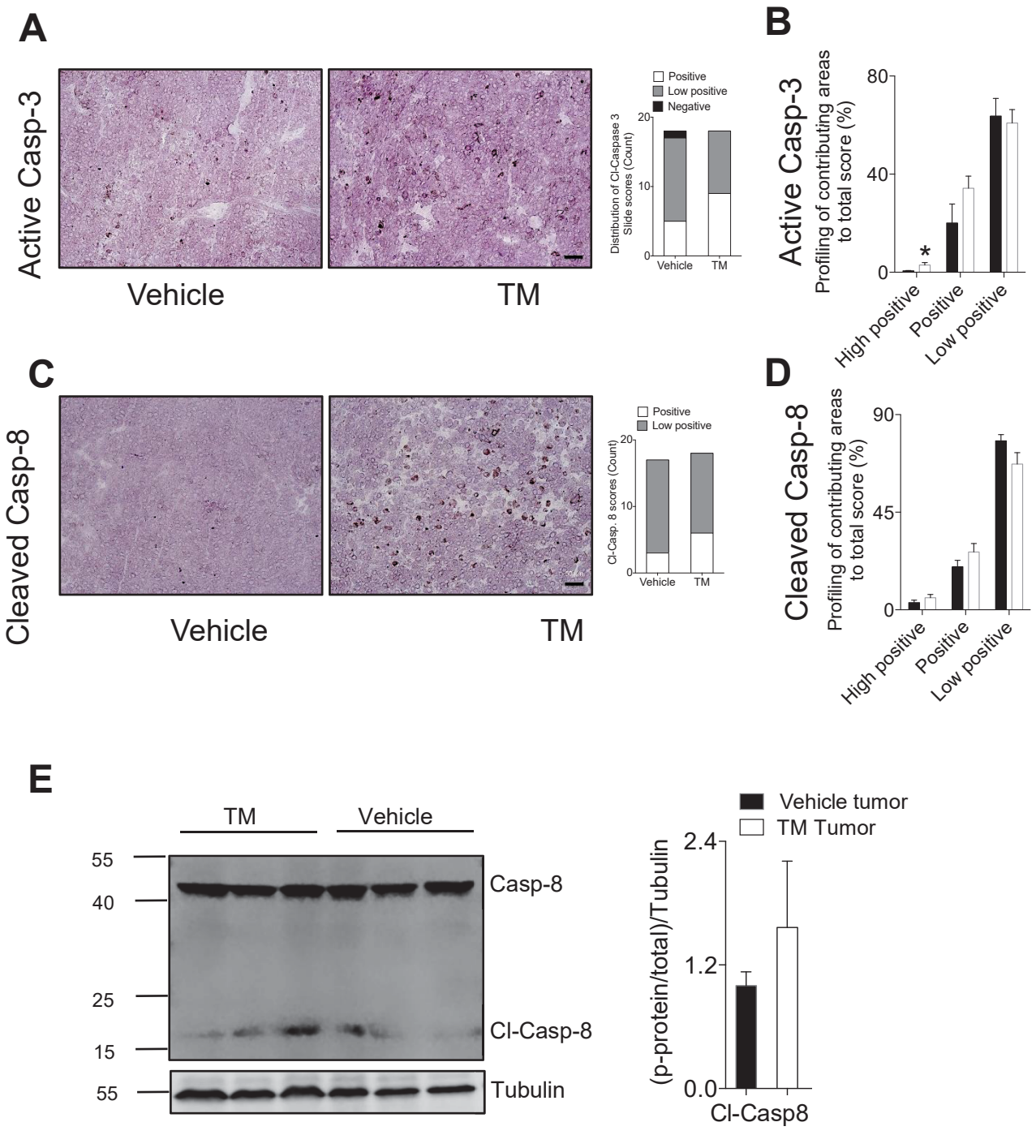
A
Active Casp-3
Vehicle
TM
Positive
Low positive
Negative
Distribution of Cl-Caspase 3 Slide scores (Count)
20
10
0
Vehicle
TM
B
Active Casp-3
Profiling of contributing areas to total score (%)
80
40
0
*
High positive
Positive
Low positive
C
Cleaved Casp-8
Vehicle
TM
Positive
Low positive
Cl-Casp. 8 scores (Count)
20
10
0
Vehicle
TM
D
Cleaved Casp-8
Profiling of contributing areas to total score (%)
90
45
0
High positive
Positive
Low positive
E
TM
Vehicle
55
40
25
15
55
Casp-8
Cl-Casp-8
Tubulin
Vehicle tumor
TM Tumor
(p-protein/total)/Tubulin
2.4
1.2
0.0
Cl-Casp8

Fig. 12. Tegaserod (TM) induces tumor cell apoptosis in vivo. C57BL/6J mice were subcutaneously injected with 5×10^5 B16.F10 cells. 7 days post-tumor injection, mice were randomized and into two groups and treated daily with Tegaserod or vehicle for five consecutive days. (A) Mice were sacrificed on Day 13 post tumor-inoculation and (A, left panel) immunohistochemical staining of tumor tissue revealed that tumors of mice treated with TM had increased active Caspase-3 expression (a representative image of n = 6 is shown). (A, right panel) The relative score distribution of tumor slides is shown (3 pictures from different fields of view were obtained of tumors from each independent mouse (n = 6), for a total of 18 tumor pictures for each stain and treatment group. (B) Quantification and profile of the active Caspase-3 staining using IHC profiler. (C, left panel) Immunohistochemical staining of cleaved caspase-8 is shown (a representative image of n = 6 mice is shown). (C, right panel) The relative score distribution and profile of tumor slides for cleaved caspase-8 is shown (3 pictures from different fields of view were obtained of tumors from each independent mouse (n = 6), for a total of 17 tumor pictures for control and 18 for TM treatment group. (D) Quantification and profile of the active Caspase-8 staining using IHC profiler. (E) Immunoblots of tumor lysates from TM or control treated mice probed for cleaved caspase 8 are shown and quantified (n = 6-9 mice, with 3 mice shown on one immunoblot). All Scale bars indicate 50 μm. Error bars in the all experiments indicate SEM. *P < 0.05 as determined by a Student´s t-test (unpaired, 2 tailed).

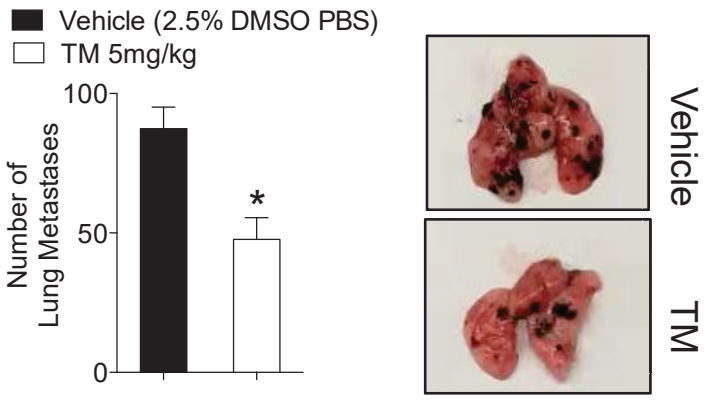

Fig. 13 Tegaserod (TM) decreases melanoma metastasis in vivo. C57BL/6J mice were intravenously injected with 2×10^5 B16.F10 cells. Starting at day 1 post inoculation, mice were treated with Tegaserod or vehicle three times a week. Mice were sacrificed at Day 14 post tumor inoculation and lung metastases counted with representative lung images shown in the right panel (n = 10). Error bars in the experiments indicate SEM. *P < 0.05 as determined by a determined by a Student´s t-test (unpaired, 2 tailed).

3.1.5 Tegaserod (TM) decreases the infiltration and FOXP3 expression of regulatory T cells and synergizes with BRAF and MEK inhibitors.

Next, we wondered whether TM treatment impacted immune infiltrates. We harvested tumors from mice at day 13 post inoculation when there were no significant differences in tumor size and found that the numbers of $NK1.1^{+}CD3^{-}$ natural killer (NK) cells, $Ly6C^{high}Ly6G^{-}$ monocytes, $Ly6C^{low}Ly6G^{high}$ granulocytes and $CD8^{+}$ T cells were not different between tumors harvested from control and TM treated mice (Fig. 14A). However, tumors harvested from TM treated mice were characterized by lower amounts of infiltrating $CD4^{+}$ T cells (Fig. 14A). As regulatory $CD4^{+}CD25^{+}$ T cells play a crucial role in suppressing anti-tumoral immunity [228] and have been shown to be susceptible to PI3K/PTEN/mTOR axis inhibition [229], we next checked whether there were any differences in the percentage of infiltrating regulatory $CD4^{+}CD25^{+}$ T cells between TM treated and control tumors. Not only was the percentage of $CD4^{+}CD25^{+}$ T cells lower in tumors harvested from TM-treated mice (Fig. 14B), but the FOXP3 expression on these cells was decreased (Fig. 14C). By contrast, surface markers of exhaustion (PD-1), activation (KLRG1, Granzyme B, perforin, Interferon gamma (IFNγ)) and death (CD95) were no different on tumor infiltrating $CD8^{+}$ T cells between TM and vehicle treated mice (Fig. 14C).

Any potential novel therapy will not be used as in a mono-therapeutic setting but will be combined with the current standard of care. We therefore ascertained whether TM could be combined with Vemurafenib, a B-Raf inhibitor approved for the treatment of late-stage melanoma [230]. We tested the combination in human cell lines harboring the $BRAF^{V600E}$ mutation targeted by Vemurafenib, namely RPMI, A375 and the SK-MEL-24 cells. TM synergized with Vemurafenib in all cell lines tested (Fig. 14D). Other kinase inhibitors currently in use for the treatment of late-stage melanoma include the MEK inhibitor Cobimetinib. TM also synergized with Cobimetinib in A375 cells at higher effective doses (ED75 and ED90) and was additive in RPMI, B16F10, MeWo and MEL-JUSO melanoma cell lines (Fig. 14D). Taken together, we have shown that TM inhibited tumor growth *in vivo* and can be successfully combined with the current standard of care.

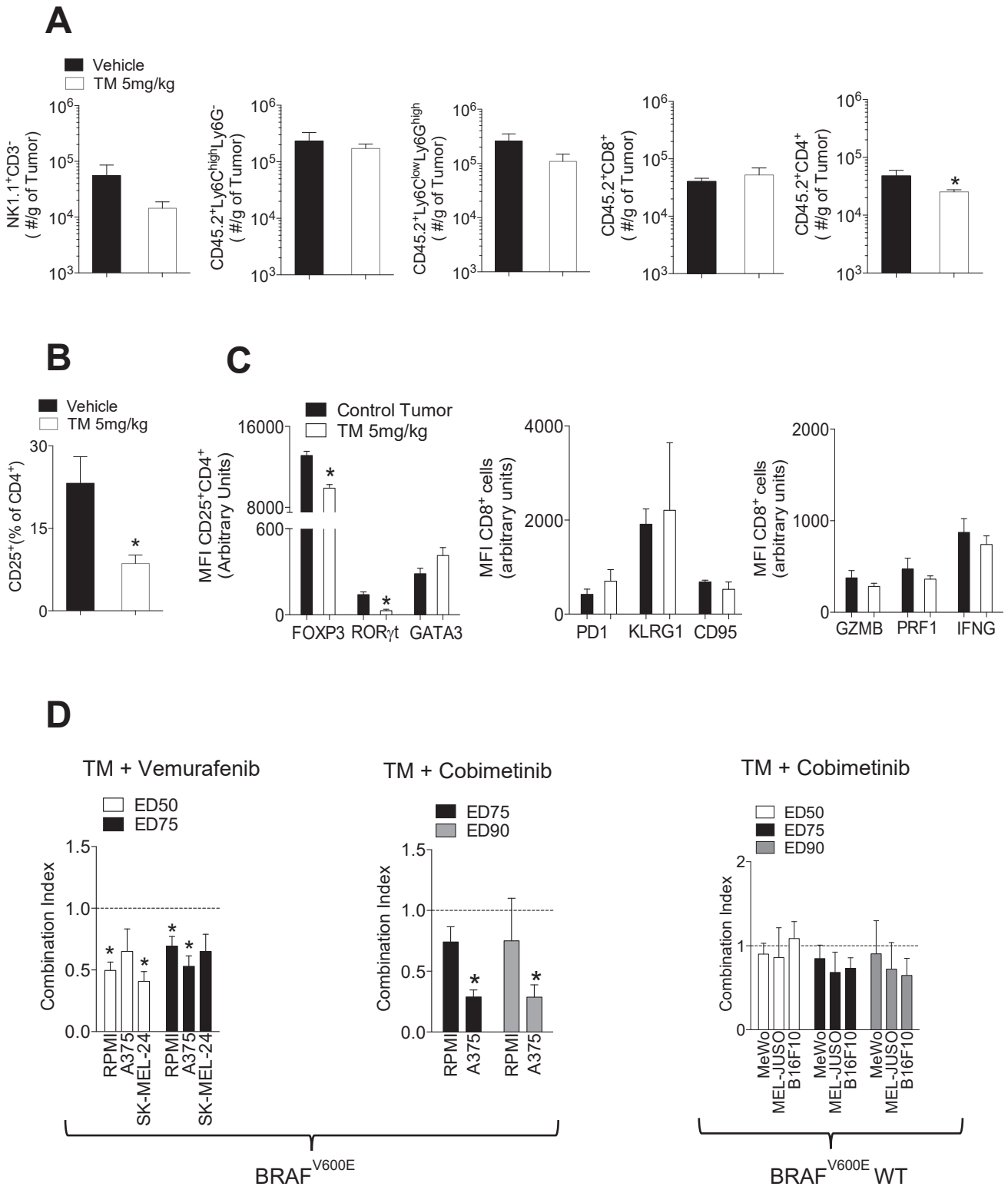
A
Vehicle
TM 5mg/kg
NK1.1+CD3-
(#/g of Tumor)
CD45.2+Ly6Chigh Ly6G-
(#/g of Tumor)
CD45.2+Ly6Clow Ly6Ghigh
(#/g of Tumor)
CD45.2+CD8+
(#/g of Tumor)
CD45.2+CD4+
(#/g of Tumor)
B
Vehicle
TM 5mg/kg
CD25+(% of CD4+)
C
Control Tumor
TM 5mg/kg
MFI CD25+CD4+
(Arbitrary Units)
FOXP3
RORγt
GATA3
MFI CD8+ cells
(arbitrary units)
PD1
KLRG1
CD95
MFI CD8+ cells
(arbitrary units)
GZMB
PRF1
IFNG
D
TM + Vemurafenib
ED50
ED75
Combination Index
RPMI
A375
SK-MEL-24
BRAFV600E
TM + Cobimetinib
ED75
ED90
Combination Index
RPMI
A375
BRAFV600E
TM + Cobimetinib
ED50
ED75
ED90
Combination Index
MeWo
MEL-JUSO
B16F10
BRAFV600E WT

Fig. 14. Tegaserod (TM) decreases tumor infiltration of $CD25^{+}CD4^{+}$ T cells and synergizes with Vemurafenib and Cobimetinib. (A-C) C57BL/6J mice were subcutaneously injected with 5×10^5 B16.F10 cells. 7 days post-tumor injection, mice were randomized and into two groups and treated daily with Tegaserod or vehicle for five consecutive days. Mice were sacrificed on Day 13 post tumor-inoculation and tumor infiltrating lymphocytes were assessed using FACS analysis (n = 3-6). (D) Melanoma cell lines harboring the $BRAFV^{600E}$ mutation, A375, RPMI-7951 (RPMI) and SK-MEL-24 were exposed to a dose range of TM and Vemurafenib in a fixed 1:1 ratio. $BRAF^{V600E}$ and BRAF WT melanoma cell lines were exposed to a dose range of TM and Cobimetinib in a fixed ratio (RPMI, 1:2, A375 64:1, MeWo 4:1, MEL-JUSO 4:1, B16.F10 1:1). Synergy was evaluated using the combination index (CI) from the dose-response curves. CI < 1 indicates synergy, CI = 1 indicates additivity, and CI > 1 indicates antagonism. The EC50 (50% effective concentration) and EC75 (75% effective concentration) or EC90 (90% effective concentration) are shown (n = 3-6). *P < 0.05 as determined by a Student´s t-test(unpaired, 2 tailed).

3.2 Function of BAFF in melanoma

3.2.1 Expression of BAFF in the tumor inhibits tumor growth.

To explore the effects of BAFF in the solid tumor microenvironment, we generated a BAFF overexpressing B16.F10.gp33 (BAFF, Tnfsf13b) cell line (Fig. 15A+B). *In vitro*, there was no difference in growth between the BAFF and control cells (Fig. 15C). When treated with apoptosis-inducing agents cycloheximide and actinomycin D, both cell lines underwent similar levels of apoptosis (Fig. 15D).

Next, we injected BAFF and control cells into C57BL/6 (B6) mice subcutaneously and followed the tumor growth. BAFF tumors grew slower and tumor volume was smaller than their controls (Fig. 16A + B). While systemic serum BAFF levels were not different between BAFF and control tumor bearing mice (Fig. 16C), BAFF mRNA and protein expression in BAFF tumors was maintained throughout the course of tumor growth and confirmed at an early time point of tumor growth (Day 13) when there were no significant differences between tumor weight and volume, and later time point (Day 18) at sacrifice (Fig. 16D + E).

Taken together, BAFF expression within the TME delays tumor growth, a phenomenon that is independent of intrinsic differences between BAFF and control cells as they behaved similarly *in vitro* in terms of growth and response to apoptotic stimuli.

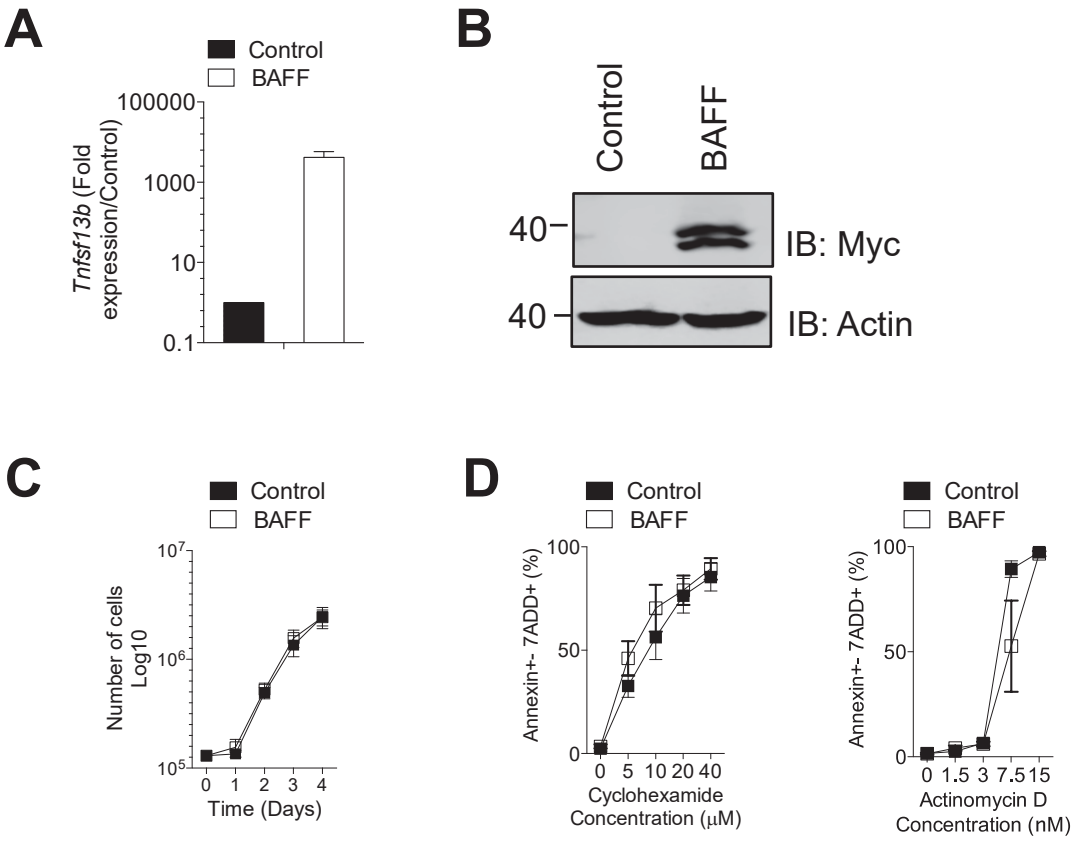

Fig. 15. Expression of BAFF in B16.F10.gp33 melanoma cells. BAFF over-expressing B16.F10.gp33 (BAFF) monoclonal cell population was generated using lentiviral transduction followed by clonal dilution. (A) *Tnfsf13B* expression levels were confirmed in the BAFF cells. Expression was normalized to *GAPDH* (n = 3). (B) BAFF protein over-expression was confirmed by immunoblotting for the Myc tag (a representative immunoblot of n = 4 is shown). (C) The growth of BAFF and control cells was compared *in vitro* (n = 3). (D) Apoptosis following treatment of BAFF and control cells with several apoptosis-inducing agents was assessed by Annexin V/7AAD staining. Percent apoptosis was ascertained by summing up the Annexin $V^+/7AAD^-$ and Annexin $V^+/7AAD^+$ populations (n = 3). Error bars in all experiments indicate SEM; *$P < 0.05$ as determined by a Student´s t-test (unpaired, 2 tailed)

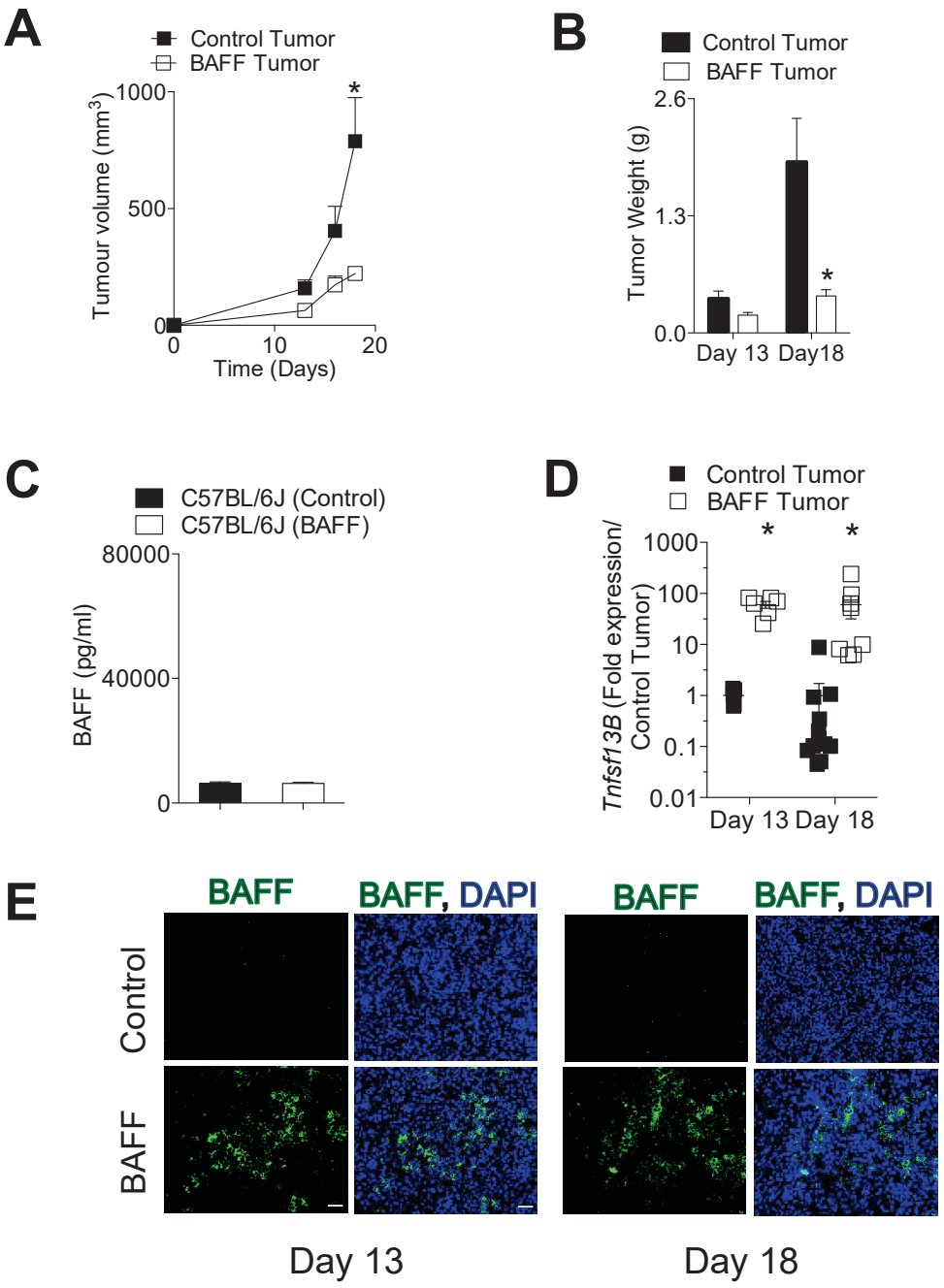
A
Control Tumor
BAFF Tumor
Tumour volume (mm3)
1000
500
0
0
10
20
Time (Days)
*
B
Control Tumor
BAFF Tumor
Tumor Weight (g)
2.6
1.3
0.0
*
Day 13
Day18
C
C57BL/6J (Control)
C57BL/6J (BAFF)
BAFF (pg/ml)
80000
40000
0
D
Control Tumor
BAFF Tumor
Tnfsf13B (Fold expression/ Control Tumor)
1000
100
10
1
0.1
0.01
*
*
Day 13
Day 18
E
BAFF
BAFF, DAPI
BAFF
BAFF, DAPI
Control
BAFF
Day 13
Day 18

Fig. 16. Elevated BAFF in the tumor slows tumor growth. (A) Tumor growth of 5×10^5 subcutaneously injected BAFF and control cells in C57BL/6 mice are shown (n = 5-6) as are tumor weights (B, n = 5-7, pooled from two independent *in vivo* experiments). (C) The level of BAFF in the serum of mice intravenously inoculated with BAFF or control cells was determined using ELISA. BAFF serum levels were determined 18 days post inoculation (n = 3). (D) Gene expression level of BAFF (*Tnfsf13B*) was determined in whole tumors harvested at the indicated time points. Expression was normalized to *GAPDH* (n = 5-12, pooled from two independent *in vivo* experiments). (E) BAFF protein expression was confirmed using immunohistochemical staining of tumor tissue at the indicated time points post subcutaneous tumor inoculation (representative images of n = 5-12 separate mice pooled from three independent in vivo experiments are shown. Pictures from 3 different fields of view were obtained of tumors from each independent mouse). Scale bar indicates 50 μm. Error bars in the all experiments indicate SEM; *P < 0.05 as determined by a Student´s t-test (unpaired, 2 tailed).

3.2.2 BAFF tumors are characterized by increased apoptosis and lower immunosuppressive factors including PD-L1.

Next, we attempted to uncover the differences between the BAFF and control tumors that could account for the observed phenotype. When we stained tumor sections harvested at early and late time points during tumor growth, we observed increases in cleaved Caspase-8 and cleaved Caspase-3 (Fig. 17A) in BAFF tumors. Cleaved Caspase-8 activates the downstream effector Caspase-3, which like Caspase-8 is also active when cleaved; both Caspases, when cleaved, are indicative of cells undergoing apoptosis.

To further characterize the differences between BAFF and control tumors on a molecular whole-tumor level, we assayed the mRNA expression of a variety of growth factors, ligands, cytokines and interferon responsive genes known to impact tumor growth. The expression of immunosuppressive factors such as *Tgfb1*, *Il-10*, *Pdgfb* and *Fgfr1* were significantly lower in the BAFF tumors at Day 13 post tumor injection (Fig. 17B). The effects of secreted TGFβ1 and IL-10 on tumor growth and surrounding immune cells are complex, often paradoxical, and can be pro or anti-tumorigenic depending on the context and stage of tumor progression [231, 232]. We verified whether the mRNA results reflected differences in secreted TGFβ1 and IL-10. We were unable to detect secreted IL-10 (data not shown) within the tumor and there was no difference in secreted TGFβ1 at the early time point between BAFF and control tumors (Fig. 17C), leading us to conclude that IL-10 or TGFβ1 were not responsible for the observed phenotype. The expression of the programmed death-ligand 1 (PD-L1) was also lower in the BAFF tumors when compared to controls at both early and late time points (Fig. 17B). PD-L1 is a crucial inhibitory ligand expressed on immune cells of the myeloid lineage, activated cells of lymphoid and epithelial origin including cancer cells [233]. PD-L1 binding to PD1 expressed on T cells decreases T cell activation and function, therefore consequentially blunting anti-tumor immunity [234, 235]. We decided to uncover the source of the differences in PD-L1 expression. As primary human and murine tumors have been shown to express PD-L1, including those generated from B16 cells [236], we assessed PD-L1 expression in the tumor cells and

stroma ($CD45.2^-$) cells. Indeed, the percentage of PD-L1 expressing $CD45.2^-$ cells in the BAFF tumor was significantly lower than in control tumors (Fig. 18A). Next, we assessed tumor infiltrating immune cells using FACS analysis and focused on myeloid populations as they have been shown to have tumor immunosuppressive functions. PD-L1 expression was significantly lower on infiltrating $CD11b^+Ly6G^{high}Ly6C^{low}$ granulocytes and $CD11b^+Ly6C^{high}Ly6G^-$ monocytes but not $CD11b^+F4/80^{high}Ly6C^{low}Ly6G^-$ tumor-associated macrophages (TAMs) (Fig. 18B + C). Taken together, BAFF tumors were characterized by increased apoptosis and decreased expression of immunosuppressive factors including PD-L1 whose expression was decreased on tumor cells, infiltrating monocytes and granulocytes.

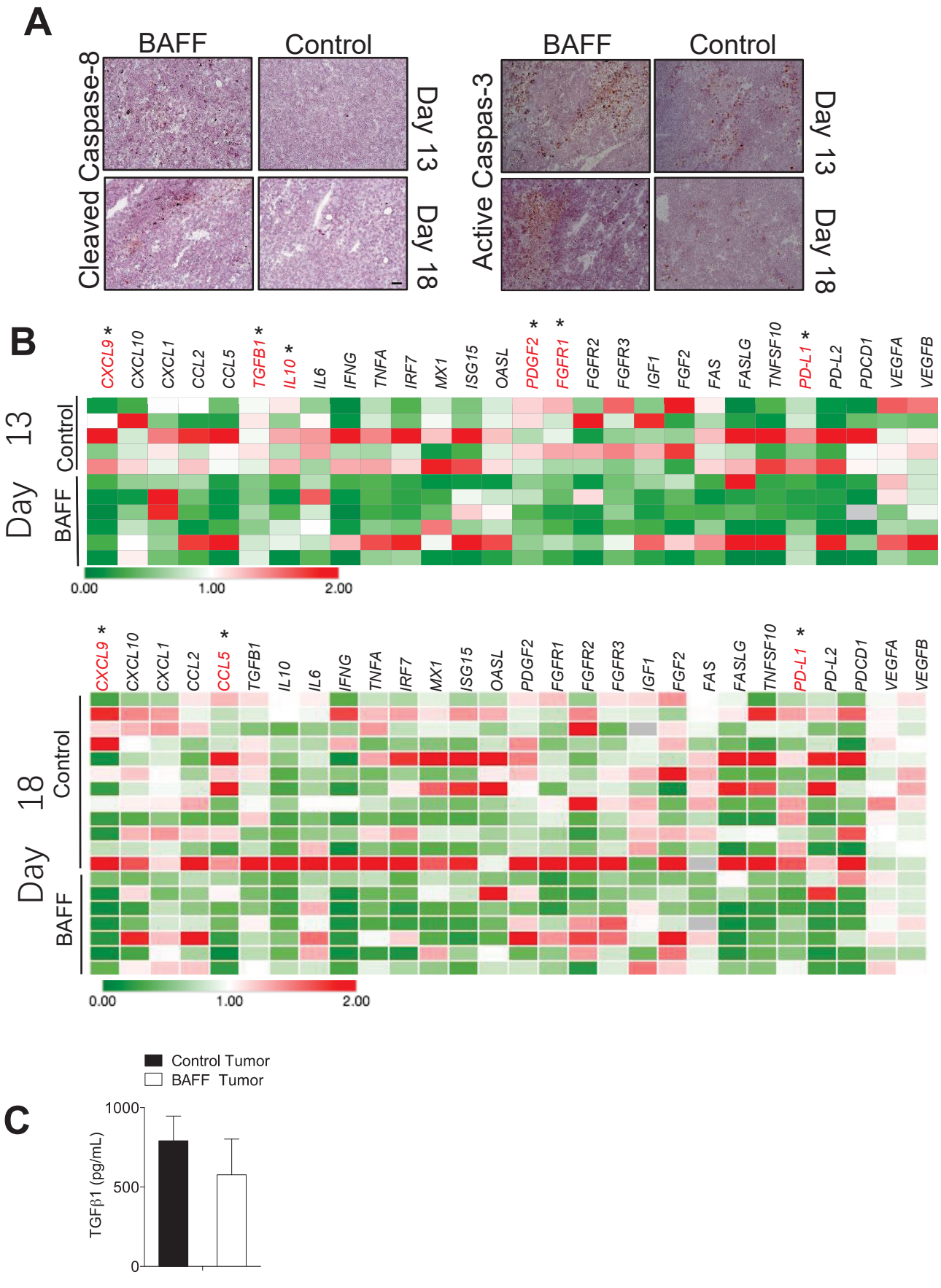
A
BAFF
Control
Cleaved Caspase-8
Active Caspas-3
Day 13
Day 18
B
CXCL9 *
CXCL10
CXCL1
CCL2
CCL5
TGFB1 *
IL10 *
IL6
IFNG
TNFA
IRF7
MX1
ISG15
OASL
PDGF2 *
FGFR1 *
FGFR2
FGFR3
IGF1
FGF2
FAS
FASLG
TNFSF10
PD-L1 *
PD-L2
PDCD1
VEGFA
VEGFB
Day 13
Control
BAFF
0.00
1.00
2.00
Day 18
C
Control Tumor
BAFF Tumor
TGFβ1 (pg/mL)
1000
500
0

Fig. 17. BAFF tumors are characterized by increased apoptosis and decreased expression of PD-L1. C57BL/6 mice were inoculated subcutaneously with 5×10^5 of BAFF or control cells and tumors were analyzed as indicated. Tumor apoptosis was assessed using conventional immunohistochemical staining for (A) Cleaved Caspase-3 and Cleaved Caspase-8 (representative images of n = 3-4 mice are shown). Pictures of 3 different fields of view were obtained of tumors from each mouse. Scale bar indicates 50 μm. (B) Gene expression level of various cytokines, growth factors and immunosuppressive and inflammatory regulators were determined in whole tumors harvested at day 13 and day 18 post tumor inoculation. Expression was normalized to *GAPDH* and then to control tumors within each independent experiment (n = 5-12, pooled from two independent *in vivo* experiments). (C) The levels of soluble TGFβ1 protein in BAFF and control tumors were determined using ELISA at the indicated time points (n = 6-7, pooled from two independent in vivo experiment). Error bars in the all experiments indicate SEM; *P < 0.05 as determined by a Student´s t-test (unpaired, 2 tailed).

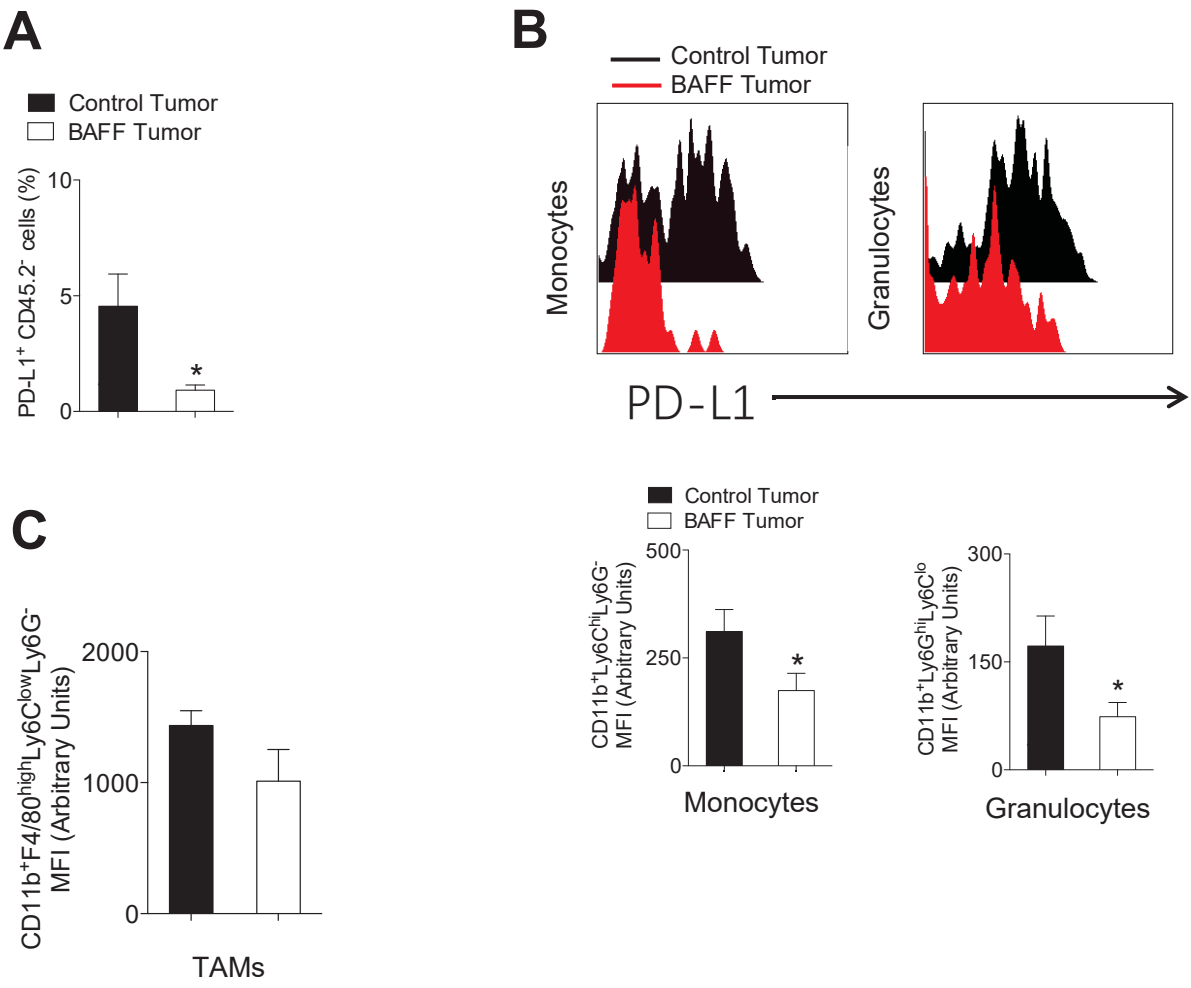

Fig. 18. The expression of PD-L1 is decreased on tumor cells, infiltrating monocytes and granulocytes. C57BL/6 mice were inoculated subcutaneously with 5 × 10^5 of BAFF or control cells and tumors were analyzed as indicated. (A) Percent of PD-L1 positive CD45.2$^-$ cells in BAFF and control tumors was assessed using FACS analysis (n = 9-13, pooled from three independent *in vivo* experiments). (B + C) PD-L1 expression was measured on monocytes, granulocytes and tumor associated macrophages (TAMs) using FACS analysis (n = 9-13, pooled from at least two independent *in vivo* experiments). Error bars in all experiments indicate SEM; *P < 0.05 as determined by a Student´s t-test (unpaired, 2 tailed).

3.2.3 B cells do not functionally contribute to BAFF mediated anti-tumor immunity.

Next, we wanted to test the potential involvement of tumor infiltrating B cells in our system. Yarchoan et al. have shown that injection of systemic BAFF upregulated the B cell compartment and markers of regulatory B cells including PD-L1 as well as CD5, increased Th1 responses and also had very specific immunoregulatory functions including the increase of Treg's in the TME [200]. In our system, there was no significant difference in B cell infiltration, and the expression of PD-L1 on $CD19^+$ B cells was not significantly different between BAFF and control tumors (Fig. 19A). The infiltration and expression of MHCII and CD5 on $CD19^+$ $B220^+IgM^+$ mature B cells was also not different in the TME between BAFF and control tumors (Fig. 19B and C). Furthermore, there was no significant difference in IgG and IgM levels in serum and tumor between BAFF and control tumor bearing mice (Fig. 19D).

Although systemic BAFF upregulated various co-stimulatory molecules on B cells [200], the actual functional importance of B cells to tumor regression is unclear. To test this, we utilized the *JHt*$^{-/-}$ knockout mouse model. The mice lack the gene for the heavy chain joining region and therefore have no functional B cells [237]. With no B cells to take up circulating BAFF, the *JHt*$^{-/-}$ mice are characterized by eight-fold higher circulating BAFF levels compared to control C57BL/6J mice (Fig. 20A). This provides the opportunity to study the effects of higher systemic BAFF without any confounding potential effects of B cells. When we inoculated B6 and *JHt*$^{-/-}$ mice with parental B16gp33 cells, the tumor growth of both cell lines was significantly delayed in the *JHt*$^{-/-}$ mice (Fig. 20B). While this result confirms the importance of systemic BAFF to a delay in tumor growth as previous study showed [200], it undermines the importance of B cells to this phenotype. Furthermore, systemic BAFF also downregulated PD-L1 on monocytes in the TME and tumor draining lymph node (Fig. 20C) and tumoral $CD45.2^-$ cells (Fig. 20D). Interestingly, from other antigen presenting cells, PD-L1 was also downregulated on dendritic cells (DC) in the TME (Fig. 20E). Taken together, higher levels of systemic BAFF maintain the difference in tumor growth and suppressive monocyte de-repression independently of B cells.

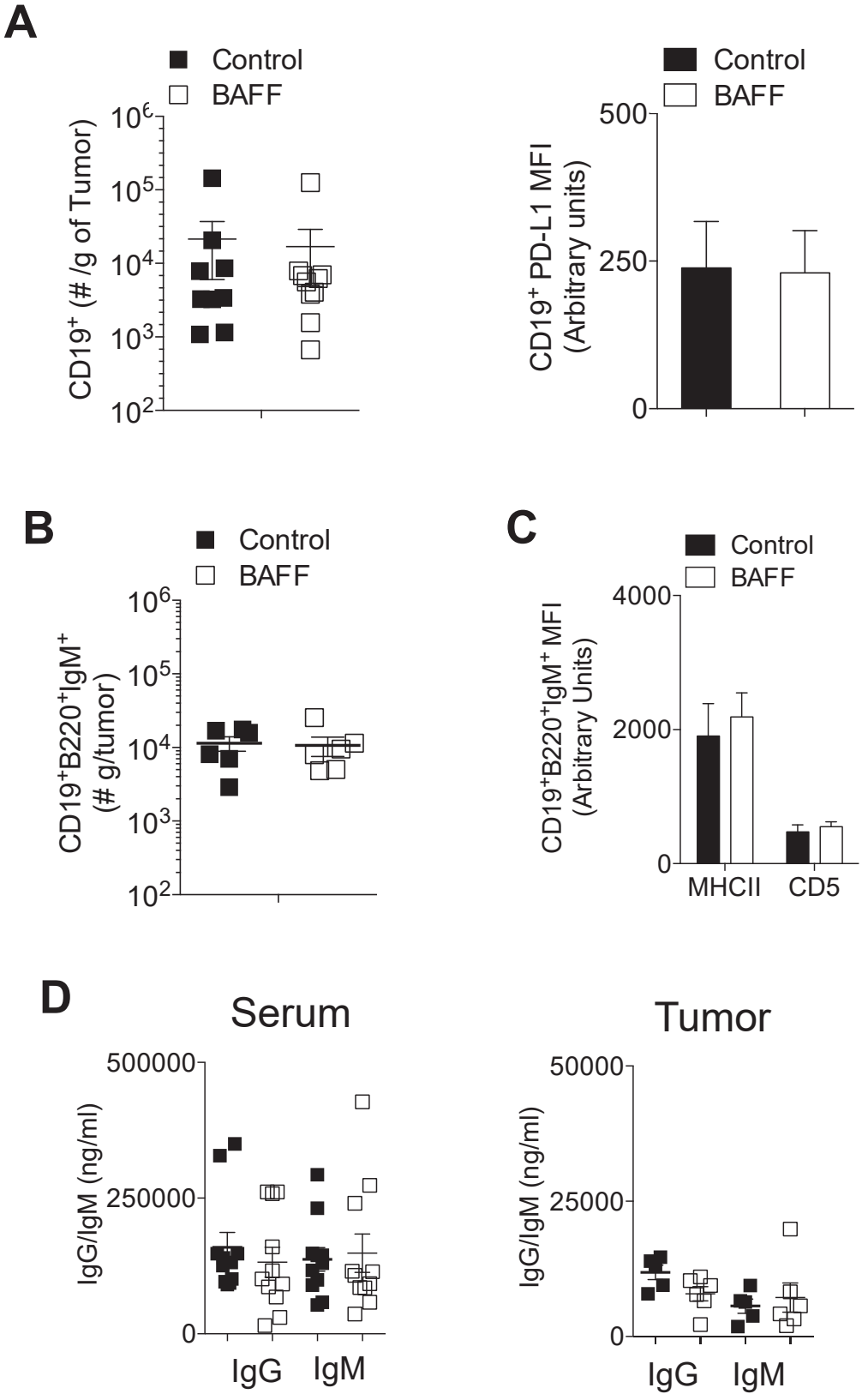
A
Control
BAFF
CD19+ (# /g of Tumor)
10^6
10^5
10^4
10^3
10^2
Control
BAFF
CD19+ PD-L1 MFI
(Arbitrary units)
500
250
0
B
Control
BAFF
CD19+B220+IgM+
(# g/tumor)
10^6
10^5
10^4
10^3
10^2
C
Control
BAFF
CD19+B220+IgM+ MFI
(Arbitrary Units)
4000
2000
0
MHCII
CD5
D
Serum
IgG/IgM (ng/ml)
500000
250000
0
IgG
IgM
Tumor
IgG/IgM (ng/ml)
50000
25000
0
IgG
IgM

Fig. 19. B cells do not functionally contribute to BAFF mediated anti-tumor immunity. C57BL/6 mice were inoculated subcutaneously with 5×10^5 of BAFF or control cells and tumors were analyzed as indicated on day 13 post tumor inoculation. (A) Numbers (left panel) and PD-L1 expression (right panel) of $CD19^+$ B cells were assessed using FACS analysis (n = 9-10, pooled from three independent *in vivo* experiments). (B) Numbers of $CD19^+$ $B220^+IgM^+$ mature B cells infiltrates in BAFF and control tumors are shown (n = 6). (C) MHCII and CD5 expression was measured by FACS on $D19^+$ $B220^+IgM^+$ mature B cells (n = 6). (D) Concentration of IgG and IgM were measured in BAFF and control tumors and serum harvested 13 days post-tumor inoculation by ELISA (n = 5-6). Error bars in the all experiments indicate SEM; *$P < 0.05$ as determined by a Student´s t-test (unpaired, 2 tailed).

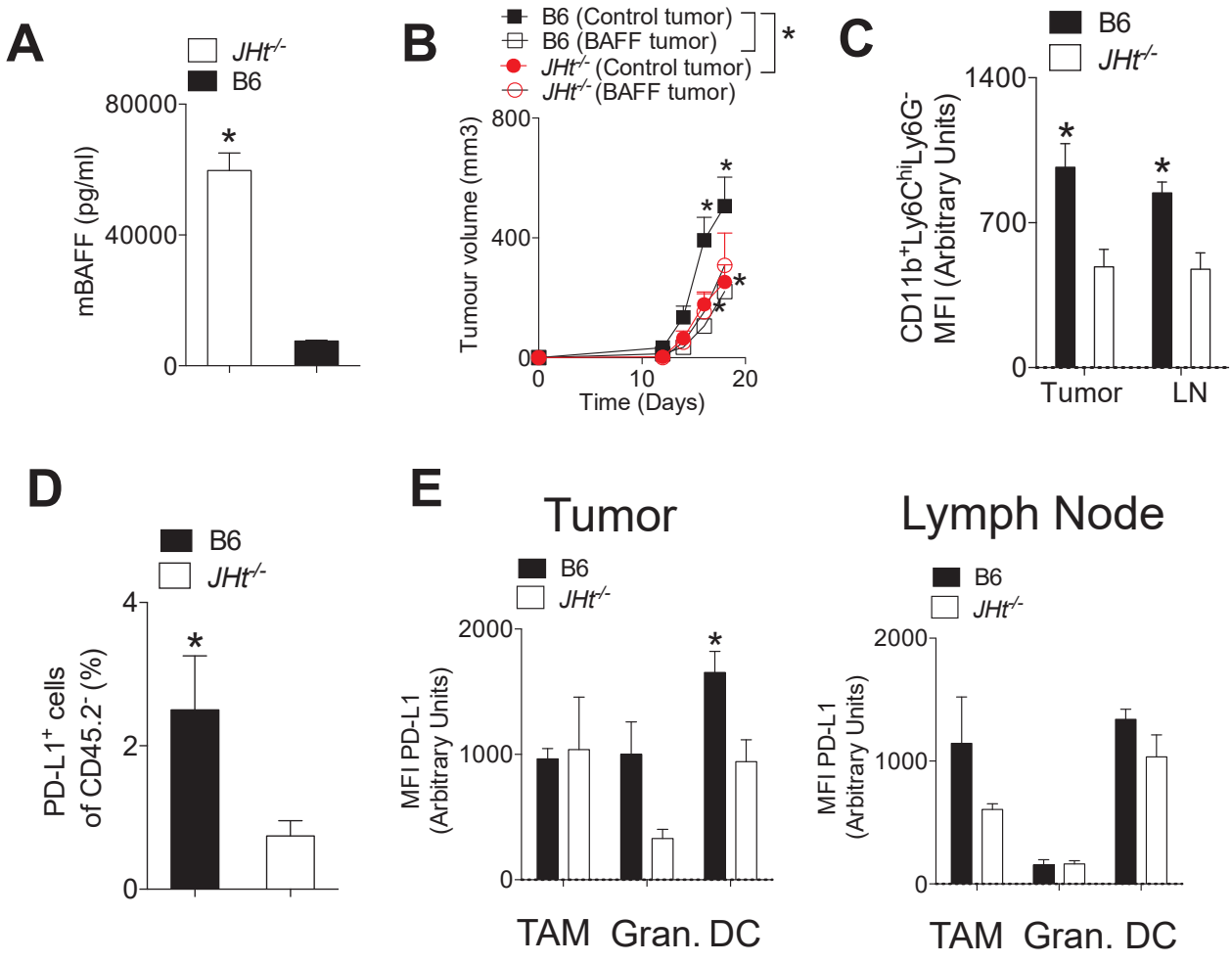

Fig. 20. Higher levels of systemic BAFF in *JHt*$^{-/-}$ mice maintain the difference. (A) Serum BAFF levels in naïve C57BL/6J and *JHt*$^{-/-}$ mice were measured by ELISA (n = 4-5). (B) *JHt*$^{-/-}$ and C57BL/6 mice were inoculated subcutaneously with 5 × 10^5 of BAFF or control cells and tumor growth was followed (n = 4-10, pooled from two independent in vivo experiments). (C) PD-L1 expression on monocytes in tumors and tumor-draining lymph nodes harvested from C57BL/6 and *JHt*$^{-/-}$ mice as assessed by FACS is shown (n = 3-8) as is the (D) percentage of PD-L1 expressing tumoral CD45.2$^-$ cells (n = 7). (E) PD-L1 expression on TAMs, granulocytes (Gran.) and dendritic cells (DC) harvested from tumors and tumor-draining lymph-nodes was assessed by FACS is shown (n = 3-8). Error bars in the all experiments indicate SEM; *P < 0.05 as determined by a Student´s t-test (unpaired, 2 tailed) or a two-way ANOVA with a post-hoc test.

3.2.4 PD-L1 and monocytes are functionally important for BAFF-mediated reduction in tumor growth which is mediated by BAFF-R signaling.

When we stained tumor section harvested from mice bearing BAFF or control tumors, we observed a decrease in Ly6C positive cell infiltrates (Fig. 21A) which was corroborated using FACS analysis (Fig. 21B). Importantly, depletion of monocytes using an anti-CCR2 antibody (Fig. 21C) was critical for the observed phenotype. To confirm the functional importance of PD-L1 to BAFF-mediated repression of PD-L1 expression, we treated mice inoculated with BAFF and control cells with an anti-PD-L1 antibody and found that while the phenotype was maintained with control treatment, it was absent with anti-PD-L1 treatment (Fig. 21D). Next, we wondered whether the observed phenotype is mediated through receptor specific signaling. We therefore injected BAFF and control cells into BAFF-R deficient (*Baffr*$^{-/-}$) mice. The growth differences between BAFF and control tumors was abolished in *Baffr*$^{-/-}$ mice indicating that the phenotype is dependent on BAFF-R signaling (Fig. 21E). Next, we assessed the expression of BAFF-R in the tumor infiltrating immune cells. Using *Baffr*$^{-/-}$ infiltrating lymphocytes as controls, we found that BAFF-R was detected in monocytes present in the inguinal lymph node as well as tumor (Fig. 21F). Furthermore, exogenous addition of BAFF to inflammatory monocytes derived from the bone marrow led to the upregulation of the BAFFr as well as engagers of adaptive immunity MHCII and CD86 (Fig. 21G). Collectively, we have demonstrated that, while myeloid immune infiltrates and tumor cells express PD-L1, the difference in PD-L1 expression between BAFF and control tumors occurs in the infiltrating monocytic populations which are functionally critical for the maintenance of BAFF-mediated differences in tumor growth.

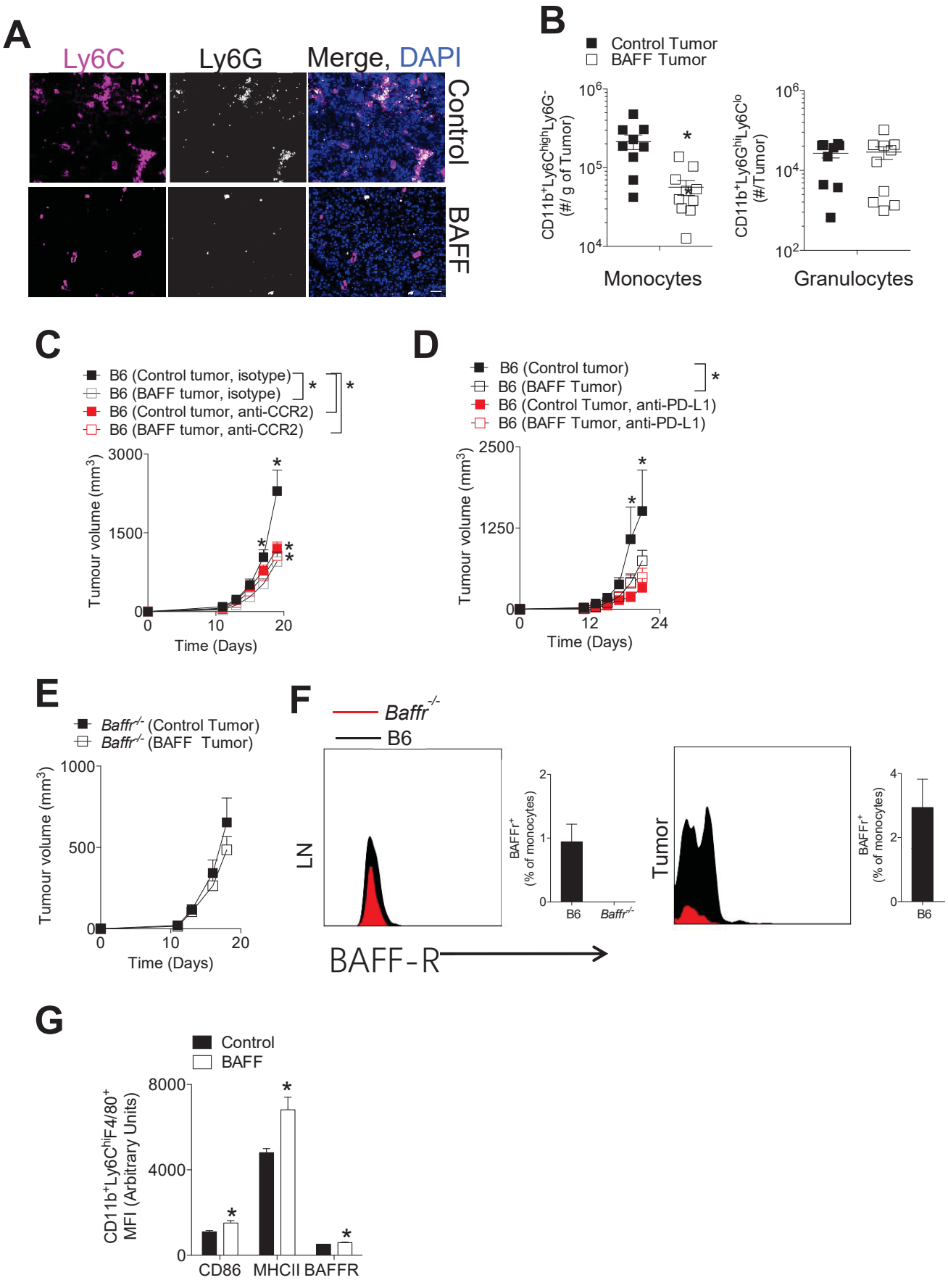
A
Ly6C
Ly6G
Merge, DAPI
Control
BAFF
B
Control Tumor
BAFF Tumor
CD11b+Ly6Chigh Ly6G-
(#/ g of Tumor)
Monocytes
CD11b+Ly6GhiLy6Clo
(#/Tumor)
Granulocytes
C
B6 (Control tumor, isotype)
B6 (BAFF tumor, isotype)
B6 (Control tumor, anti-CCR2)
B6 (BAFF tumor, anti-CCR2)
Tumour volume (mm3)
Time (Days)
D
B6 (Control tumor)
B6 (BAFF Tumor)
B6 (Control Tumor, anti-PD-L1)
B6 (BAFF Tumor, anti-PD-L1)
Tumour volume (mm3)
Time (Days)
E
Baffr-/- (Control Tumor)
Baffr-/- (BAFF Tumor)
Tumour volume (mm3)
Time (Days)
F
Baffr-/-
B6
LN
BAFFr+
(% of monocytes)
Tumor
BAFF-R
G
Control
BAFF
CD11b+Ly6ChiF4/80+
MFI (Arbitrary Units)
CD86
MHCII
BAFFR

Fig. 21. Down regulation of PD-L1 on monocytes is functionally important for the BAFF-mediated reduction in tumor growth. C57BL/6 mice were inoculated subcutaneously with 5×10^5 of BAFF or control cells and tumors were analyzed as indicated. (A) Ly6C and Ly6G protein expression in BAFF and control tumors was assessed using fluorescent immunohistochemistry at day 13 (representative images of n = 5-7 mice are shown). Pictures of 3 different fields of view were obtained of tumors from each independent mouse. Scale bar indicates 50 μm. (B) Numbers of monocyte, granulocyte in BAFF and control tumors were analyzed at the indicating time points post tumor inoculation using FACS analysis (n = 6-13, pooled from at least two independent *in vivo* experiments). (C) C57BL/6 mice treated with monocyte depleting antibody (anti-CCR2) were inoculated subcutaneously with 5×10^5 of BAFF or control cells and tumor growth was followed (n = 6-8, pooled from two independent *in vivo* experiments). (D) C57BL/6 mice treated with anti-PD-L1 antibody were inoculated subcutaneously with 5×10^5 of BAFF or control cells and tumor growth was followed (n = 4-5). (E) *Baffr*$^{-/-}$ mice were inoculated subcutaneously with 5×10^5 of BAFF or control cells and tumor growth was followed (n = 6-9). (F) BAFF-R expression was detected on monocytes in the inguinal lymph node 13 days post-inoculation with control cells and tumor 18 days post-inoculation with control cells as assessed by FACS (n = 4-6). Tumor infiltrates from *Baffr*$^{-/-}$ mice were used as a negative control. (G) Bone marrow derived inflammatory monocytes were treated with 1 ug/ml of BAFF protein for 24 hours 4 days post-isolation from the bone marrow. Expression of MHC-II, CD86 and BAFFR were analyzed using FACS (n = 4). Error bars in the all experiments indicate SEM; *$P < 0.05$ as determined by a Student´s t-test (unpaired, 2 tailed) or a two-way ANOVA with a post-hoc test.

3.2.5 BAFF induces differential gene expression in tumor infiltrating monocytes.

To determine what signaling pathways are affected by BAFF in tumoral monocytes, we sorted tumor-infiltrating monocytes from early tumors (Day 13) and performed RNA-Seq analysis (Fig. 22A). As expected, monocytes sorted from BAFF tumors were characterized by lower PD-L1 mRNA levels (Fig. 22B). Gene set enrichment analysis (GSEA) was implemented to determine prominent pathways altered between monocytes harvested from control and BAFF tumors visualized using Cytoscape (Fig. 23A). Immune response pathways featured prominently and were enriched in monocytes harvested from BAFF expressing tumors. Specifically, regulation of adaptive immune responses, interleukin, NF-κB and Apoptosis signaling pathways were enriched in monocytes harvested from BAFF expressing tumors. By contrast, cell cycle regulation and ECM/Collagen formation pathways were enriched in monocytes harvested from control tumors. Significant, individual genes differentially regulated in regulation of adaptive immune responses, apoptosis and NF-κB signaling pathways are represented in heatmaps (Fig. 23B). Genes involved in the activation of NF-κB signaling (*Tnfrs8*, *Adgrg3*, *Id1*, *Malt1*) were upregulated in monocytes harvested from BAFF tumors while negative regulators (*Traip*, *Gas6*) were downregulated. Pathways responsible for proliferation were enriched in monocytes harvested from control tumors. Fittingly, pro-apoptotic genes (*Fas*, *Tnfsf14*, *Tnfrsf12A*) were down-regulated and pro-survival (*Mybl2*, *Hells*, *Trim2*, *Pik3r3*) genes were up-regulated in monocytes harvested from control tumors. This is in accordance with the decreased numbers of infiltrating monocytes observed in BAFF tumors pointing to an expansion of PD-L1 positive immunosuppressive monocytes in control tumors. Additionally, factors such as Pglyrp1 which is also cytotoxic to cancer cells, were also upregulated in BAFF-tumoral monocytes[238]. Several factors that positively engage the adaptive arm of the immune system were increased in monocytes harvested from BAFF tumors indicating a shift in pro-inflammatory, anti-tumorigenic responses and the activation of $CD8^+$ T and NK cells. Specifically, expression of receptors and factors that activate $CD8^+$ T cells and/or NK cells *Tarm1*, *Cd80*, *Cd86*, *Tnfs14* [239] were up-regulated on monocytes harvested from BAFF tumors. This is further supported by Ingenuity Pathway Analysis (IPA)

which showed that the top upstream regulator in monocytes were IFNγ, TNF-α and IL-1β (Fig. 24A) pointing to an anti-tumorigenic phenotype[240]. In contrast, cell cycle related genes were inactivated in BAFF tumor harvested monocytes (Fig. 24B). Taken together, tumoral BAFF shifts the monocytic phenotype to an anti-tumorigenic state and curbs expansion of PD-L1 positive immune-suppressive monocytes.

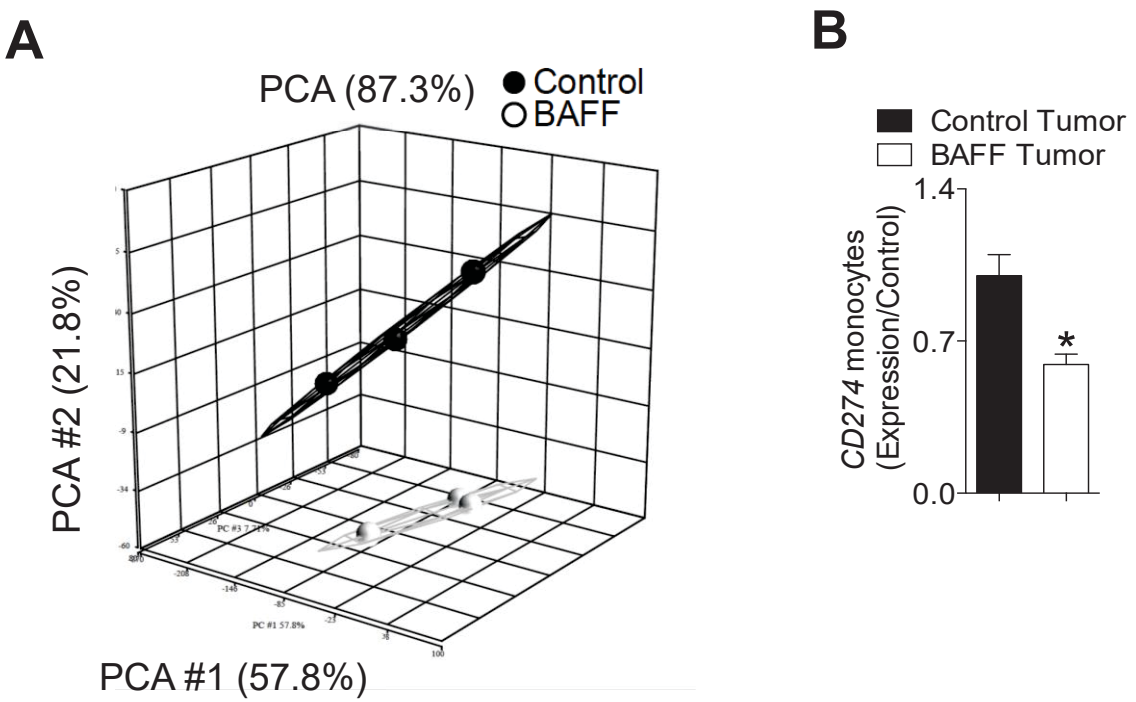

Fig. 22. RNA-Seq analysis in tumor infiltrating monocytes. C57BL/6 mice were inoculated subcutaneously with 5×10^5 of BAFF or control cells. 13 days post-inoculation, monocytes were sorted from BAFF and control tumors. Isolated monocytes were analyzed using RNA-Seq analysis. (A) A PCA plot showing the distribution of the individual samples is shown. (B) Gene expression level of PDL1 was determined in sorted monocytes. Expression was normalized to *GAPDH* and then to control tumors within each independent experiment (n = 7-12, pooled from two independent in vivo experiments). Error bars in all experiments indicate SEM; *P < 0.05 as determined by a Student´s t-test (unpaired, 2 tailed).

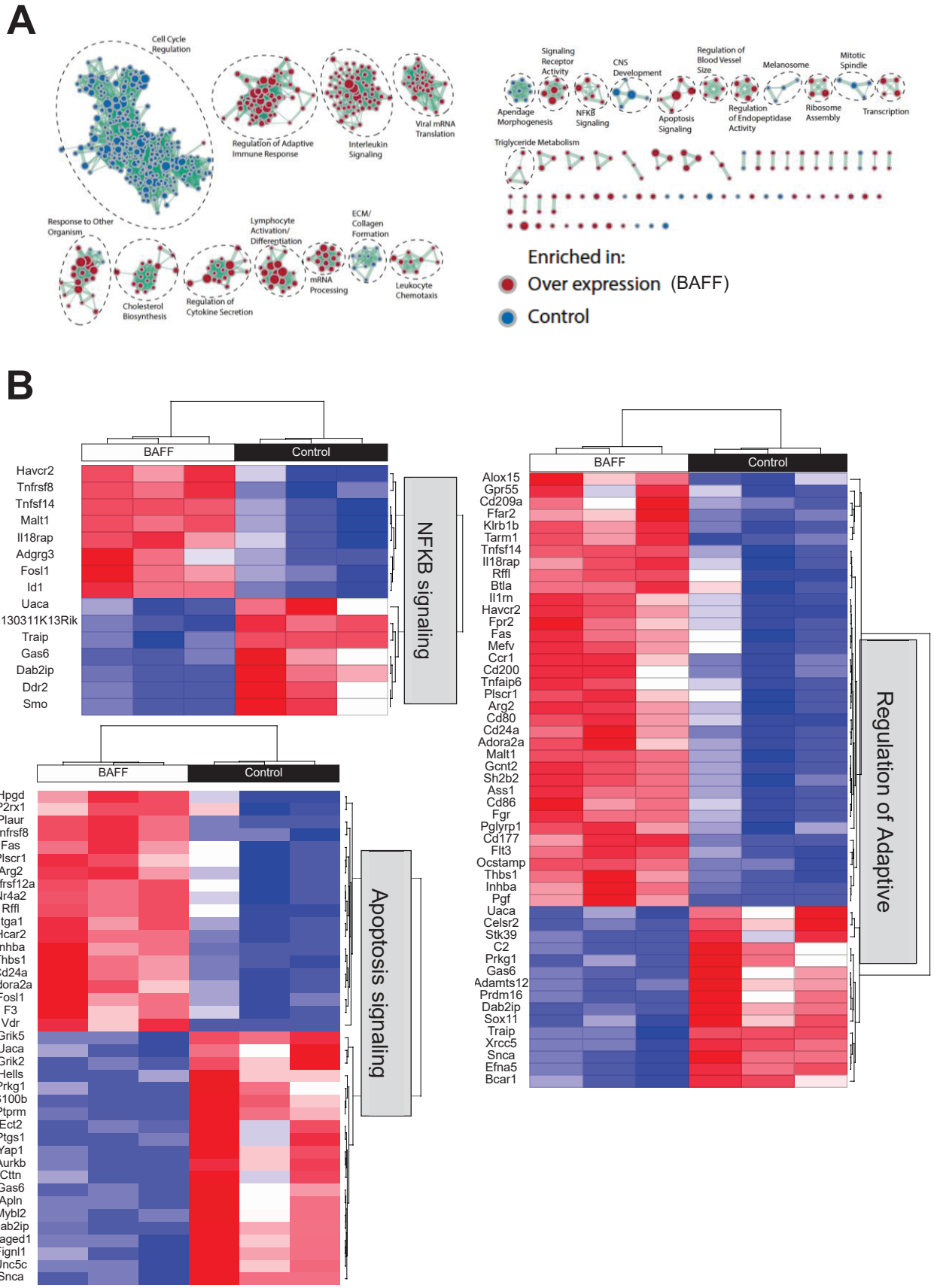
A
Cell Cycle Regulation
Regulation of Adaptive Immune Response
Interleukin Signaling
Viral mRNA Translation
Response to Other Organism
Cholesterol Biosynthesis
Regulation of Cytokine Secretion
Lymphocyte Activation/ Differentiation
mRNA Processing
ECM/ Collagen Formation
Leukocyte Chemotaxis
Signaling Receptor Activity
CNS Development
Regulation of Blood Vessel Size
Melanosome
Mitotic Spindle
Apendage Morphogenesis
NFKB Signaling
Apoptosis Signaling
Regulation of Endopeptidase Activity
Ribosome Assembly
Transcription
Triglyceride Metabolism
Enriched in:
Over expression (BAFF)
Control
B
BAFF
Control
Havcr2
Tnfrsf8
Tnfsf14
Malt1
Il18rap
Adgrg3
Fosl1
Id1
Uaca
E130311K13Rik
Traip
Gas6
Dab2ip
Ddr2
Smo
NFKB signaling
Hpgd
P2rx1
Plaur
Tnfrsf8
Fas
Plscr1
Arg2
Tnfrsf12a
Nr4a2
Rffl
Itga1
Hcar2
Inhba
Thbs1
Cd24a
Adora2a
Fosl1
F3
Vdr
Grik5
Uaca
Grik2
Hells
Prkg1
S100b
Ptprm
Ect2
Ptgs1
Yap1
Aurkb
Cttn
Gas6
Apln
Mybl2
Dab2ip
Maged1
Fignl1
Unc5c
Snca
Apoptosis signaling
Alox15
Gpr55
Cd209a
Ffar2
Klrb1b
Tarm1
Tnfsf14
Il18rap
Rffl
Btla
Il1rn
Havcr2
Fpr2
Fas
Mefv
Ccr1
Cd200
Tnfaip6
Plscr1
Arg2
Cd80
Cd24a
Adora2a
Malt1
Gcnt2
Sh2b2
Ass1
Cd86
Fgr
Pglyrp1
Cd177
Flt3
Ocstamp
Thbs1
Inhba
Pgf
Uaca
Celsr2
Stk39
C2
Prkg1
Gas6
Adamts12
Prdm16
Dab2ip
Sox11
Traip
Xrcc5
Snca
Efna5
Bcar1
Regulation of Adaptive

Fig. 23. BAFF induces differential gene expression in tumor infiltrating monocytes. (A) Gene set enrichment analysis (GSEA) was implemented to determine prominent pathways altered between monocytes harvested from control and BAFF tumors. (B) Significant, individual genes differentially regulated in Regulation of Adaptive Immune Responses, Apoptosis and NF-κB signaling pathways are shown as heatmaps.

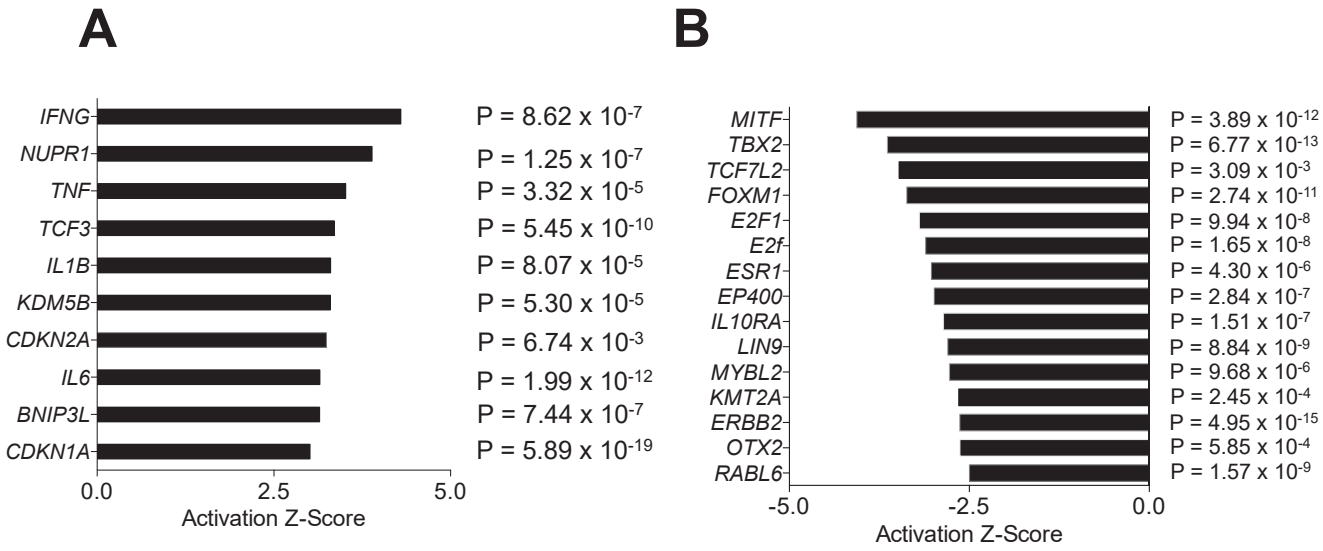

Fig. 24. BAFF induces differential upstream regulator in tumor infiltrating monocytes. (A-B) Top upstream regulator as assessed by Ingenuity Pathway Analysis (IPA) in monocytes harvested form BAFF tumors are shown. (n = 3).

3.2.6 BAFF-triggered differences in tumor growth are mediated by NK cells.

As shown by the RNA-Seq data, monocytes from BAFF tumors were enriched for factors activating cytotoxic lymphocyte $CD8^+$ T and NK cells, which are directly responsible mediating tumor cell death [241]. We therefore wondered about the effects of BAFF on cytotoxic lymphocytes. First, we evaluated tumor infiltrating $CD8^+$ T cells using FACS analysis and found that there were no differences in infiltrating $CD8^+$ T cell numbers between BAFF and control tumors (Fig. 25A). Expression of surface molecule exhaustion markers Programmed Cell Death 1 (PD-1) and interleukin 7 receptor (IL-7R) were not different between $CD8^+$ T cells isolated from BAFF and control tumors (Fig. 25B). Similarly, there was no difference in markers indicating improved T cell immunity such as Granzyme B or Eomes between $CD8^+$ T cells harvested from BAFF and control tumors (Fig. 25B). When *Cd8*$^{-/-}$ mice were inoculated with BAFF and control cells, there were significant differences in tumor growth between BAFF and control tumors (Fig. 25C) indicating that the phenotype is largely not dependent on $CD8^+$ T cells. This finding is not unexpected given that activation of cytotoxic T cells is an MHC class I bound antigen specific process. Although our B16 cells also express the H-2Db-restricted GP33 peptide CTL epitope (residues 33 to 41 of the glycoprotein from the lymphocytic choriomeningitis virus (LCMV)) CTL epitope [242], numbers of tetramer specific $CD8^+$ T cells, while present, were low in the tumor and inguinal lymph node (Fig. 25D).

In addition to $CD8^+$ T cells, cytotoxic lymphocytic elimination of cancer cells can also be mediated by natural killer (NK) cells whose cytotoxic tumor-killing functions are independent of MHC-mediated antigen presentation [241, 243]. BAFF and control tumors were characterized by similar levels of NK infiltrates (Fig. 26A). Upon depletion of NK cells, there was no difference in growth between the BAFF and control tumors (Fig. 26B) indicating that NK cells contribute to the observed phenotype. Indeed, NK cells in BAFF tumors were characterized by increased expression of Granzyme B and IFNγ as compared to NK cells in control tumors (Fig. 26C). The pleiotropic cytokine interferon gamma (IFNγ) which is produced by activated lymphocytes including NK cells, has a complex, often beneficial role in anti-tumor immunity and

has been shown to be an effector of cytotoxic NK cells [243]. When we inoculated IFNγ knockout mice (*Ifng*$^{-/-}$) with BAFF and control tumor cell lines, there was no difference between BAFF tumor and control tumor growth (Fig. 26D). The growth of both BAFF and control tumors in the *Ifng*$^{-/-}$ mice was comparable to the control tumors in B6 mice. There were no differences in tumoral IFNγ levels at the early time points although at day 18 post tumor inoculation IFNγ levels were higher in BAFF tumors but comparisons are difficult due to the size differential between BAFF and control tumors at the later time points (Fig. 26E). Addition of BAFF to *ex vivo* cultures of NK cells did not alter their ability to kill target cells (Fig. 26F) indicating that the engagement of the other immune infiltrates is needed to alter their phenotype in the context of BAFF and control tumors. However, when we isolated monocytes from BAFF and control tumors and added them to *ex vivo* cultures of NK cells and RMA/S cells, there was no difference in NK cell killing ability (Fig. 26G). Taken together, while NK cells rather than $CD8^+$ T cells were the main contributors to the observed growth differences between BAFF and control tumors, the effects are likely not mediated between a direct monocyte-NK cell interaction.

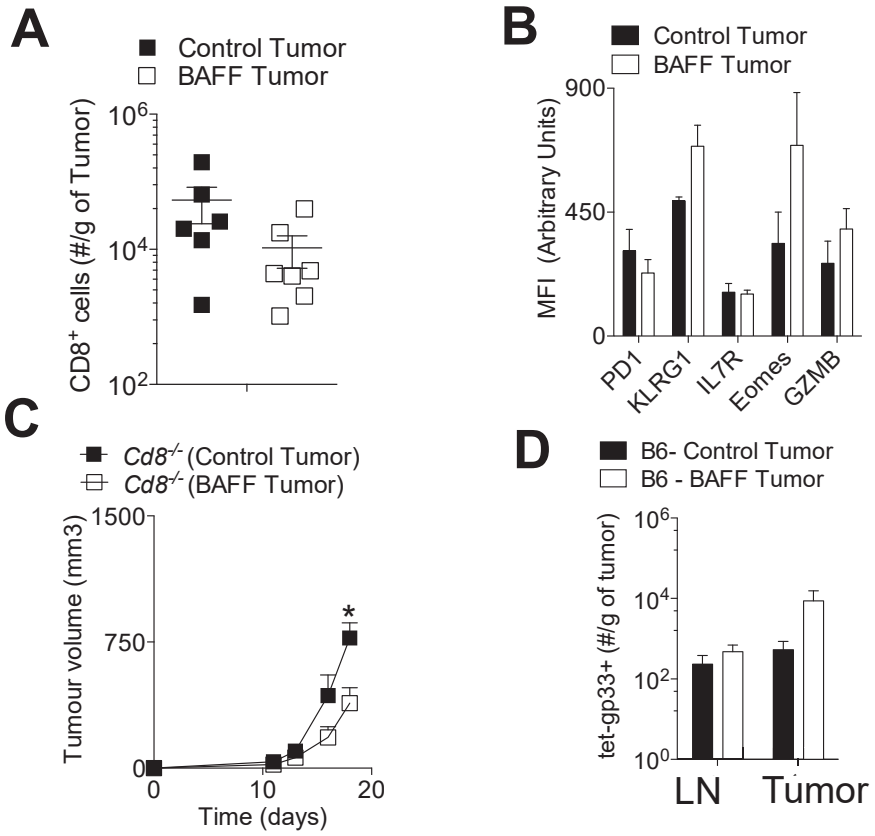

Fig. 25. BAFF-triggered difference in tumor growth is not dependent on T cells. (A-C) C57BL/6 mice were inoculated subcutaneously with 5×10^5 of BAFF or control cells and tumors were analyzed as indicated. (A) Numbers of $CD8^+$ T cell infiltrates in BAFF and control tumors were analyzed at the indicating time points post tumor inoculation using FACS analysis (n = 6-7, pooled from two independent in vivo experiments). (B)Tumor infiltrating $CD8^+$ T cells were stained for markers of activation and exhaustion using FACS analysis (n = 3-9). (C) *Cd8*$^{-/-}$ mice were inoculated subcutaneously with 5×10^5 of BAFF or control cells and tumor growth was followed (n = 3-6). (D) Numbers of gp-33 specific tetramer $CD8^+$ T in BAFF and control tumors as well as inguinal lymph nodes were analyzed at day 13 post tumor inoculation using FACS analysis (n = 3-4). Error bars in the all experiments indicate SEM; *P < 0.05 as determined by a Student´s t-test (unpaired, 2 tailed).

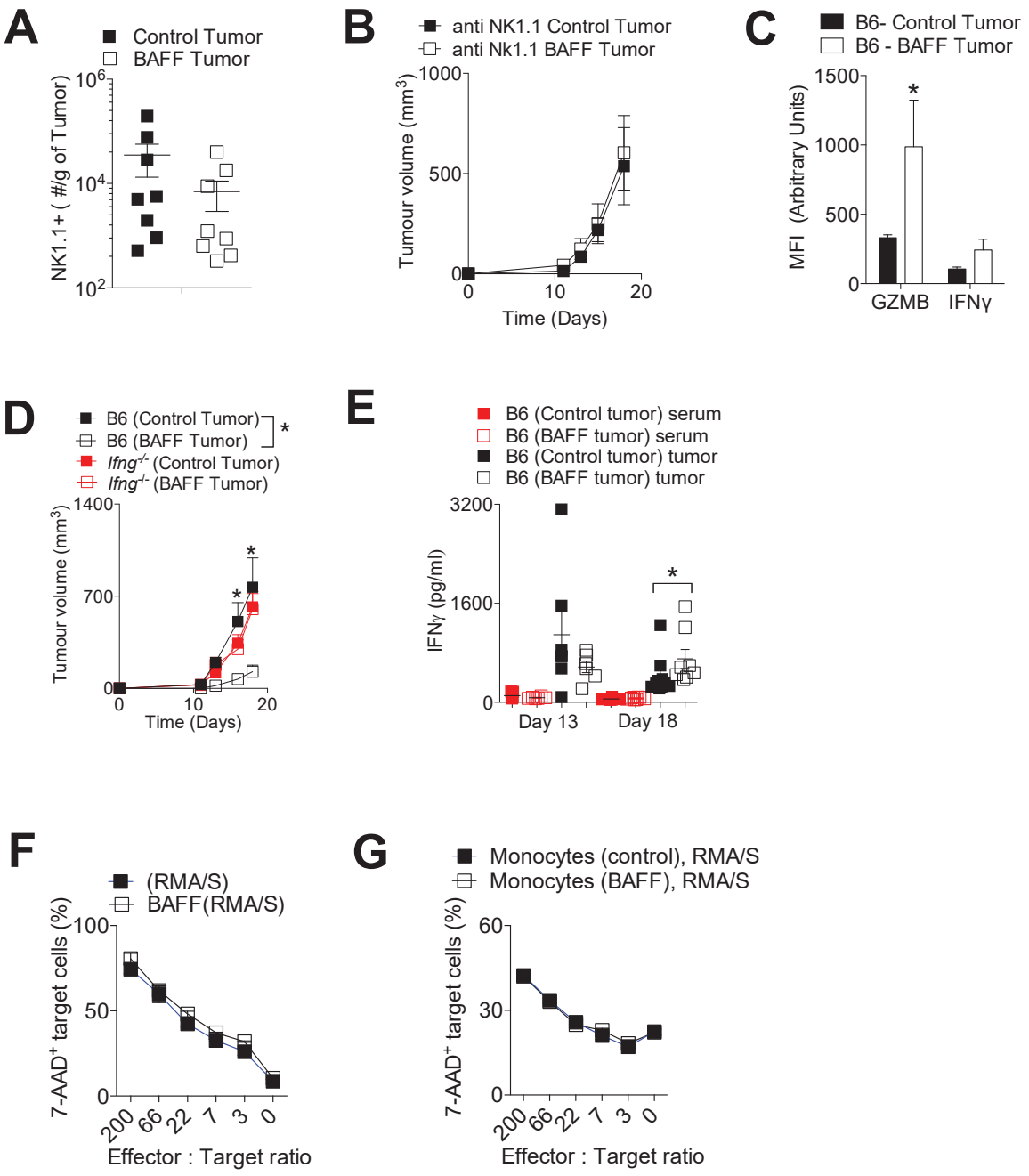
A
Control Tumor
BAFF Tumor
NK1.1+ (#/g of Tumor)
B
anti NK1.1 Control Tumor
anti Nk1.1 BAFF Tumor
Tumour volume (mm3)
Time (Days)
C
B6- Control Tumor
B6 - BAFF Tumor
MFI (Arbitrary Units)
GZMB
IFNγ
D
B6 (Control Tumor)
B6 (BAFF Tumor)
Ifng-/- (Control Tumor)
Ifng-/- (BAFF Tumor)
Tumour volume (mm3)
Time (Days)
E
B6 (Control tumor) serum
B6 (BAFF tumor) serum
B6 (Control tumor) tumor
B6 (BAFF tumor) tumor
IFNγ (pg/ml)
Day 13
Day 18
F
(RMA/S)
BAFF(RMA/S)
7-AAD+ target cells (%)
Effector : Target ratio
G
Monocytes (control), RMA/S
Monocytes (BAFF), RMA/S
7-AAD+ target cells (%)
Effector : Target ratio

Fig. 26. NK cells mediate BAFF-triggered differences in tumor growth. (A) C57BL/6 mice were inoculated subcutaneously with 5×10^5 of BAFF or control cells. Numbers of $NK1.1^+$ cell infiltrates in BAFF and control tumors were analyzed at day 13 post tumor inoculation using FACS analysis (n = 8-10, pooled from two independent *in vivo* experiments). (B) C57BL/6 mice treated with NK cell depleting antibody (anti-Nk1.1) were inoculated subcutaneously with 5×10^5 of BAFF or control cells and tumor growth was followed (n = 5, pooled from two independent *in vivo* experiments). (C) Granzyme B (GZMB) and IFNγ intracellular expression was measured in tumor infiltrating NK1.1 cells using FACS analysis at day 13 post tumor inoculation (n = 4-5). (D) *Ifng*$^{-/-}$ and C57BL/6 mice were inoculated subcutaneously with 5×10^5 of BAFF or control cells and tumor growth was followed (n = 5-8, pooled from two independent *in vivo* experiments). (E) The levels of IFNγ in BAFF and control tumors were determined using ELISA at the indicated time points (n = 6-10), pooled from two independent *in vivo* experiments). (F) The cytotoxic activity of BAFF (250 ng/ml) treated NK cells to RMA/S cell was measured at the indicated effector/target ratios (n = 3). (G) The NK cells combined with monocytes harvest from BAFF or control tumors to kill RMA/S cell was measured at the indicated effector/target ratios (n = 3). Error bars in the all experiments indicate SEM; *$P < 0.05$ as determined by a Student´s t-test (unpaired, 2 tailed) or a two-way ANOVA with a post-hoc test.

4 Discussion

4.1 Anti-tumor effect of small molecules in melanoma [201]

Our screen identified several potential hits with anti-melanoma activity including serotonin agonists and other compounds, such as statins, anthelmintics and antifungals which are already being re-purposed as anti-cancer agents pre-clinically or in the clinical setting. The serotonin signaling class of compounds that were positive hits in the original screen included serotonin agonists as well as the anti-depressants indatraline and maprotiline. The latter two are multi-functional and not only prevent the re-uptake of serotonin but also dopamine and norepinephrine and did not have appreciable anti-melanoma activity when compared to the other compounds in the serotonin signaling class including TM. Serotonin signaling occurs when serotonin, a neurotransmitter present in the gut, blood platelets and the central nervous system (CNS), binds to serotonin receptors (5-HTRs) resulting in complex physiological and behavioral changes affecting mood, cognition, digestion, pain perception [214, 244]. The pharmacological opportunities to modulate these physiological processes and impact human disease are vast and have resulted in a plethora of 5-HTR agonist and antagonist ligands. There are seven families of human serotonin receptors mostly part of the G-protein coupled receptor family differentially expressed throughout the CNS, liver, kidney, heart, gut [214]. We were intrigued by the possibility of investigating TM because the role of serotonin signaling in cancer remains controversial. Serotonin and 5-HTR2A agonists were found to induce melanogenesis in melanoma cell lines [245]. Jiang et al. reported increased levels of serotonin and 5-HTR2B in human pancreatic ductal adenocarcinomas which promoted pancreatic tumor growth in mice [246]. Many other studies have similarly reported growth stimulatory effects of serotonin signaling through various 5-HTRs and inhibitory effects of 5-HTR antagonists in many tumor types [247, 248]. However, there have also been reports, albeit much fewer, suggesting that treatment with serotonin agonists might also have anti-cancer effects in glioma [249] and breast cancer cells [250]. Involvement within the autocrine loops and

activation of the MAPK, JNK, PI3K/Akt/mTOR [246, 247] pathways has been implicated in serotonin's mitogenic role.

We did not observe any pro or anti-mitogenic effects following treatment with serotonin (5-HT) in melanoma cells. Co-treatment of TM with 5-HT did not affect the compound's ability to induce apoptosis in the melanoma cells. This suggests that the affinity of the synthetic ligand TM is stronger for the 5-HTR's than for the natural ligand 5-HT, and/or that the pro-apoptotic effects of TM can be uncoupled from serotonin signaling. Treatment with 5-HTR ligands, agonists or antagonist presents a complex scenario. As previously reported [247] treatment with one ligand can yield opposing concentration dependent results. Serotonin signaling following TM treatment might occur through other 5-HTRs. TM has been reported to be an agonist for the 5-HTR1A-D and an antagonist for 5-HTR2A-B [251]. In our case, we used doses in the low micromolar range, high enough to elicit tumor apoptosis inducing pleiotropic effects [251, 252]. Although we did not observe significant changes in cAMP levels and 5-HT responsive genes following TM treatment in most of the cell lines, increased p-CREB levels were observed in the SH4 and MEL-JUSO cells suggesting a possible involvement of other serotonin receptors including ones previously unidentified as being targets for TM. However, other antagonists and agonists present in the screen including the 5-HTR4 agonists (Cisparide) that did not have any anti-cancer effects further suggesting that TM is uniquely acting to distinctly target other molecules, likely upstream receptors or kinases upstream of the PI3K/Akt/mTOR pathways.

The current repertoire of clinically approved treatment options in melanoma encompasses agents that inhibit proliferation and induce cell death [253]. This includes targeted inhibitors of the BRAF pathway and checkpoint inhibitors. The former class of agents such as Vemurafenib cause cell arrest and trigger apoptosis [230, 254] while the checkpoint inhibitors cause immunogenic cell death through lytic and apoptotic cell death mediated by activated $CD8^+$ T and NK cells respectively [253, 255]. Resistance to the targeted inhibitors and variable checkpoint inhibitor response rates has shifted the focus in recent years interest to finding novel combination treatments to overcome resistance and increase response rates [256]. Strategies include targeting other forms of

cell death such as necroptosis [257], inhibiting MAPK reactivation that occurs following targeted therapy treatment, and concomitantly inhibiting other pathways including the PI3K/Akt/mTOR [258, 259].

Recently, a report has shown phosphorylation of S6 to be a marker of sensitivity to BRAF mutated melanoma and that suppression of S6 after MAPK treatment was a predictor of progression-free survival [219]. In our investigation, TM's suppression of p-S6 and its strong synergy with vemurafenib in BRAF mutated human melanoma cell lines is in accordance with the above report. Importantly, TM also suppressed S6 phosphorylation in non-BRAF mutated melanoma cell lines indicating a broader therapeutic potential of TM in patients without the BRAF mutation but where the PI3K/Akt/mTOR pathway is activated such as in patients harboring NRAS mutations [259]. The suppression of S6 phosphorylation is likely mediated by decreased mTORC1 activity as phosphorylation of the direct upstream regulator of S6, p70 S6 kinase was also blunted. mTORC1 integrates several upstream pathways related to cellular growth and metabolism including MAPK through RSK [218], PI3K/Akt [221] as well as the liver kinase B1 (LKB1)-adenosine monophosphate-activated protein kinase (AMPK) [260]. As TM did not perturb the MAPK pathway but decreased Akt phosphorylation at a residue known to be phosphorylated by mTORC2 [223], it's likely that S6 is affected through the PI3K/Akt pathway although the potential contribution of AMPK would also have to be explored. Interestingly, Yoon et al. found that dual mTORC1/2 inhibition following treatment with Torin1 in A375 melanoma cells induced focal adhesion re-organization increased the size of focal adhesions and increased migration and invasion in vitro [225]. TM did not phenocopy Torin 1 using B16F10 cells, as treatment with TM decreased the number of metastases in vivo in an immuno-competent murine model where the presence of tumor infiltrating lymphocytes was considered. The immunosuppressive and pro-tumorigenic contribution of regulatory $CD4^+$ T cells in the tumor microenvironment is well established [261]. As the infiltration and FOXP3 expression on regulatory $CD4^+$ T cells in TM treated tumors was decreased, this likely contributes to TM's anti-cancer effects *in vivo*.

Tegaserod (Zelnorm, Zelmac) which is used for the treatment of irritable bowel syndrome (IBS) [262, 263] was also shown to be effective against chronic constipation [264]. Although Tegaserod was well-tolerated and effective, it was removed off the market in the Unites States in 2007 at the FDA's request [265] chiefly due cardiovascular (CV) safety concerns raised through retrospective clinical trial analysis. However, all adverse cardiovascular events occurred in patients with CV disease and/or CV risk factors. Furthermore, the link between Tegaserod and adverse CV outcomes was not recapitulated in subsequent epidemiological studies [266, 267] which found no association between Tegaserod use and adverse CV's. The tolerability and availability of the drug would likely outweigh the relatively low cardiovascular risk (0.1%) associated with Tegaserod usage especially in melanoma patients with few treatment options. *In vivo*, TM retarded decreased metastatic and primary tumor growth, induced apoptosis and suppressed p-Akt and p-S6 in tumor cells. TM is available in generic form and has the potential to be re-purposed as an anti-melanoma agent. The dose we used in mice is roughly equivalent to a Human Equivalent Dose (HED) [268]. Given that TM is available as a 6 mg pill administered twice daily, the doses we used in our in vivo studies are within the physiological range. Furthermore, as the compound synergized with Vemurafenib and other kinase inhibitors currently used in melanoma patients with late-stage disease, this is likely a favorable point of clinical entry especially since most patients eventually develop resistance to Vemurafenib and other kinase inhibitors [256, 258]. Furthermore, as the BRAF WT cohort of patients are a diverse group, treatment options are much less clear cut [253, 269] although immunotherapies, as with $BRAF^{V600E}$ melanoma are a promising albeit costly treatment approach [108]. Currently there are a lot of different combinations in clinical trials using MEK in combination with inhibitors of the PI3K/AKT/mTOR axis (NCT01941927, NCT01363232, NCT01337765) [269].

4.2 Function of BAFF in melanoma

BAFF plays a crucial role in anti-tumor immunity through its effects on immune cells within the TME, lymph nodes and systemic circulation. While the recent study by Yarchoan et al. has focused on the application of systemic BAFF and effects on B cells [200], through tumor-specific expression of BAFF, we found that monocytes were critical to maintaining the delay in tumor growth in BAFF expressing tumors. Within the TME, monocytes are crucial in maintaining an immunosuppressive, pro-tumorigenic phenotype that can hinder immunotherapy and this has been demonstrated in several tumor types including melanoma [236, 270-274]. Monocytes, particularly PD-L1 positive monocytes also termed myeloid-derived suppressor cells (MDSC), can exert their immunosuppressive effects through inhibition of anti-tumor functions of T and NK cells, secretion of immunoregulatory cytokines and presentation of surface inhibitory molecules [236, 271, 275].

In our model system, monocyte numbers were decreased in BAFF tumors indicating that BAFF inhibited their infiltration and/or expansion within the TME. Given that pro-apoptotic genes were upregulated and proliferation genes downregulated in monocytes harvested from BAFF tumors, the latter explanation is plausible. Positive regulators of NF-κB signaling were upregulated in monocytes harvested from BAFF tumors while negative regulators were downregulated. Signaling cascades caused by binding of BAFF to the BAFF-R are mediated NF-κB signaling. As BAFF-R was detected on monocytes in the tumor draining lymph node and TME and the phenotype was abrogated in *Baffr*$^{-/-}$ mice, we postulate that forward signalling directly through the BAFF receptor on monocytes is occurring in our system. This is supported by studies that have demonstrated the direct effects of BAFF on monocytes and cell lines. Chang et al. found that *ex vivo* treatment with BAFF promoted activation and differentiation of primary monocytes that expressed TACI following stimulation with BAFF or IL-10 [276]. Others have shown that BAFF-mediated reverse or forward signalling in the monocytic THP-1 cell line inhibited trans-migrational and phagocytic activities and increased inflammatory activation [184, 185]. BAFF mediated forward

signalling can occur when BAFF is solubilized or tethered [147]. Although soluble BAFF was detected in *in vitro* cultured BAFF cells, within the context of the tumor micro-environment, increased BAFF expression was detected via immunofluorescent surface staining. Although the BAFF antibody was raised against soluble portion of BAFF and the antibody would recognize both tethered and soluble BAFF, the lack of difference in soluble BAFF as measured by ELISA suggests that the BAFF in our system was not cleaved.

The resulting lower expression of PD-L1 on tumor infiltrating monocytes in BAFF tumors is likely a result of a general shift in balance in monocytic immunosuppressive functions rather than a direct consequence of BAFF-induced signaling. Furthermore, it remains to be elucidated how PD-L1 was downregulated on CD45.2^{-} cells. However, clearly the differences in PD-L1 monocytic and/or tumoral expression have functional consequences as blocking PD-L1 using a monoclonal antibody abrogated the phenotype *in vivo.* Although many studies investigating the PD-1/PD-L1 axis have focused on the suppressive effects of exhausted T cells [277, 278], PD-L1 signaling can also affect other immune populations. Hartley et al. demonstrated that PD-L1 signaling in TAMs impacted tumor growth and that treatment with an anti-PD-L1 antibody decreased PD-L1 mediated constitutive negative signals to macrophages. TAM activation through stimulation with an anti-PD-L1 antibody increased anti-tumor effects through mTOR pathway activity and increased inflammatory activity [279]. Tumor-bearing *Rag*$^{-/-}$ mice, which lack T and B cells, were responsive to combined anti-PD-L1 and anti-PD1 therapy suggesting that the expression of PD-L1 on immune cells influences their immunosuppressive phenotype and can subsequently shape the tumor micro-environment independently of T cells.

Upregulation of PD-L1 in the tumor microenvironment has been shown to be mediated by IFNγ [280] and interferon receptor signaling pathways [281] as well as by monocyte-derived IL-10 [270] and TNF-α [282]. Although IFNγ was shown to be crucial for the growth difference maintenance between BAFF and control tumors, it is likely not a causative factor for the differences in PD-L1 expression as there was no difference in IFNγ levels within the tumor at the early time point and higher secreted

IFNγ in BAFF tumors at later time points. Secreted IL-10 within the tumor was not detectable and, as determined by tumor expression data, there were also no difference in interferon signalling and TNF-α making it unlikely that decreased PD-L1 expression on monocytes within BAFF tumors was caused by these factors. mRNA expression of platelet-derived growth factor subunit B *(PDGF2)* and fibroblast growth factor receptor 1 (*FGFR1*) was downregulated in BAFF tumors and it's possible that this difference contributed to the observed differences in PD-L1 expression. In a syngeneic breast tumor model, inhibition of FGFR1 was recently shown to enhance the immunogenicity of the pulmonary tumor microenvironment and reduce the numbers of myeloid suppressor cells [283, 284]. Thus, the possible contribution of these factors in shaping the TME remains to be further explored. Taken together host and tumor derived PD-L1 expression particularly in the myeloid compartment is crucial regulating anti-tumor immunity and is involved in tumor evasion in cell lines of varying immunogenicity [285].

In the B16.F10 melanoma system, NK cell depletion abolished the difference in growth between BAFF and control tumors, and we can conclude that NK-mediated cytotoxicity plays a crucial role in maintaining the phenotype. NK cytotoxic effector function is governed by a balance between expression of inhibitory and activating receptors on NK cells and their subsequent interactions with corresponding ligands[243]. Others have shown that monocytes can directly inhibit NK cytotoxicity including through the PD-1/PD-L1 axis [286, 287] and that PD-1 plays a role in NK cell cytotoxic functions [288]. In our experimental system, decreased PD-L1 expression on monocytes might increase NK cell activation. However, as *ex vivo* incubation of NK cells, monocytes and BAFF did not lead to increased NK cytotoxicity we cannot state that this is the case in our system. However, the limitation of an *ex vivo* assay in recapitulating the TME, does not entirely rule out this possibility. Furthermore, the role of tumoral BAFF on $CD8^+$ T cells in a more immunogenic system should be further explored especially as Yarchoan et al. demonstrated that systemic BAFF increased TH1 polarization [200]. Although *CXCL9* mRNA was increased in control tumors, we observed no differences in $CD8^+$ T cell infiltrates, function and exhaustion/activation

markers. The chemokine Cxcl9 is produced by myeloid cells and can have both context specific anti and pro-tumoral roles within the TME [289] and its function in our system is subject to further investigation.

Increasing BAFF levels within the tumor could be an attractive therapeutic option. As already shown by Yarchoan et al., this could be accomplished by use of BAFF as a vaccine adjuvant [200] and/or incorporation of BAFF into virus-based therapeutic vaccines or oncolytic viruses. To increase antigen processing through the endoplasmic reticulum (ER), Wu et al. fused BAFF with an E7 antigen in a tumor-specific DNA vaccine and found that the presence of BAFF enhanced E7-specific $CD8^+$ T cell responses [290]. Another strategy would be to trigger tumor-infiltrating cells to produce BAFF within the tumor micro-environment. It is expected that therapies which currently attempt to increase T cell stimulation and IFNγ production might also result in increased BAFF production from infiltrating innate immune cells. However, the unintended consequences of raising tumoral BAFF levels in the context of applied immunotherapies and decreased PD-L1 expression require further exploration.

5 Conclusion

To screening out new effective molecules for melanoma treatment, we identified a compound, Tegaserod, that was effective in inducing apoptosis in both $BRAF^{V600E}$ and BRAF WT melanoma. Tegaserod blunted phosphorylation of S6 through inhibition of the PI3K/Akt/mTOR pathway *in vitro* and *in vivo*. Tegaserod synergized with Vemurafenib in $BRAF^{V600E}$ human cell lines and could also be combined with Cobimetinib in BRAF WT cell lines. Tegaserod has the potential to be readily translated to the clinic especially in the case of BRAF WT melanoma where fewer approved treatment options exist.

To better understand the contribution of the BAFF cytokine in the solid tumor microenvironment, we generated BAFF overexpressing melanoma cell lines and examined the ability to influence primary tumor growth. We identified a novel role for the BAFF cytokine in the context of melanoma tumor growth. We have shown BAFF to decrease the numbers and suppressive phenotype of infiltrating monocytes and as a consequence, alleviate the immunosuppressive tumor environment. Taken together, the second section in this thesis highlights the important role of BAFF in anti-tumor immunity.

6 References

1. *Globocan 2018, International Agency for Research on Cancer, World Health Organization.* 2018.
2. *Globocan 2020, International Agency for Research on Cancer, World Health Organization.* 2020.
3. *GLOBOCAN 2020. Melanoma of skin. Available from:https://gco.iarc.fr/today/data/factsheets/cancers/16-Melanoma-of-skin-fact-sheet.pdf.* 2020.
4. Hanahan, D. and R.A.J.c. Weinberg, *Hallmarks of cancer: the next generation.* 2011. **144**(5): p. 646-674.
5. Abdel-Malek, Z., et al., *The melanocortin-1 receptor and human pigmentation.* Ann N Y Acad Sci, 1999. **885**: p. 117-33.
6. Abdel-Malek, Z., et al., *Mitogenic and melanogenic stimulation of normal human melanocytes by melanotropic peptides.* Proc Natl Acad Sci U S A, 1995. **92**(5): p. 1789-93.
7. Lerner, A.B. and J.S. McGuire, *Melanocyte-Stimulating Hormone and Adrenocorticotrophic Hormone. Their Relation to Pigmentation.* N Engl J Med, 1964. **270**: p. 539-46.
8. Tsatmali, M., J. Ancans, and A.J. Thody, *Melanocyte function and its control by melanocortin peptides.* J Histochem Cytochem, 2002. **50**(2): p. 125-33.
9. Linos, E., et al., *Increasing Burden of Melanoma in the United States.* Journal of Investigative Dermatology, 2009. **129**(7): p. 1666-1674.
10. Erdei, E. and S.M. Torres, *A new understanding in the epidemiology of melanoma.* Expert Review of Anticancer Therapy, 2010. **10**(11): p. 1811-1823.
11. *American Cancer Society. Cancer facts and figures. Atlanta:American Cancer Society.* 2020.
12. Rastrelli, M., et al., *Melanoma: Epidemiology, Risk Factors, Pathogenesis, Diagnosis and Classification.* In Vivo, 2014. **28**(6): p. 1005-1011.
13. Raimondi, S., M. Suppa, and S. Gandini, *Melanoma Epidemiology and Sun Exposure.* Acta Derm Venereol, 2020. **100**(11): p. adv00136.
14. Armstrong, B.K., A.J.J.o.p. Kricker, and p.B. Biology, *The epidemiology of UV induced skin cancer.* 2001. **63**(1-3): p. 8-18.
15. O'Sullivan, D.E., et al., *Estimates of the current and future burden of melanoma attributable to ultraviolet radiation in Canada.* 2019. **122**: p. 81-90.
16. Gandini, S., et al., *Meta-analysis of risk factors for cutaneous melanoma: II. Sun exposure.* 2005. **41**(1): p. 45-60.
17. Gielen, M., et al., *Body mass index is negatively associated with telomere length: a collaborative cross-sectional meta-analysis of 87 observational studies.* American Journal of Clinical Nutrition, 2018. **108**(3): p. 453-475.
18. Popinat, G., et al., *Sub-cutaneous Fat Mass measured on multislice computed tomography of pretreatment PET/CT is a prognostic factor of stage IV non-small cell lung cancer treated by nivolumab.* Oncoimmunology, 2019. **8**(5).
19. Newton-Bishop, J.A., et al., *Serum 25-Hydroxyvitamin D(3) Levels Are Associated With Breslow Thickness at Presentation and Survival From Melanoma.* Journal of Clinical Oncology, 2009. **27**(32): p. 5439-5444.

20. O'Shea, S.J., J.R. Davies, and J.A. Newton-Bishop, *Vitamin D, vitamin A, the primary melanoma transcriptome and survival.* British Journal of Dermatology, 2016. **175**: p. 30-34.
21. Bishop, D.T., et al., *Geographical variation in the penetrance of CDKN2A mutations for melanoma.* Journal of the National Cancer Institute, 2002. **94**(12): p. 894-903.
22. Potrony, M., et al., *Update in genetic susceptibility in melanoma.* Annals of Translational Medicine, 2015. **3**(15).
23. Begg, C.B., et al., *Lifetime risk of melanoma in CDKN2A mutation carriers in a population-based sample.* Jnci-Journal of the National Cancer Institute, 2005. **97**(20): p. 1507-1515.
24. Puntervoll, H.E., et al., *Melanoma prone families with CDK4 germline mutation: phenotypic profile and associations with MC1R variants.* Journal of Medical Genetics, 2013. **50**(4): p. 264-U82.
25. Horn, S., et al., *TERT promoter mutations in familial and sporadic melanoma.* Science, 2013. **339**(6122): p. 959-61.
26. Aoude, L.G., et al., *Nonsense mutations in the shelterin complex genes ACD and TERF2IP in familial melanoma.* J Natl Cancer Inst, 2015. **107**(2).
27. Robles-Espinoza, C.D., et al., *POT1 loss-of-function variants predispose to familial melanoma.* Nat Genet, 2014. **46**(5): p. 478-481.
28. Wiesner, T., et al., *Germline mutations in BAP1 predispose to melanocytic tumors.* Nat Genet, 2011. **43**(10): p. 1018-21.
29. Aoude, L.G., et al., *POLE mutations in families predisposed to cutaneous melanoma.* Fam Cancer, 2015. **14**(4): p. 621-8.
30. Wadt, K.A., et al., *Germline RAD51B truncating mutation in a family with cutaneous melanoma.* Fam Cancer, 2015. **14**(2): p. 337-40.
31. Gudbjartsson, D.F., et al., *ASIP and TYR pigmentation variants associate with cutaneous melanoma and basal cell carcinoma.* Nat Genet, 2008. **40**(7): p. 886-91.
32. Bastian, B.C., *The molecular pathology of melanoma: an integrated taxonomy of melanocytic neoplasia.* Annu Rev Pathol, 2014. **9**: p. 239-71.
33. Law, M.H., et al., *Genome-wide meta-analysis identifies five new susceptibility loci for cutaneous malignant melanoma.* Nat Genet, 2015. **47**(9): p. 987-995.
34. NEWTON-BISHOP, J.A., D.T. Bishop, and M.J.A.d.-v. Harland, *Melanoma Genomics.* 2020. **100**.
35. Roh, M.R., et al., *Genetics of melanocytic nevi.* 2015. **28**(6): p. 661-672.
36. Hodis, E., et al., *A landscape of driver mutations in melanoma.* 2012. **150**(2): p. 251-263.
37. Yan, J., et al., *Increased AURKA Gene Copy Number Correlates with Poor Prognosis and Predicts the Efficacy of High-dose Interferon Therapy in Acral Melanoma.* 2018. **9**(7): p. 1267.
38. Chernoff, K.A., et al., *GAB2 amplifications refine molecular classification of melanoma.* 2009. **15**(13): p. 4288-4291.
39. Yeh, I., et al., *Targeted genomic profiling of acral melanoma.* 2019. **111**(10): p. 1068-1077.
40. Sauter, E.R., et al., *Cyclin D1 is a candidate oncogene in cutaneous melanoma.* 2002. **62**(11): p. 3200-3206.
41. Curtin, J.A., et al., *Distinct sets of genetic alterations in melanoma.* 2005. **353**(20): p. 2135-2147.

42. Liang, W.S., et al., *Integrated genomic analyses reveal frequent TERT aberrations in acral melanoma.* 2017. **27**(4): p. 524-532.
43. Wan, P.T., et al., *Mechanism of activation of the RAF-ERK signaling pathway by oncogenic mutations of B-RAF.* 2004. **116**(6): p. 855-867.
44. Mitin, N., K.L. Rossman, and C.J.J.C.B. Der, *Signaling interplay in Ras superfamily function.* 2005. **15**(14): p. R563-R574.
45. Repasky, G.A., E.J. Chenette, and C.J.J.T.i.c.b. Der, *Renewing the conspiracy theory debate: does Raf function alone to mediate Ras oncogenesis?* 2004. **14**(11): p. 639-647.
46. Vredeveld, L.C., et al., *Abrogation of BRAFV600E-induced senescence by PI3K pathway activation contributes to melanomagenesis.* 2012. **26**(10): p. 1055-1069.
47. Bello, D.M., C.E. Ariyan, and R.D.J.C.C. Carvajal, *Melanoma mutagenesis and aberrant cell signaling.* 2013. **20**(4): p. 261-281.
48. Joyce, K.M., *Surgical Management of Melanoma*, in *Cutaneous Melanoma: Etiology and Therapy*, W.H. Ward and J.M. Farma, Editors. 2017: Brisbane (AU).
49. Bub, J.L., et al., *Management of lentigo maligna and lentigo maligna melanoma with staged excision: a 5-year follow-up.* Arch Dermatol, 2004. **140**(5): p. 552-8.
50. Morton, D.L., et al., *Technical details of intraoperative lymphatic mapping for early stage melanoma.* Arch Surg, 1992. **127**(4): p. 392-9.
51. Wagner, J.D., et al., *Patterns of initial recurrence and prognosis after sentinel lymph node biopsy and selective lymphadenectomy for melanoma.* Plast Reconstr Surg, 2003. **112**(2): p. 486-97.
52. Faries, M.B., et al., *Completion Dissection or Observation for Sentinel-Node Metastasis in Melanoma.* N Engl J Med, 2017. **376**(23): p. 2211-2222.
53. Lens, M.B., et al., *Elective lymph node dissection in patients with melanoma: systematic review and meta-analysis of randomized controlled trials.* Arch Surg, 2002. **137**(4): p. 458-61.
54. Leiter, U., et al., *Sentinel Lymph Node Dissection in Head and Neck Melanoma has Prognostic Impact on Disease-Free and Overall Survival.* Ann Surg Oncol, 2015. **22**(12): p. 4073-80.
55. Hein, D.W. and R.L. Moy, *Elective lymph node dissection in stage I malignant melanoma: a meta-analysis.* Melanoma Res, 1992. **2**(4): p. 273-7.
56. Sondak, V.K., et al., *Evidence-based clinical practice guidelines on the use of sentinel lymph node biopsy in melanoma.* Am Soc Clin Oncol Educ Book, 2013.
57. Dummer, R., et al., *Cutaneous melanoma: ESMO Clinical Practice Guidelines for diagnosis, treatment and follow-up.* Ann Oncol, 2012. **23 Suppl 7**: p. vii86-91.
58. Little, J.B., et al., *Repair of potentially lethal radiation damage in vitro and in vivo.* Radiology, 1973. **106**(3): p. 689-94.
59. Rofstad, E.K., *Radiation biology of malignant melanoma.* Acta Radiol Oncol, 1986. **25**(1): p. 1-10.
60. Overgaard, J., et al., *Some factors of importance in the radiation treatment of malignant melanoma.* Radiother Oncol, 1986. **5**(3): p. 183-92.
61. Jenrette, J.M., *Malignant melanoma: the role of radiation therapy revisited.* Semin Oncol, 1996. **23**(6): p. 759-62.

62. Stevens, G. and M.J. McKay, *Dispelling the myths surrounding radiotherapy for treatment of cutaneous melanoma.* Lancet Oncol, 2006. **7**(7): p. 575-83.
63. Barranco, S.C., M.M. Romsdahl, and R.M. Humphrey, *The radiation response of human malignant melanoma cells grown in vitro.* Cancer Res, 1971. **31**(6): p. 830-3.
64. Sause, W.T., et al., *Fraction size in external beam radiation therapy in the treatment of melanoma.* Int J Radiat Oncol Biol Phys, 1991. **20**(3): p. 429-32.
65. Dvorak, E., R.E. Haas, and E.J. Liebner, *Contribution of radiotherapy to the management of malignant melanoma. A ten year experience at the University of Illinois Hospital in Chicago.* Neoplasma, 1993. **40**(6): p. 387-99.
66. Fenig, E., et al., *Role of radiation therapy in the management of cutaneous malignant melanoma.* Am J Clin Oncol, 1999. **22**(2): p. 184-6.
67. Chang, D.T., et al., *Adjuvant radiotherapy for cutaneous melanoma: comparing hypofractionation to conventional fractionation.* Int J Radiat Oncol Biol Phys, 2006. **66**(4): p. 1051-5.
68. Strojan, P., et al., *Melanoma metastases to the neck nodes: role of adjuvant irradiation.* Int J Radiat Oncol Biol Phys, 2010. **77**(4): p. 1039-45.
69. Fogarty, G.B., et al., *Radiotherapy for lentigo maligna: a literature review and recommendations for treatment.* Br J Dermatol, 2014. **170**(1): p. 52-8.
70. Agrawal, S., et al., *The benefits of adjuvant radiation therapy after therapeutic lymphadenectomy for clinically advanced, high-risk, lymph node-metastatic melanoma.* Cancer, 2009. **115**(24): p. 5836-44.
71. Hellman, S. and R.R. Weichselbaum, *Oligometastases.* J Clin Oncol, 1995. **13**(1): p. 8-10.
72. Wilson, M.A. and L.M. Schuchter, *Chemotherapy for Melanoma.* Cancer Treat Res, 2016. **167**: p. 209-29.
73. Bajetta, E., et al., *Metastatic melanoma: chemotherapy.* Semin Oncol, 2002. **29**(5): p. 427-45.
74. Li, Y. and E.F. McClay, *Systemic chemotherapy for the treatment of metastatic melanoma.* Semin Oncol, 2002. **29**(5): p. 413-26.
75. Yung, W.K., *Temozolomide in malignant gliomas.* Semin Oncol, 2000. **27**(3 Suppl 6): p. 27-34.
76. Yung, W.K., et al., *A phase II study of temozolomide vs. procarbazine in patients with glioblastoma multiforme at first relapse.* Br J Cancer, 2000. **83**(5): p. 588-93.
77. Agarwala, S.S., et al., *Temozolomide for the treatment of brain metastases associated with metastatic melanoma: a phase II study.* J Clin Oncol, 2004. **22**(11): p. 2101-7.
78. Bleehen, N.M., et al., *Cancer Research Campaign phase II trial of temozolomide in metastatic melanoma.* J Clin Oncol, 1995. **13**(4): p. 910-3.
79. Hill, G.J., 2nd, et al., *Chemotherapy of malignant melanoma with dimethyl traizeno imidazole carboxamide (DITC) and nitrosourea derivatives (BCNU, CCNU).* Ann Surg, 1974. **180**(2): p. 167-74.
80. Evans, L.M., E.S. Casper, and R. Rosenbluth, *Phase II trial of carboplatin in advanced malignant melanoma.* Cancer Treat Rep, 1987. **71**(2): p. 171-2.
81. Legha, S.S., et al., *A phase II trial of taxol in metastatic melanoma.* Cancer, 1990. **65**(11): p. 2478-81.

82. Bedikian, A.Y., et al., *Phase II trial of docetaxel in patients with advanced cutaneous malignant melanoma previously untreated with chemotherapy.* J Clin Oncol, 1995. **13**(12): p. 2895-9.
83. Bajetta, E., et al., *Multicenter phase III randomized trial of polychemotherapy (CVD regimen) versus the same chemotherapy (CT) plus subcutaneous interleukin-2 and interferon-alpha2b in metastatic melanoma.* Ann Oncol, 2006. **17**(4): p. 571-7.
84. Hofmann, M.A., et al., *Prospective evaluation of supportive care with or without CVD chemotherapy as a second-line treatment in advanced melanoma by patient's choice: a multicentre Dermatologic Cooperative Oncology Group trial.* Melanoma Res, 2011. **21**(6): p. 516-23.
85. Margolin, K.A., et al., *Phase II study of carmustine, dacarbazine, cisplatin, and tamoxifen in advanced melanoma: a Southwest Oncology Group study.* J Clin Oncol, 1998. **16**(2): p. 664-9.
86. Chapman, P.B., et al., *Improved survival with vemurafenib in melanoma with BRAF V600E mutation.* N Engl J Med, 2011. **364**(26): p. 2507-16.
87. Creagan, E.T., et al., *Phase III clinical trial of the combination of cisplatin, dacarbazine, and carmustine with or without tamoxifen in patients with advanced malignant melanoma.* J Clin Oncol, 1999. **17**(6): p. 1884-90.
88. McClay, E.F., et al., *Effective combination chemo/hormonal therapy for malignant melanoma: experience with three consecutive trials.* Int J Cancer, 1992. **50**(4): p. 553-6.
89. Flaherty, K.T., *Targeting metastatic melanoma.* Annu Rev Med, 2012. **63**: p. 171-83.
90. Livingstone, E., et al., *BRAF, MEK and KIT inhibitors for melanoma: adverse events and their management.* 2014. **3**(3): p. 29.
91. Ballantyne, A.D. and K.P.J.D. Garnock-Jones, *Dabrafenib: first global approval.* 2013. **73**(12): p. 1367-1376.
92. Domingues, B., et al., *Melanoma treatment in review.* Immunotargets Ther, 2018. **7**: p. 35-49.
93. Gata, V.A., et al., *Tumor infiltrating lymphocytes as a prognostic factor in malignant melanoma. Review of the literature.* J BUON, 2017. **22**(3): p. 592-598.
94. Mantovani, A., et al., *Cancer-related inflammation.* Nature, 2008. **454**(7203): p. 436-44.
95. Krieg, C., et al., *Improved IL-2 immunotherapy by selective stimulation of IL-2 receptors on lymphocytes and endothelial cells.* Proc Natl Acad Sci U S A, 2010. **107**(26): p. 11906-11.
96. Bright, R., et al., *Clinical Response Rates From Interleukin-2 Therapy for Metastatic Melanoma Over 30 Years' Experience: A Meta-Analysis of 3312 Patients.* J Immunother, 2017. **40**(1): p. 21-30.
97. Bhatia, S., S.S. Tykodi, and J.A. Thompson, *Treatment of metastatic melanoma: an overview.* Oncology (Williston Park), 2009. **23**(6): p. 488-96.
98. Sanlorenzo, M., et al., *Role of interferon in melanoma: old hopes and new perspectives.* Expert Opin Biol Ther, 2017. **17**(4): p. 475-483.
99. Lindenmann, J., *Induction of chick interferon: procedures of the original experiments.* Methods Enzymol, 1981. **78**(Pt A): p. 181-8.
100. Pestka, S., et al., *Interferons and their actions.* Annu Rev Biochem, 1987. **56**: p. 727-77.

101. Rafique, I., J.M. Kirkwood, and A.A. Tarhini, *Immune checkpoint blockade and interferon-alpha in melanoma.* Semin Oncol, 2015. **42**(3): p. 436-47.
102. Kirkwood, J.M., et al., *High-dose interferon alfa-2b significantly prolongs relapse-free and overall survival compared with the GM2-KLH/QS-21 vaccine in patients with resected stage IIB-III melanoma: results of intergroup trial E1694/S9512/C509801.* J Clin Oncol, 2001. **19**(9): p. 2370-80.
103. Roh, M.R., et al., *Difference of interferon-alpha and interferon-beta on melanoma growth and lymph node metastasis in mice.* Melanoma Res, 2013. **23**(2): p. 114-24.
104. Ives, N.J., et al., *Adjuvant interferon-alpha for the treatment of high-risk melanoma: An individual patient data meta-analysis.* Eur J Cancer, 2017. **82**: p. 171-183.
105. Eggermont, A.M., et al., *Long term follow up of the EORTC 18952 trial of adjuvant therapy in resected stage IIB-III cutaneous melanoma patients comparing intermediate doses of interferon-alpha-2b (IFN) with observation: Ulceration of primary is key determinant for IFN-sensitivity.* Eur J Cancer, 2016. **55**: p. 111-21.
106. Raedler, L.A., *Opdivo (Nivolumab): Second PD-1 Inhibitor Receives FDA Approval for Unresectable or Metastatic Melanoma.* Am Health Drug Benefits, 2015. **8**(Spec Feature): p. 180-3.
107. Specenier, P., *Nivolumab in melanoma.* Expert Rev Anticancer Ther, 2016. **16**(12): p. 1247-1261.
108. Robert, C., et al., *Pembrolizumab versus Ipilimumab in Advanced Melanoma.* N Engl J Med, 2015. **372**(26): p. 2521-32.
109. Robert, C., et al., *Anti-programmed-death-receptor-1 treatment with pembrolizumab in ipilimumab-refractory advanced melanoma: a randomised dose-comparison cohort of a phase 1 trial.* Lancet, 2014. **384**(9948): p. 1109-17.
110. Ribas, A., et al., *Pembrolizumab versus investigator-choice chemotherapy for ipilimumab-refractory melanoma (KEYNOTE-002): a randomised, controlled, phase 2 trial.* Lancet Oncol, 2015. **16**(8): p. 908-18.
111. Brunet, J.F., et al., *A new member of the immunoglobulin superfamily--CTLA-4.* Nature, 1987. **328**(6127): p. 267-70.
112. Waterhouse, P., et al., *Lymphoproliferative disorders with early lethality in mice deficient in Ctla-4.* Science, 1995. **270**(5238): p. 985-8.
113. Ribas, A., et al., *Intratumoral immune cell infiltrates, FoxP3, and indoleamine 2,3-dioxygenase in patients with melanoma undergoing CTLA4 blockade.* Clin Cancer Res, 2009. **15**(1): p. 390-9.
114. Hodi, F.S., et al., *Improved survival with ipilimumab in patients with metastatic melanoma.* N Engl J Med, 2010. **363**(8): p. 711-23.
115. Panelli, M.C., et al., *Phase 1 study in patients with metastatic melanoma of immunization with dendritic cells presenting epitopes derived from the melanoma-associated antigens MART-1 and gp100.* J Immunother, 2000. **23**(4): p. 487-98.
116. Yuan, J., et al., *Safety and immunogenicity of a human and mouse gp100 DNA vaccine in a phase I trial of patients with melanoma.* Cancer Immun, 2009. **9**: p. 5.
117. Kanzler, H., et al., *Therapeutic targeting of innate immunity with Toll-like receptor agonists and antagonists.* Nat Med, 2007. **13**(5): p. 552-9.

118. Barton, G.M. and J.C. Kagan, *A cell biological view of Toll-like receptor function: regulation through compartmentalization.* Nat Rev Immunol, 2009. **9**(8): p. 535-42.
119. Royal, R.E., et al., *A toll-like receptor agonist to drive melanoma regression as a vaccination adjuvant or by direct tumor application*. 2017, American Society of Clinical Oncology.
120. Pol, J., G. Kroemer, and L. Galluzzi, *First oncolytic virus approved for melanoma immunotherapy.* Oncoimmunology, 2016. **5**(1): p. e1115641.
121. Dudley, M.E., et al., *Adoptive cell therapy for patients with metastatic melanoma: evaluation of intensive myeloablative chemoradiation preparative regimens.* 2008. **26**(32): p. 5233.
122. Huang, V., et al., *Cutaneous toxic effects associated with vemurafenib and inhibition of the BRAF pathway.* Arch Dermatol, 2012. **148**(5): p. 628-33.
123. Peuvrel, L., et al., *Severe radiotherapy-induced extracutaneous toxicity under vemurafenib.* Eur J Dermatol, 2013. **23**(6): p. 879-81.
124. Merten, R., et al., *Increased skin and mucosal toxicity in the combination of vemurafenib with radiation therapy.* Strahlenther Onkol, 2014. **190**(12): p. 1169-72.
125. Hecht, M., et al., *Radiosensitization by BRAF inhibitor therapy-mechanism and frequency of toxicity in melanoma patients.* Ann Oncol, 2015. **26**(6): p. 1238-1244.
126. Ly, D., et al., *Local control after stereotactic radiosurgery for brain metastases in patients with melanoma with and without BRAF mutation and treatment.* J Neurosurg, 2015. **123**(2): p. 395-401.
127. Patel, K.R., et al., *BRAF inhibitor and stereotactic radiosurgery is associated with an increased risk of radiation necrosis.* Melanoma Res, 2016. **26**(4): p. 387-94.
128. Xu, Z., et al., *BRAF V600E mutation and BRAF kinase inhibitors in conjunction with stereotactic radiosurgery for intracranial melanoma metastases.* J Neurosurg, 2017. **126**(3): p. 726-734.
129. Derer, A., et al., *Chemoradiation Increases PD-L1 Expression in Certain Melanoma and Glioblastoma Cells*. Front Immunol, 2016. **7**: p. 610.
130. Sunshine, J.C., et al., *PD-L1 Expression in Melanoma: A Quantitative Immunohistochemical Antibody Comparison.* Clin Cancer Res, 2017. **23**(16): p. 4938-4944.
131. Buchbinder, E. and F.S. Hodi, *Cytotoxic T lymphocyte antigen-4 and immune checkpoint blockade.* J Clin Invest, 2015. **125**(9): p. 3377-83.
132. Witz, I.P. and O.J.C.I. Levy-Nissenbaum, *The tumor microenvironment in the post-PAGET era.* 2006. **242**(1): p. 1-10.
133. Fridman, W.H., et al., *The immune contexture in human tumours: impact on clinical outcome.* 2012. **12**(4): p. 298-306.
134. Milne, K., et al., *Systematic analysis of immune infiltrates in high-grade serous ovarian cancer reveals CD20, FoxP3 and TIA-1 as positive prognostic factors.* 2009. **4**(7): p. e6412.
135. Coronella, J.A., et al., *Evidence for an antigen-driven humoral immune response in medullary ductal breast cancer.* 2001. **61**(21): p. 7889-7899.
136. Andreu, P., et al., *FcRγ activation regulates inflammation-associated squamous carcinogenesis.* 2010. **17**(2): p. 121-134.
137. De Visser, K.E., L.V. Korets, and L.M.J.C.c. Coussens, *De novo carcinogenesis promoted by chronic inflammation is B lymphocyte dependent.* 2005. **7**(5): p. 411-423.

138. Balkwill, F.R., M. Capasso, and T. Hagemann, *The tumor microenvironment at a glance*. 2012, The Company of Biologists Ltd.
139. Ugel, S., et al., *Monocytes in the Tumor Microenvironment.* 2021. **16**: p. 93-122.
140. Mackay, F. and P.J.N.r.i. Schneider, *Cracking the BAFF code.* 2009. **9**(7): p. 491-502.
141. Nardelli, B., et al., *Synthesis and release of B-lymphocyte stimulator from myeloid cells.* 2001. **97**(1): p. 198-204.
142. Novak, A.J., et al., *Aberrant expression of B-lymphocyte stimulator by B chronic lymphocytic leukemia cells: a mechanism for survival.* 2002. **100**(8): p. 2973-2979.
143. Gorelik, L., et al., *Normal B cell homeostasis requires B cell activation factor production by radiation-resistant cells.* 2003. **198**(6): p. 937-945.
144. Sjöstrand, M., et al., *The expression of BAFF is controlled by IRF transcription factors.* 2016. **196**(1): p. 91-96.
145. Thompson, J.S., et al., *BAFF-R, a newly identified TNF receptor that specifically interacts with BAFF.* 2001. **293**(5537): p. 2108-2111.
146. Gross, J.A., et al., *TACI and BCMA are receptors for a TNF homologue implicated in B-cell autoimmune disease.* 2000. **404**(6781): p. 995-999.
147. Schneider, P., et al., *BAFF, a novel ligand of the tumor necrosis factor family, stimulates B cell growth.* The Journal of experimental medicine, 1999. **189**(11): p. 1747-56.
148. Batten, M., et al., *BAFF mediates survival of peripheral immature B lymphocytes.* 2000. **192**(10): p. 1453-1466.
149. Schiemann, B., et al., *An essential role for BAFF in the normal development of B cells through a BCMA-independent pathway.* 2001. **293**(5537): p. 2111-2114.
150. Gross, J.A., et al., *TACI-Ig neutralizes molecules critical for B cell development and autoimmune disease: impaired B cell maturation in mice lacking BLyS.* 2001. **15**(2): p. 289-302.
151. Mackay, F., et al., *Mice transgenic for BAFF develop lymphocytic disorders along with autoimmune manifestations.* 1999. **190**(11): p. 1697-1710.
152. Khare, S.D., et al., *Severe B cell hyperplasia and autoimmune disease in TALL-1 transgenic mice.* 2000. **97**(7): p. 3370-3375.
153. Xu, S., K.-P.J.M. Lam, and C. Biology, *B-cell maturation protein, which binds the tumor necrosis factor family members BAFF and APRIL, is dispensable for humoral immune responses.* 2001. **21**(12): p. 4067-4074.
154. von Bülow, G.-U., J.M. van Deursen, and R.J.J.I. Bram, *Regulation of the T-independent humoral response by TACI.* 2001. **14**(5): p. 573-582.
155. Yan, M., et al., *Activation and accumulation of B cells in TACI-deficient mice.* 2001. **2**(7): p. 638-643.
156. Lam, K.-P., R. Kühn, and K.J.C. Rajewsky, *In vivo ablation of surface immunoglobulin on mature B cells by inducible gene targeting results in rapid cell death.* 1997. **90**(6): p. 1073-1083.
157. Kraus, M., et al., *Survival of resting mature B lymphocytes depends on BCR signaling via the Igα/β heterodimer.* 2004. **117**(6): p. 787-800.
158. Yan, M., et al., *Identification of a novel receptor for B lymphocyte stimulator that is mutated in a mouse strain with severe B cell deficiency.* 2001. **11**(19): p. 1547-1552.

159. Sasaki, Y., et al., *TNF family member B cell-activating factor (BAFF) receptor-dependent and-independent roles for BAFF in B cell physiology.* 2004. **173**(4): p. 2245-2252.
160. Claudio, E., et al., *BAFF-induced NEMO-independent processing of NF-κB2 in maturing B cells.* 2002. **3**(10): p. 958-965.
161. Kayagaki, N., et al., *BAFF/BLyS receptor 3 binds the B cell survival factor BAFF ligand through a discrete surface loop and promotes processing of NF-κB2.* 2002. **17**(4): p. 515-524.
162. Pieper, K., et al., *B-cell biology and development.* 2013. **131**(4): p. 959-971.
163. Patke, A., et al., *BAFF controls B cell metabolic fitness through a PKCβ-and Akt-dependent mechanism.* 2006. **203**(11): p. 2551-2562.
164. Matsushita, T., et al., *BAFF inhibition attenuates fibrosis in scleroderma by modulating the regulatory and effector B cell balance.* 2018. **4**(7): p. eaas9944.
165. Huard, B., et al., *BAFF production by antigen-presenting cells provides T cell co-stimulation.* 2004. **16**(3): p. 467-475.
166. Morimoto, S., et al., *Expression of B-cell activating factor of the tumour necrosis factor family (BAFF) in T cells in active systemic lupus erythematosus: the role of BAFF in T cell-dependent B cell pathogenic autoantibody production.* 2007.
167. Lavie, F., et al., *Expression of BAFF (BLyS) in T cells infiltrating labial salivary glands from patients with Sjögren's syndrome.* The Journal of Pathology, 2004. **202**(4): p. 496-502.
168. Yoshimoto, K., et al., *Aberrant expression of BAFF in T cells of systemic lupus erythematosus, which is recapitulated by a human T cell line, Loucy.* 2006. **18**(7): p. 1189-1196.
169. Ng, L.G., et al., *B cell-activating factor belonging to the TNF family (BAFF)-R is the principal BAFF receptor facilitating BAFF costimulation of circulating T and B cells.* 2004. **173**(2): p. 807-817.
170. Huard, B., et al., *T cell costimulation by the TNF ligand BAFF.* 2001. **167**(11): p. 6225-6231.
171. Shan, X., et al., *Effects of human soluble BAFF synthesized in Escherichia coli on CD4+ and CD8+ T lymphocytes as well as NK cells in mice.* 2006. **55**(3).
172. Zhu, X.-j., et al., *The effects of BAFF and BAFF-R-Fc fusion protein in immune thrombocytopenia.* 2009. **114**(26): p. 5362-5367.
173. Hu, S., et al., *BAFF promotes T cell activation through the BAFF-BAFF-R-PI3K-Akt signaling pathway.* 2019. **114**: p. 108796.
174. Sutherland, A.P., et al., *BAFF augments certain Th1-associated inflammatory responses.* 2005. **174**(9): p. 5537-5544.
175. Walters, S., et al., *Increased CD4+ Foxp3+ T cells in BAFF-transgenic mice suppress T cell effector responses.* 2009. **182**(2): p. 793-801.
176. Zhou, X., et al., *BAFF promotes Th17 cells and aggravates experimental autoimmune encephalomyelitis.* 2011. **6**(8): p. e23629.
177. Lam, Q.L.K., et al., *Local BAFF gene silencing suppresses Th17-cell generation and ameliorates autoimmune arthritis.* 2008. **105**(39): p. 14993-14998.
178. Scapini, P., et al., *Myeloid cells, BAFF, and IFN-γ establish an inflammatory loop that exacerbates autoimmunity in Lyn-deficient mice.* 2010. **207**(8): p. 1757-1773.
179. Ye, Q., et al., *BAFF binding to T cell-expressed BAFF-R costimulates T cell proliferation and alloresponses.* 2004. **34**(10): p. 2750-2759.

180. Craxton, A., et al., *Macrophage-and dendritic cell—dependent regulation of human B-cell proliferation requires the TNF family ligand BAFF.* 2003. **101**(11): p. 4464-4471.
181. Wei, F., et al., *BAFF and its receptors involved in the inflammation progress in adjuvant induced arthritis rats.* 2016. **31**: p. 1-8.
182. Moisini, I., A.J.C. Davidson, and E. Immunology, *BAFF: a local and systemic target in autoimmune diseases.* 2009. **158**(2): p. 155-163.
183. Chang, S.K., S.A. Mihalcik, and D.F.J.T.J.o.I. Jelinek, *B lymphocyte stimulator regulates adaptive immune responses by directly promoting dendritic cell maturation.* 2008. **180**(11): p. 7394-7403.
184. Jeon, S.T., et al., *Reverse signaling through BAFF differentially regulates the expression of inflammatory mediators and cytoskeletal movements in THP-1 cells.* Immunol Cell Biol, 2010. **88**(2): p. 148-56.
185. Lee, S.-M., et al., *BAFF and APRIL induce inflammatory activation of THP-1 cells through interaction with their conventional receptors and activation of MAPK and NF-κB.* Inflammation Research, 2011. **60**(9): p. 807-15.
186. Groom, J., et al., *Association of BAFF/BLyS overexpression and altered B cell differentiation with Sjögren's syndrome.* 2002. **109**(1): p. 59-68.
187. Dörner, T., C.J.A.R. Putterman, and Therapy, *B cells, BAFF/zTNF4, TACI, and systemic lupus erythematosus.* 2001. **3**(4): p. 197.
188. Rahman, Z.S., et al., *Normal induction but attenuated progression of germinal center responses in BAFF and BAFF-R signaling–deficient mice.* 2003. **198**(8): p. 1157-1169.
189. Zhang, J., et al., *Cutting edge: a role for B lymphocyte stimulator in systemic lupus erythematosus.* 2001. **166**(1): p. 6-10.
190. Bosello, S., et al., *Concentrations of BAFF correlate with autoantibody levels, clinical disease activity, and response to treatment in early rheumatoid arthritis.* 2008. **35**(7): p. 1256-1264.
191. Steri, M., et al., *Overexpression of the cytokine BAFF and autoimmunity risk.* 2017. **376**(17): p. 1615-1626.
192. Strand, V., et al., *Improvements in health-related quality of life with belimumab, a B-lymphocyte stimulator-specific inhibitor, in patients with autoantibody-positive systemic lupus erythematosus from the randomised controlled BLISS trials.* 2014. **73**(5): p. 838-844.
193. Lemancewicz, D., et al., *Evaluation of TNF superfamily molecules in multiple myeloma patients: correlation with biological and clinical features.* 2013. **37**(9): p. 1089-1093.
194. Novak, A.J., et al., *Expression of BLyS and its receptors in B-cell non-Hodgkin lymphoma: correlation with disease activity and patient outcome.* 2004. **104**(8): p. 2247-2253.
195. Grimaldi, F., et al., *Exploring the Possible Prognostic Role of B-Lymphocyte Stimulator (BLyS) in a Large Series of Patients with Neuroendocrine Tumors.* 2018. **18**(6): p. 618-625.
196. Pelekanou, V., et al., *Expression of TNF-superfamily members BAFF and APRIL in breast cancer: immunohistochemical study in 52 invasive ductal breast carcinomas.* 2008. **8**(1): p. 76.
197. Koizumi, M., et al., *Increased B cell-activating factor promotes tumor invasion and metastasis in human pancreatic cancer.* 2013. **8**(8): p. e71367.
198. Shurin, M.R., et al., *BAFF and APRIL from Activin A–Treated Dendritic Cells Upregulate the Antitumor Efficacy of Dendritic Cells In Vivo.* 2016. **76**(17): p. 4959-4969.

199. Di Carlo, E., et al., *The lack of epithelial interleukin-7 and BAFF/BLyS gene expression in prostate cancer as a possible mechanism of tumor escape from immunosurveillance.* 2009. **15**(9): p. 2979-2987.
200. Yarchoan, M., et al., *Effects of B cell-activating factor on tumor immunity.* JCI Insight, 2020. **5**(10).
201. Liu, W., et al., *Repurposing the serotonin agonist Tegaserod as an anticancer agent in melanoma: molecular mechanisms and clinical implications.* J Exp Clin Cancer Res, 2020. **39**(1): p. 38.
202. Chou, T.C. and P. Talalay, *Quantitative analysis of dose-effect relationships: the combined effects of multiple drugs or enzyme inhibitors.* Adv Enzyme Regul, 1984. **22**: p. 27-55.
203. Varghese, F., et al., *IHC Profiler: an open source plugin for the quantitative evaluation and automated scoring of immunohistochemistry images of human tissue samples.* PLoS One, 2014. **9**(5): p. e96801.
204. Barretina, J., et al., *The Cancer Cell Line Encyclopedia enables predictive modelling of anticancer drug sensitivity.* Nature, 2012. **483**(7391): p. 603-7.
205. Goldman, M., et al., *The UCSC Cancer Genomics Browser: update 2015.* Nucleic Acids Res, 2015. **43**(Database issue): p. D812-7.
206. Xu, H.C., et al., *Type I interferon protects antiviral CD8+ T cells from NK cell cytotoxicity.* Immunity, 2014. **40**(6): p. 949-60.
207. Mack, M., et al., *Expression and characterization of the chemokine receptors CCR2 and CCR5 in mice.* J Immunol, 2001. **166**(7): p. 4697-704.
208. Huang, A., et al., *Progranulin prevents regulatory NK cell cytotoxicity against antiviral T cells.* JCI Insight, 2019. **4**(17).
209. Minden, M.D., et al., *Lovastatin induced control of blast cell growth in an elderly patient with acute myeloblastic leukemia.* Leuk Lymphoma, 2001. **40**(5-6): p. 659-62.
210. Spagnuolo, P.A., et al., *The antihelmintic flubendazole inhibits microtubule function through a mechanism distinct from Vinca alkaloids and displays preclinical activity in leukemia and myeloma.* Blood, 2010. **115**(23): p. 4824-33.
211. Liang, G., et al., *Itraconazole exerts its anti-melanoma effect by suppressing Hedgehog, Wnt, and PI3K/mTOR signaling pathways.* Oncotarget, 2017. **8**(17): p. 28510-28525.
212. Cameron, D., et al., *Accelerated versus standard epirubicin followed by cyclophosphamide, methotrexate, and fluorouracil or capecitabine as adjuvant therapy for breast cancer in the randomised UK TACT2 trial (CRUK/05/19): a multicentre, phase 3, open-label, randomised, controlled trial.* Lancet Oncol, 2017. **18**(7): p. 929-945.
213. Mikami, T., et al., *Contribution of active and inactive states of the human 5-HT4d receptor to the functional activities of 5-HT4-receptor agonists.* J Pharmacol Sci, 2008. **107**(3): p. 251-9.
214. Nichols, D.E. and C.D. Nichols, *Serotonin receptors.* Chem Rev, 2008. **108**(5): p. 1614-41.
215. Dominguez-Soto, A., et al., *Serotonin drives the acquisition of a profibrotic and anti-inflammatory gene profile through the 5-HT7R-PKA signaling axis.* Sci Rep, 2017. **7**(1): p. 14761.
216. Paluncic, J., et al., *Roads to melanoma: Key pathways and emerging players in melanoma progression and oncogenic signaling.* Biochim Biophys Acta, 2016. **1863**(4): p. 770-84.

217. Burnett, P.E., et al., *RAFT1 phosphorylation of the translational regulators p70 S6 kinase and 4E-BP1.* Proceedings of the National Academy of Sciences of the United States of America, 1998. **95**(4): p. 1432-7.
218. Roux, P.P., et al., *RAS/ERK signaling promotes site-specific ribosomal protein S6 phosphorylation via RSK and stimulates cap-dependent translation.* The Journal of biological chemistry, 2007. **282**(19): p. 14056-64.
219. Corcoran, R.B., et al., *TORC1 suppression predicts responsiveness to RAF and MEK inhibition in BRAF-mutant melanoma.* Sci Transl Med, 2013. **5**(196): p. 196ra98.
220. Kleffel, S., et al., *Melanoma Cell-Intrinsic PD-1 Receptor Functions Promote Tumor Growth.* Cell, 2015. **162**(6): p. 1242-56.
221. Manning, B.D., et al., *Identification of the tuberous sclerosis complex-2 tumor suppressor gene product tuberin as a target of the phosphoinositide 3-kinase/akt pathway.* Molecular cell, 2002. **10**(1): p. 151-62.
222. Meyuhas, O., *Ribosomal Protein S6 Phosphorylation: Four Decades of Research.* International review of cell and molecular biology, 2015. **320**: p. 41-73.
223. Sarbassov, D.D., et al., *Phosphorylation and regulation of Akt/PKB by the rictor-mTOR complex.* Science (New York, N Y), 2005. **307**(5712): p. 1098-101.
224. Feng, J., et al., *Identification of a PKB/Akt hydrophobic motif Ser-473 kinase as DNA-dependent protein kinase.* The Journal of biological chemistry, 2004. **279**(39): p. 41189-96.
225. Yoon, S.-O., et al., *Focal Adhesion- and IGF1R-Dependent Survival and Migratory Pathways Mediate Tumor Resistance to mTORC1/2 Inhibition.* Molecular cell, 2017. **67**(3): p. 512-527.e4.
226. Di Maira, G., et al., *Protein kinase CK2 phosphorylates and upregulates Akt/PKB.* Cell death and differentiation, 2005. **12**(6): p. 668-77.
227. Gulen, M.F., et al., *Inactivation of the enzyme GSK3alpha by the kinase IKKi promotes AKT-mTOR signaling pathway that mediates interleukin-1-induced Th17 cell maintenance.* Immunity, 2012. **37**(5): p. 800-12.
228. Ohue, Y. and H. Nishikawa, *Regulatory T (Treg) cells in cancer: Can Treg cells be a new therapeutic target?* Cancer science, 2019. **110**(7): p. 2080-2089.
229. Ali, K., et al., *Inactivation of PI(3)K p110delta breaks regulatory T-cell-mediated immune tolerance to cancer.* Nature, 2014. **510**(7505): p. 407-411.
230. Larkin, J., et al., *Vemurafenib in patients with BRAF(V600) mutated metastatic melanoma: an open-label, multicentre, safety study.* Lancet Oncol, 2014. **15**(4): p. 436-44.
231. Bellomo, C., L. Caja, and A. Moustakas, *Transforming growth factor beta as regulator of cancer stemness and metastasis.* Br J Cancer, 2016. **115**(7): p. 761-9.
232. Geginat, J., et al., *The light and the dark sides of Interleukin-10 in immune-mediated diseases and cancer.* Cytokine Growth Factor Rev, 2016. **30**: p. 87-93.
233. Gibbons Johnson, R.M. and H. Dong, *Functional Expression of Programmed Death-Ligand 1 (B7-H1) by Immune Cells and Tumor Cells.* Front Immunol, 2017. **8**: p. 961.
234. Merelli, B., et al., *Targeting the PD1/PD-L1 axis in melanoma: biological rationale, clinical challenges and opportunities.* Crit Rev Oncol Hematol, 2014. **89**(1): p. 140-65.
235. Wang, Y., et al., *Regulation of PD-L1: Emerging Routes for Targeting Tumor Immune Evasion.* Front Pharmacol, 2018. **9**: p. 536.

236. Lin, H., et al., *Host expression of PD-L1 determines efficacy of PD-L1 pathway blockade-mediated tumor regression.* J Clin Invest, 2018. **128**(2): p. 805-815.
237. Gu, H., Y.R. Zou, and K. Rajewsky, *Independent control of immunoglobulin switch recombination at individual switch regions evidenced through Cre-loxP-mediated gene targeting.* Cell, 1993. **73**(6): p. 1155-64.
238. Yashin, D.V., et al., *Tag7 (PGLYRP1) in Complex with Hsp70 Induces Alternative Cytotoxic Processes in Tumor Cells via TNFR1 Receptor.* J Biol Chem, 2015. **290**(35): p. 21724-31.
239. Chen, L. and D.B. Flies, *Molecular mechanisms of T cell co-stimulation and co-inhibition.* Nat Rev Immunol, 2013. **13**(4): p. 227-42.
240. Lin, Y., J. Xu, and H. Lan, *Tumor-associated macrophages in tumor metastasis: biological roles and clinical therapeutic applications.* J Hematol Oncol, 2019. **12**(1): p. 76.
241. Martinez-Lostao, L., A. Anel, and J. Pardo, *How Do Cytotoxic Lymphocytes Kill Cancer Cells?* Clin Cancer Res, 2015. **21**(22): p. 5047-56.
242. Prevost-Blondel, A., et al., *Tumor-infiltrating lymphocytes exhibiting high ex vivo cytolytic activity fail to prevent murine melanoma tumor growth in vivo.* J Immunol, 1998. **161**(5): p. 2187-94.
243. Lopez-Soto, A., et al., *Control of Metastasis by NK Cells.* Cancer Cell, 2017. **32**(2): p. 135-154.
244. Berger, M., J.A. Gray, and B.L. Roth, *The expanded biology of serotonin.* Annu Rev Med, 2009. **60**: p. 355-66.
245. Lee, H.J., et al., *Serotonin induces melanogenesis via serotonin receptor 2A.* Br J Dermatol, 2011. **165**(6): p. 1344-8.
246. Jiang, S.H., et al., *Increased Serotonin Signaling Contributes to the Warburg Effect in Pancreatic Tumor Cells Under Metabolic Stress and Promotes Growth of Pancreatic Tumors in Mice.* Gastroenterology, 2017. **153**(1): p. 277-291 e19.
247. Sarrouilhe, D., et al., *Serotonin and cancer: what is the link?* Curr Mol Med, 2015. **15**(1): p. 62-77.
248. Etxabe, A., et al., *Inhibition of serotonin receptor type 1 in acute myeloid leukemia impairs leukemia stem cell functionality: a promising novel therapeutic target.* Leukemia, 2017. **31**(11): p. 2288-2302.
249. Pollard, S.M., et al., *Glioma stem cell lines expanded in adherent culture have tumor-specific phenotypes and are suitable for chemical and genetic screens.* Cell Stem Cell, 2009. **4**(6): p. 568-80.
250. Jose, J., et al., *Serotonin Analogues as Inhibitors of Breast Cancer Cell Growth* Medicinal Chemistry Letters, 2017. **8**: p. 1072-1076.
251. De Maeyer, J.H., R.A. Lefebvre, and J.A. Schuurkes, *5-HT4 receptor agonists: similar but not the same.* Neurogastroenterol Motil, 2008. **20**(2): p. 99-112.
252. Beattie, D.T., et al., *The 5-HT4 receptor agonist, tegaserod, is a potent 5-HT2B receptor antagonist in vitro and in vivo.* Br J Pharmacol, 2004. **143**(5): p. 549-60.
253. Mattia, G., et al., *Cell death-based treatments of melanoma:conventional treatments and new therapeutic strategies.* Cell death & disease, 2018. **9**(2): p. 112.
254. Joseph, E.W., et al., *The RAF inhibitor PLX4032 inhibits ERK signaling and tumor cell proliferation in a V600E BRAF-selective manner.* Proceedings of the National Academy of Sciences of the United States of America, 2010. **107**(33): p. 14903-8.

255. Schachter, J., et al., *Pembrolizumab versus ipilimumab for advanced melanoma: final overall survival results of a multicentre, randomised, open-label phase 3 study (KEYNOTE-006).* Lancet, 2017. **390**(10105): p. 1853-1862.
256. Keller, H.R., et al., *Overcoming resistance to targeted therapy with immunotherapy and combination therapy for metastatic melanoma.* Oncotarget, 2017. **8**(43): p. 75675-75686.
257. Broussard, L., et al., *Melanoma Cell Death Mechanisms.* Chonnam medical journal, 2018. **54**(3): p. 135-142.
258. Torres-Collado, A.X., J. Knott, and A.R. Jazirehi, *Reversal of Resistance in Targeted Therapy of Metastatic Melanoma: Lessons Learned from Vemurafenib (BRAFV600E-Specific Inhibitor).* Cancers, 2018. **10**(6).
259. Posch, C., et al., *Combined targeting of MEK and PI3K/mTOR effector pathways is necessary to effectively inhibit NRAS mutant melanoma in vitro and in vivo.* Proceedings of the National Academy of Sciences of the United States of America, 2013. **110**(10): p. 4015-20.
260. Inoki, K., et al., *TSC2 integrates Wnt and energy signals via a coordinated phosphorylation by AMPK and GSK3 to regulate cell growth.* Cell, 2006. **126**(5): p. 955-68.
261. Togashi, Y., K. Shitara, and H. Nishikawa, *Regulatory T cells in cancer immunosuppression - implications for anticancer therapy.* Nature reviews Clinical oncology, 2019. **16**(6): p. 356-371.
262. Muller-Lissner, S.A., et al., *Tegaserod, a 5-HT(4) receptor partial agonist, relieves symptoms in irritable bowel syndrome patients with abdominal pain, bloating and constipation.* Aliment Pharmacol Ther, 2001. **15**(10): p. 1655-66.
263. Nyhlin, H., et al., *A double-blind, placebo-controlled, randomized study to evaluate the efficacy, safety and tolerability of tegaserod in patients with irritable bowel syndrome.* Scand J Gastroenterol, 2004. **39**(2): p. 119-26.
264. Johanson, J.F., et al., *Effect of tegaserod in chronic constipation: a randomized, double-blind, controlled trial.* Clin Gastroenterol Hepatol, 2004. **2**(9): p. 796-805.
265. Thompson, C.A., *Novartis suspends tegaserod sales at FDA's request.* Am J Health Syst Pharm, 2007. **64**(10): p. 1020.
266. Anderson, J.L., et al., *Lack of association of tegaserod with adverse cardiovascular outcomes in a matched case-control study.* J Cardiovasc Pharmacol Ther, 2009. **14**(3): p. 170-5.
267. Loughlin, J., et al., *Tegaserod and the risk of cardiovascular ischemic events: an observational cohort study.* J Cardiovasc Pharmacol Ther, 2010. **15**(2): p. 151-7.
268. Nair, A.B. and S. Jacob, *A simple practice guide for dose conversion between animals and human.* Journal of basic and clinical pharmacy, 2016. **7**(2): p. 27-31.
269. Johnpulle, R.A.N., D.B. Johnson, and J.A. Sosman, *Molecular Targeted Therapy Approaches for BRAF Wild-Type Melanoma.* Current oncology reports, 2016. **18**(1): p. 6.
270. Kuang, D.M., et al., *Activated monocytes in peritumoral stroma of hepatocellular carcinoma foster immune privilege and disease progression through PD-L1.* J Exp Med, 2009. **206**(6): p. 1327-37.
271. Fleming, V., et al., *Melanoma Extracellular Vesicles Generate Immunosuppressive Myeloid Cells by Upregulating PD-L1 via TLR4 Signaling.* Cancer Res, 2019. **79**(18): p. 4715-4728.

272. Weber, R., et al., *Myeloid-Derived Suppressor Cells Hinder the Anti-Cancer Activity of Immune Checkpoint Inhibitors.* Front Immunol, 2018. **9**: p. 1310.
273. Groth, C., et al., *Immunosuppression mediated by myeloid-derived suppressor cells (MDSCs) during tumour progression.* Br J Cancer, 2019. **120**(1): p. 16-25.
274. Witkowski, M.T., et al., *Extensive Remodeling of the Immune Microenvironment in B Cell Acute Lymphoblastic Leukemia.* Cancer Cell, 2020. **37**(6): p. 867-882 e12.
275. Cane, S., et al., *The Endless Saga of Monocyte Diversity.* Front Immunol, 2019. **10**: p. 1786.
276. Chang, S.K., et al., *A role for BLyS in the activation of innate immune cells.* Blood, 2006. **108**(8): p. 2687-94.
277. Barber, D.L., et al., *Restoring function in exhausted CD8 T cells during chronic viral infection.* Nature, 2006. **439**(7077): p. 682-7.
278. Ayers, M., et al., *IFN-gamma-related mRNA profile predicts clinical response to PD-1 blockade.* J Clin Invest, 2017. **127**(8): p. 2930-2940.
279. Hartley, G.P., et al., *Programmed Cell Death Ligand 1 (PD-L1) Signaling Regulates Macrophage Proliferation and Activation.* Cancer Immunol Res, 2018.
280. Spranger, S., et al., *Up-regulation of PD-L1, IDO, and T(regs) in the melanoma tumor microenvironment is driven by CD8(+) T cells.* Sci Transl Med, 2013. **5**(200): p. 200ra116.
281. Garcia-Diaz, A., et al., *Interferon Receptor Signaling Pathways Regulating PD-L1 and PD-L2 Expression.* Cell Rep, 2017. **19**(6): p. 1189-1201.
282. Hartley, G., et al., *Regulation of PD-L1 expression on murine tumor-associated monocytes and macrophages by locally produced TNF-alpha.* Cancer Immunol Immunother, 2017. **66**(4): p. 523-535.
283. Akhand, S.S., et al., *Pharmacological inhibition of FGFR modulates the metastatic immune microenvironment and promotes response to immune checkpoint blockade.* Cancer Immunol Res, 2020.
284. Juneja, V.R., et al., *PD-L1 on tumor cells is sufficient for immune evasion in immunogenic tumors and inhibits CD8 T cell cytotoxicity.* J Exp Med, 2017. **214**(4): p. 895-904.
285. Tang, F. and P. Zheng, *Tumor cells versus host immune cells: whose PD-L1 contributes to PD-1/PD-L1 blockade mediated cancer immunotherapy?* Cell Biosci, 2018. **8**: p. 34.
286. Vari, F., et al., *Immune evasion via PD-1/PD-L1 on NK cells and monocyte/macrophages is more prominent in Hodgkin lymphoma than DLBCL.* Blood, 2018. **131**(16): p. 1809-1819.
287. Veglia, F., M. Perego, and D. Gabrilovich, *Myeloid-derived suppressor cells coming of age.* Nat Immunol, 2018. **19**(2): p. 108-119.
288. Oyer, J.L., et al., *PD-L1 blockade enhances anti-tumor efficacy of NK cells.* Oncoimmunology, 2018. **7**(11): p. e1509819.
289. Neo, S.Y. and A. Lundqvist, *The Multifaceted Roles of CXCL9 Within the Tumor Microenvironment.* Adv Exp Med Biol, 2020. **1231**: p. 45-51.
290. Wu, C.C., et al., *Enhanced anti-tumor therapeutic efficacy of DNA vaccine by fusing the E7 gene to BAFF in treating human papillomavirus-associated cancer.* Oncotarget, 2017. **8**(20): p. 33024-33036.

Acknowledgements

It's my great honor to take this opportunity to express special thanks to many people who have helped me a lot during the past four years. Without their support and encouragement, I could not have completed my PhD projects and thesis.

Firstly, I have to thank my supervisor, Professor Philipp Lang, who is an excellent professor and expert. I really appreciate his generous support and constant guidance in the past 4 years. His enthusiasm in science has positively impacted my outlook on science. He taught me how to read literature efficiently, how to deal with difficulties in scientific research, and how to be a good scientist. Without his support, I could not have finished my PhD projects. I have great respect to him.

Secondly, I would like to thank my second supervisor, Professor Bernhard Homey, who has patiently listened to all my progress reports and provided very valuable advice. Moreover, I have to thank him for revising my thesis.

In particular, I would like to thank Dr. Aleksandra A. Pandyra for helping me in all my projects. During the 4 years, she has patiently guided me not only in designing experiments and collecting the original data but also in designing new research methods and analyzing data, from which I have benefitted greatly. I learned how to be optimistic to face difficulties in experiments and how to balance my work and life. I also have to thank her for revising my thesis. I am very lucky and appreciate working with her.

Furthermore, I also would like to thank my workmate, Pawel. I feel so lucky to work with him and I will never forget his help and company in the past 4 years. Many thanks to Chris, Anfei, Rui, Yuan, Jun, Prashant and Nikkitha for helping me to learn all the methods and for their advice about experiments. I would like to thank Anna Bornikoel who helped with some German translation. And I would like to say another special thanks to Anfei, Xiaoli, Rui, Jun and Yuan: thank you for your company when I missed home. I would like to thank everyone in the lab, it was really nice to work with them over the years.

I would like to thank my friends in China. Thanks for their company on the phone when I was feeling down. Cangcang and Yangyang, thanks very much for lending me

money when I came to Germany in my first year. I would like to thank Dr. Zhao for understanding and support in the past 10 years. He is a great teacher.

Last but not least, I have to thank my family. Thanks for your understanding and your continual support throughout the years. Thanks for encouraging me to overcome the obstacles over the years.